

TRANSIENT SIMULATION OF THE IMMISCIBLE
FRESH-WATER/SALT-WATER INTFERFACE
IN AQUIFERS

By

ROOP DASARI KUMAR

Bachelor of Technology

Osmania University

Hyderabad, India

1980

Submitted to the Faculty of the Graduate College
of the Oklahoma State University
in partial fulfillment of the requirements
for the Degree of
MASTER OF SCIENCE
May, 1984

1984

1984

1984

1984

1984

1984

1984

1984

1984

1984

1984

1984

1984

1984

1984

1984

1984

1984

1984

1984

1984

1984

1984

1984

1984

1984

1984

1984

1984

Thesis

1984

K96t


cop.2

1984

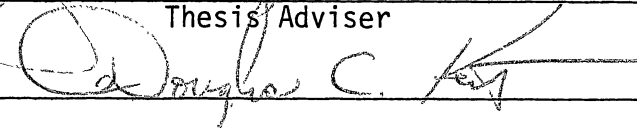


TRANSIENT SIMULATION OF THE IMMISCIBLE
FRESH-WATER/SALT-WATER INTERFACE
IN AQUIFERS


Thesis Approved:




Thesis Adviser



Douglas C. Key



Ardibaldy Hill



Norman N. Durhan
Dean of the Graduate College

ACKNOWLEDGMENTS

The author wishes to express his gratitude to his major advisor, Dr. Jan Wagner, for his guidance and encouragement during the course of this study. Appreciation is also expressed to the University Computing Center for providing computer time necessary for the successful completion of this report.

A note of thanks is due to Ms. Nannie Mathews for a typing job well done. The author also wishes to acknowledge the National Center for Groundwater Research for funding the project.

TABLE OF CONTENTS

Chapter	Page
I. INTRODUCTION	1
II. REVIEW OF LITERATURE	3
Analytical Models	4
Immiscible Fluid Flow	5
Numerical Models	7
III. MODEL DEVELOPMENT	10
Interface Conditions	11
Unconfined Aquifers	13
Confined Aquifers	23
IV. FINITE-ELEMENT MODEL	27
Unconfined Aquifers	28
Confined Aquifers	33
Other Aspects of the Finite-Element Technique	36
Finite-Element Computer Model	37
V. TESTING OF THE NUMERICAL MODEL	38
Upconing in an Unconfined Aquifer	39
Effect of Capillarity on Ground-Water Mounds	48
Salt-Water Intrusion in a Confined Coastal Aquifer	51
VI. CONCLUSIONS AND RECOMMENDATIONS	60
REFERENCES	62
APPENDIXES	64
APPENDIX A - INPUT CODES FOR PROGRAM	65
APPENDIX B - SUMMARY OF COMPUTER PROGRAM	71
APPENDIX C - SOURCE CODES FOR COMPUTER PROGRAM	75
APPENDIX D - INPUT DATA FOR NUMERICAL SIMULATION	92
APPENDIX E - RESULTS OF NUMERICAL SIMULATION	118
APPENDIX F - FINITE ELEMENT MESH LAYOUTS	136

LIST OF TABLES

Table	Page
I. Input Data for Case 1	93
II. Input Data for Case 2	96
III. Input Data for Case 3	99
IV. Input Data for Case 4	102
V. Input Data for Case 5	105
VI. Input Data for Confined Aquifer Example	108
VII. Input Data for Recharge Mound Example with Capillarity . . .	110
VIII. Input Data for Recharge Mound Example without Capillarity. .	116
IX. Sample Output for Case 1	119
X. Sample Output for Case 2	120
XI. Sample Output for Case 3	121
XII. Sample Output for Case 4	124
XIII. Sample Output for Case 5	125
XIV. Analytical Solution for Confined Aquifer	128
XV. Sample Output for Confined Aquifer Example	129
XVI. Sample Output for Recharge Mound Example with Capillarity. .	130
XVII. Sample Output for Recharge Mound Example without Capillarity	133

LIST OF FIGURES

Figure	Page
1. The Ghyben-Herzberg Interface Approximation for a Coastal Aquifer	6
2. Movement of the Salt-Water Front in a Confined Coastal Aquifer	12
3. Vertical Cross-Section of an Unconfined Coastal Aquifer	14
4. Capillary Pressure Profile in a Soil Column	20
5. Vertical Cross-Section of a Confined Coastal Aquifer	24
6. Sahni's Experimental Model for Salt-Water Upconing in a Phreatic Aquifer	40
7. Finite Element Mesh Simulation of Sahni's Physical Model	42
8. Steady State Solutions Employing Different Mesh Layouts	43
9. Transient Numerical Analyses Employing Different Mesh Layouts	44
10. Experimental Observations Versus Steady State Solution Obtained Using the Expanded Mesh	46
11. Experimental Results Versus Transient Analysis of the Numerical Model Obtained Using the Expanded Mesh	47
12. Groundwater Mounding Due to Vertical Percolation from Surface Recharge Areas	49
13. Finite Element Mesh Simulation of the Experimental Model of Ortiz, et al.	50
14. Experimental Results Versus Numerical Solution	52
15. Comparison of Numerical Results With and Without the Influence of Capillary Effects	53
16. Sea-Water Wedge in a Confined Coastal Aquifer	54
17. Finite Element Mesh Simulation of the Analytical Model	57
18. Analytical Solution Versus Numerical Results	58

Figure	Page
19. Detailed Finite Element Mesh Layout of Sahni's Model	137
20. Expanded Finite Element Mesh Layout of Sahni's Model	138
21. Finite Element Mesh Layout of the Experimental Model of Ortiz, et al.	139
22. Finite Element Mesh Layout of Henry's Analytical Model.	140

NOMENCLATURE

A	Cross-sectional area of aquifer, L^2
B	Saturated thickness of the confined aquifer, L
C_1, C_2, C_3, C_4	Coefficients in the finite element equations, L^2/T
dh/dl	Hydraulic gradient
H_e	Equivalent saturated height, L
H_f	Total head in the aquifer, L
H_j	Hydraulic head of fluid j, L
H_K	Equivalent permeable height, L
H_s	Salt water head, L
H_T	Phreatic surface elevation, L
H'	Distance from water table to the soil surface, L
H	Change in hydraulic head, L
h	Hydraulic head, L
h^*	Piezometric head, L
K	Hydraulic conductivity, L/T
K_m	Saturated hydraulic conductivity, L/T
K_{rw}	Relative permeability of the wetting phase
k	Permeability of the medium, L^2
k'	Product of permeability and buoyancy
$L(H_f)$	Differential equation governing H_f
l_x, l_y	Directional cosines
N_i	Shape function of the i^{th} node

N'_x, N'_y	Dervatives of the shape function with respect to the x and y coordinates
n	Unit vector normal to the interface
p	Fluid pressure head, L
P_b	Bubbling pressure head, L
P_c	Capillary pressure head, L
p	Scaled capillary pressure
Q	Volumetric discharge, L^3/T
Q_f, Q_s	Fresh and salt water sources or sinks if areal, L/T if nodal, L^3/T
Q'	Fresh water flow per unit length of shore line, L^2/T
q	Superficial recharge velocity, L/T
q_i	Superficial velocity in x, y and z directions, L/T
q_j	Superficial discharge rate of fluid j, L/T
q_x, q_y, q_z	Darcy velocities in x, y and z directions, L/T
S	Stiffness matrix
S	Storativity of confined aquifer
S	Saturation
S_e	Effective saturation
S_r	Residual saturation
S_s	Specific storage coefficient, L^{-1}
S_y	Specific yield
V	Specific discharge, L/T
V_i	Pore velocity, L/T
x, y, z	Spatial coordinates

X	Horizontal distance from shore towards land, L
Y	Distance from impermeable confining layer to interface, L
Z	Elevation above datum, L
γ	Excess of the specific gravity of sea water over fresh water, M/L^2T^2
γ_f	Unit weight of fresh water, M/L^2T^2
γ_j	Unit weight of fluid j, M/L^2T^2
γ_s	Unit weight of salt water, M/L^2T^2
η	Interface elevation, L
θ	Porosity of the medium
θ	Integration parameter
γ	Pore size distribution index
ξ	Height of ocean above the top of the aquifer, L

CHAPTER I

INTRODUCTION

Increasing surface water contamination has required the development of groundwater as an alternative source of water for human, industrial and irrigation purposes. Unfortunately, groundwater resources have been utilized to such an extent that water tables have declined drastically. Efficient use of aquifers as reservoirs can be achieved if the impact of imposed conditions - natural or artificial - on hydrologic systems can be simulated successfully.

Aquifers, inland or coastal, may consist of fresh-water with the heavier salt-water lying underneath. Fresh-water and salt-water are actually mixible fluids but under certain conditions, the width of the transition zone caused by hydrodynamic dispersion is relatively small, so that an abrupt interface can be assumed to separate the two fluids. As a result of the simultaneous movement of both, fresh-water and salt-water, the interface does not remain static but moves accordingly. Water balance of groundwater can be achieved only when the rate of discharge is less than or equal to the rate of natural and/or artificial recharge. If the pumping rate is in excess of the replenishment rate, the water table elevation will drop and as a result the interface will start upconing under the discharge well. As long as the critical discharge rate is not exceeded, fresh-water can be continuously pumped out of the aquifer. Once the critical discharge is exceeded, the upconed interface becomes unstable and salt-water starts flowing out of the well.

Furthermore, due to increasing concern about surface pollution, liquid and solid wastes are being introduced into the subsurface environment thereby endangering groundwater supplies. As a result, the simulation of the dynamic fluid-fluid interface is of utmost importance in determining the course of subsurface water management policies.

The soil between the water table and the ground surface is only partially saturated with water. In this zone, the effect of capillary pressure on the water table elevation and the specific yield of the aquifer is not negligible. If flow in the unsaturated region has some impact on the water table, the salt-water interface will also be affected accordingly.

The prediction of the location of the fresh-water/salt-water interface will also be useful towards gaining an insight into the mechanism of sea-water intrusion into coastal aquifers. This problem is a particularly difficult one as it involves tracking a boundary which is moving and limited in extent.

This research, therefore, intends to develop a general model based on the governing partial differential equations to simulate the dynamic interface in a two phase subsurface reservoir. Flow of fresh-water and salt-water will be considered in a horizontal two-dimensional plane as a three dimensional model is useful only when changes in vertical head components are too large to ignore. The numerical model will be tested against existing analytical and experimental models to determine its accuracy and utility in the real world.

CHAPTER II

REVIEW OF LITERATURE

Flow problems involving nonlinear partial differential equations have been solved using various numerical techniques such as finite differences, the method of characteristics, etc. These methods were inadequate for certain types of problems, and the need for a new method was stressed. This led to the introduction of finite-element methods in hydrology and reservoir engineering. These numerical techniques are applied to obtain solutions to partial differential equations after certain assumptions have been made to simplify the flow domain, boundary conditions, physical characteristics of the porous medium, and fluid characteristics.

The study of homogeneous and inhomogeneous fluid flow can be classified as follows:

1. Single phase flow
2. Multiphase flow
 - a. miscible flow
 - b. immiscible flow

The simultaneous flow of two fluids that are soluble in each other is termed miscible displacement. In this case, there is no distinct fluid-fluid interface, instead there is a convective-dispersion zone. Immiscible displacement occurs when the fluids displace each other without mixing, and there is a distinct fluid-fluid interface between each fluid phase.

The fresh water and salt water are treated independently and the interface elevation is evaluated from the boundary condition over the fluid-fluid interface.

The presence of capillarity in unconfined aquifers involves the solution of a set of nonlinear differential equations which describe the capillary pressure and the saturated and permeable heights.

Analytical Models

The basis of groundwater hydrology is Darcy's Law which was propounded by Henry Darcy in 1856. As a result of his experiments, the following empirical relationship evolved:

$$Q = -KA \frac{dh}{dl} \text{ or } V = \frac{Q}{A} = -K \frac{dh}{dl} \quad (1)$$

where:

h = hydraulic head,

dh/dl = hydraulic gradient,

K = hydraulic conductivity,

V = specific discharge,

Q = volumetric discharge, and

A = cross-sectional area.

From this simple empirical base, researchers have developed complex equations which describe flow in aquifers for single, as well as multi-phase, fluid flow. Dupuit (1863) and Forchheimer (1930) postulated that for flow in unconfined systems bounded by a free surface (1) flowlines can be assumed to be horizontal with vertical equipotentials and (2) the hydraulic gradient can be assumed to be equal to the slope of the free surface and to be invariant with depth. The Dupuit-Forchheimer assumptions

are not applicable in regions where the vertical flow components are significant. However, these assumptions are important tools for treating unconfined flows due to their simplicity and relatively small errors in many cases.

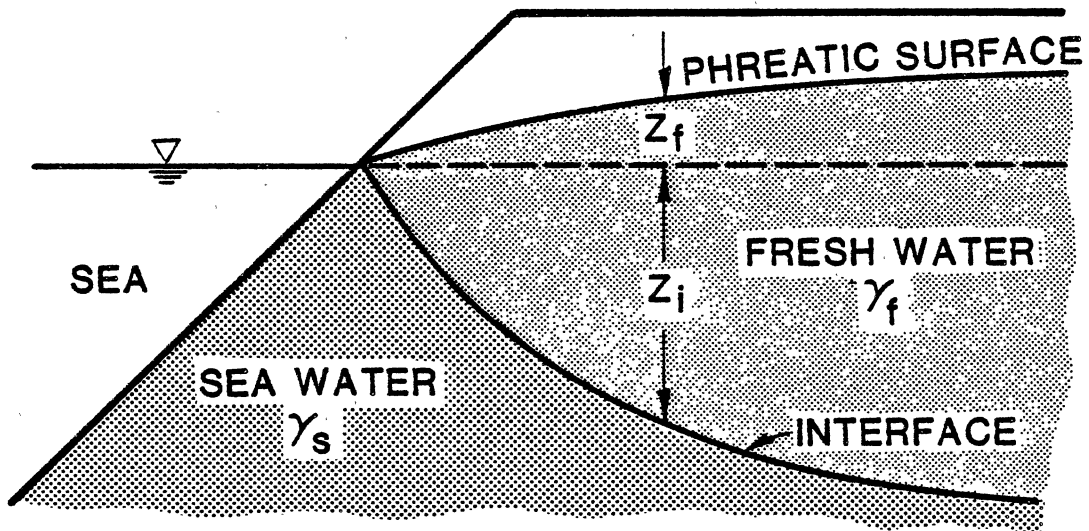
Immiscible Fluid Flow

Pioneering research on the position of the interface in coastal aquifers was conducted by Badon-Ghyben and Herzberg in 1888 and 1901, respectively. Their analyses assumed simple hydrostatic conditions in a homogeneous, unconfined coastal aquifer. Essentially, both Ghyben and Herzberg assumed static equilibrium and a hydrostatic pressure distribution in the fresh-water body with the sea-water being stationary. Figure 1 depicts the idealized Ghyben-Herzberg model for the phreatic surface and interface position in an unconfined coastal aquifer.

The Ghyben-Herzberg principle states that at any distance from the sea, the depth of the stationary interface below sea level is approximately forty times the height of the fresh-water above it. Near the seashore, however, dynamic factors become important. If static conditions alone were to prevail, the fresh-water body would narrow and there would be no way for the fresh-water to escape to the sea. When dynamic factors are considered, the fresh-water flows through a narrow gap between a fresh-water/salt-water interface and the water table outcrop at the coast.

Based on this theory, Glover (1959) developed a relationship to relate the interface elevation to the rate of fresh-water withdrawal from a confined coastal aquifer at steady state conditions. The equation describing this relationship is

$$y^2 - \frac{2Q'}{\gamma k} x - \frac{Q'^2}{\gamma^2 k^2} = 0 \quad (2)$$



$$Z_i = Z_f \left(\frac{\gamma_f}{\gamma_s - \gamma_f} \right) \approx 40 Z_f$$

Figure 1. The Ghyben-Herzberg Interface Approximation for a Coastal Aquifer

where γ = excess of the specific gravity of sea-water over fresh-water,

x = horizontal distance from shore towards land,

k = permeability of the medium,

y = vertical downward distance from sea level, and

Q' = fresh-water flow per unit length of shore line.

A somewhat analogous relationship was presented by Henry (1959) by the use of hodograph planes and complex potentials. His relationship is

$$\left(\frac{yk'}{Q'}\right)^2 - 2\left(\frac{xk'}{Q'}\right) - 1 = 0 \quad (3)$$

where

$$k' = \frac{k(\gamma_s - \gamma_f)}{\gamma_f}$$

and x = horizontal distance landwards,

y = vertical distance downward,

k' = product of permeability and buoyancy,

γ_s = specific weight of salt-water, and

γ_f = specific weight of fresh-water.

When sea-water intrudes into a coastal aquifer, both fluids will be moving under transient conditions. Because the zone underlain by the sea-water wedge is limited, the problem becomes more complicated since there is a moving boundary to deal with.

Numerical Models

The petroleum industry is responsible for developing many of the reservoir simulation techniques. The basis behind these techniques is the immiscible displacement of fluids. The fundamental laws governing the displacement problem are Darcy's law, the law of conservation of

mass of both fluids, and the pressure balance across the interface. The highly nonlinear partial differential equations that result are extremely difficult to solve, analytically or numerically. Simplifying assumptions have to be made before a solution can be obtained.

The numerical solution can be accomplished by numerous techniques available. The most common solution techniques are the finite-difference and finite-element methods. One of the problems in flow through porous media involves sharp fronts. A sharp front refers to a large change in a dependent variable over a small distance. It was observed that finite-difference methods, when applied to sharp-front problems, tend to oscillate and cause instability (Mercer and Faust, 1977). Hence, there has been a growing tendency to use the finite-element method to solve sharp front problems. Pinder and Page (1976) developed a finite-element model to simulate salt-water intrusion on Long Island. Segol, Pinder and Gray (1973), Pinder and Cooper (1970), Bredehoeft and Pinder (1970), Neuman and Witherspoon (1970) and others have used the finite-element technique with excellent results. Layla (1980) developed a general model based on the Galerkin finite-element method to predict the interface elevations in coastal aquifers. His model was found to have some discrepancies regarding the development of the necessary flow equations.

In developing the fresh-water and salt-water flow equations for confined aquifers, Layla neglected to integrate the specific storage term with respect to the vertical fluid phase elevation. He also makes an assumption that the change in interface elevation with time is zero so as to simplify the formulation of the fresh-water equation in the Galerkin finite-element approximation. Contradictorily, he retains the term during the salt-water region Galerkin approximation. Time inte-

gration of the finite-element matrix equations is accomplished but the derivation is subject to mathematical errors.

Layla's finite-element algorithm is fundamentally correct and his solution technique error-free. The choice of quadratic, triangular elements leads to great accuracy and low computation times and costs. However, the subroutines for evaluating the equivalent saturated and permeable heights are conceptually incorrect. Layla integrates the necessary differential equations to arrive at relationships which describe the permeable and saturated heights in the presence of capillary pressure. He then uses the unintegrated differential equations to build his algorithms for evaluating the equivalent saturated and permeable heights and apparent specific yield.

The integration routine used in the algorithms does not cover the entire flow domain, and the change in the equivalent saturated height with respect to the change in water-table elevation is also evaluated incorrectly.

All-in-all, the Layla model has to be redeveloped from a fundamental basis so that the head distributions in aquifers can be predicted with a reasonable degree of accuracy. The next few chapters will be devoted to developing the necessary flow equations and solving them using the Galerkin finite-element algorithms developed by Layla.

CHAPTER III

MODEL DEVELOPMENT

The areal distribution of the dynamic fresh-water/salt-water interface in unconfined aquifers is considered first. This will enable the model to be checked with existing experimental data. Next, the effect of capillarity on the value of specific yield and the water table height in unconfined aquifers is considered. Finally, the necessary flow equations for fluid movement in confined aquifers are developed.

The assumptions underlying the formulation of the flow equations for an unconfined aquifer are:

1. Darcy's law is valid for both fluid phases,
2. An abrupt interface approximation is justified since the transition zone between fresh and salt water is very small when compared to the saturated thickness of the aquifer,
3. The Dupuit-Forchheimer approximations are applicable,
4. Soil and fluid properties do not change with time,
5. Both fluids are incompressible,
6. Isothermal conditions prevail in the flow domain,
7. The effect of the capillary fringe on the water table elevation is not negligible, and
8. Elastic properties of the formulation and fluids are negligible.

Interface Conditions

At steady state, the magnitude of seaward fresh-water flow, $Q_f(L, 0)$, is constant everywhere and equals $Q_f(x, 0)$. The boundary condition along the interface (Figure 2a) is the same as that of the impervious boundary conditions; i.e.,

$$\vec{q}_j \cdot \vec{n} = 0 \quad (4)$$

where j represents fluid phase and n is the unit vector normal to the interface.

If equilibrium is disturbed, the interface will shift accordingly due to hydraulic gradients. Suppose at $t=t_1$, the seaward fresh-water flow is increased to $Q_f(L, t_1)$. The interface will continue moving landward until a new equilibrium is established (Figure 2b). During the transition, the boundary condition described by Equation 4 is no longer applicable along the interface. Continuity requires that

$$q_{nj} = -K \frac{\partial H_j}{\partial n} \quad (5)$$

where q_{nj} is the velocity component normal to the interface and

$$H_j = \frac{P}{\gamma_j} + n \quad (6)$$

where H_j = hydraulic head of fluid j ,

γ_j = unit weight of fluid j ,

P = fluid pressure, and

n = interface elevation.

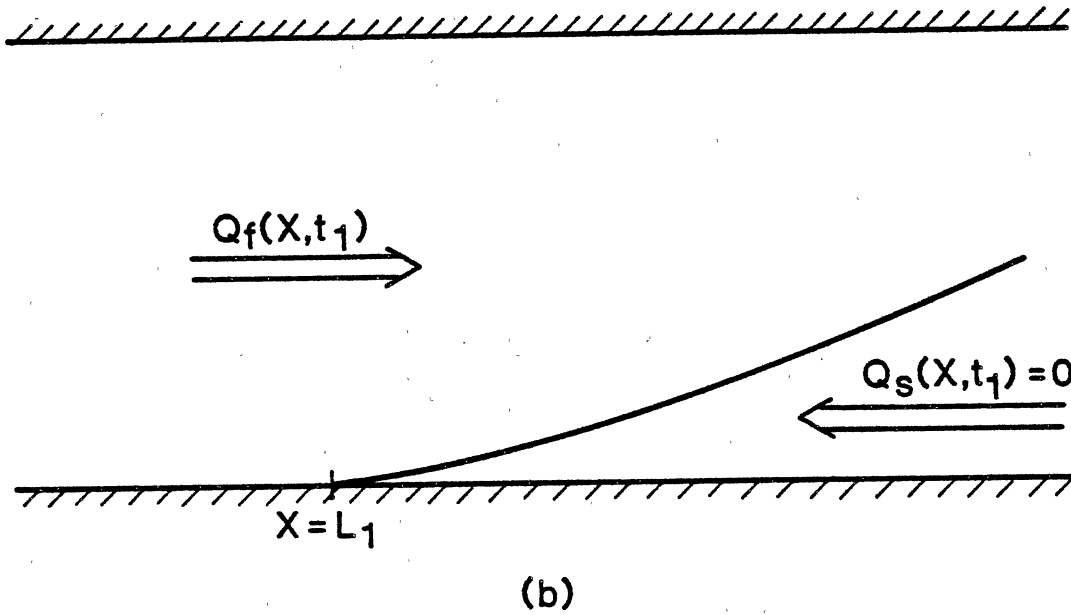
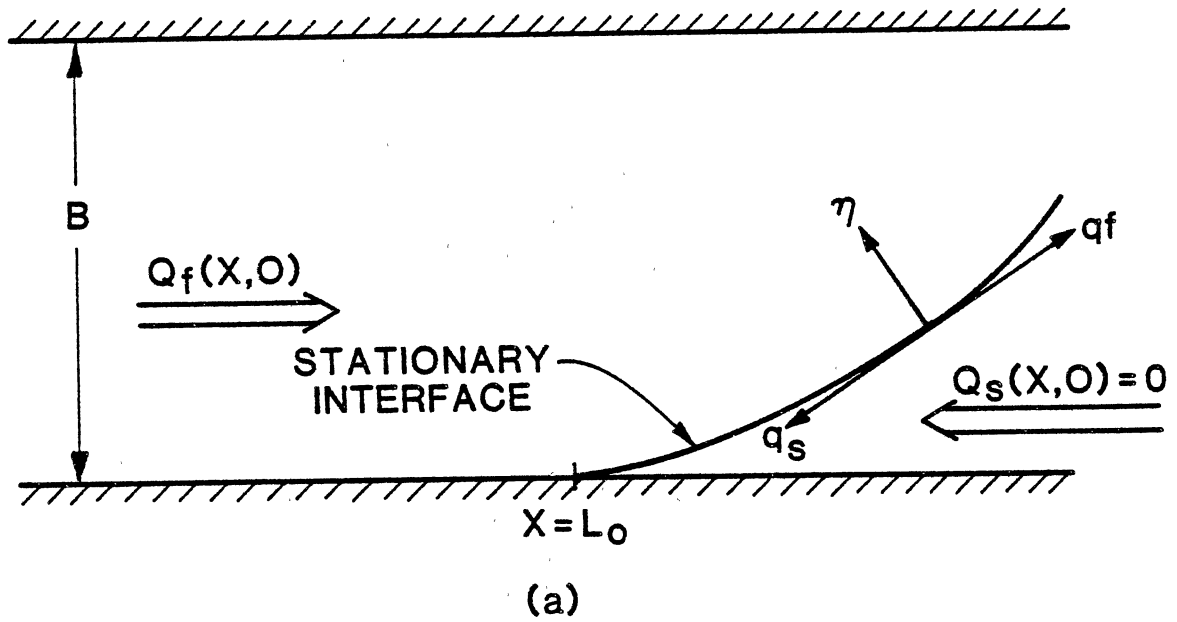


Figure 2. Movement of the Salt-Water Front in a Confined Coastal Aquifer

Continuity also requires equality of fluid pressure across the interface. Hence, equating the pressure term in Equation 6 for both fluids yields

$$P = (H_S - n)\gamma_S = (H_f - n)\gamma_f \quad (7)$$

which simplifies to:

$$n = \alpha_S H_S - \alpha_f H_f \quad (8)$$

where $\alpha_f = \gamma_f/\Delta\gamma$ and $\alpha_S = \gamma_S/\Delta\gamma$, and f and s denote fresh-water and salt water, respectively. Equation 8 is the dynamic boundary condition on the interface.

Unconfined Aquifers

The elevations of the phreatic surface and the interface (Figure 3) can be expressed as follows (Bear, 1979):

$$F_1(x, y, z, t) = z - H_T(x, y, t) \quad (9)$$

$$F_2(x, y, z, t) = z - n(x, y, t) \quad (10)$$

where H_T = phreatic surface elevation,

n = elevation of salt-water/fresh-water interface,

z = elevation above datum, and

t = time.

Since the phreatic surface and the interface are material surfaces which are always composed of the same fluid particles,

$$\frac{DF}{Dt} = \frac{\partial F}{\partial t} + V_i \cdot \nabla F = 0 \quad (11)$$

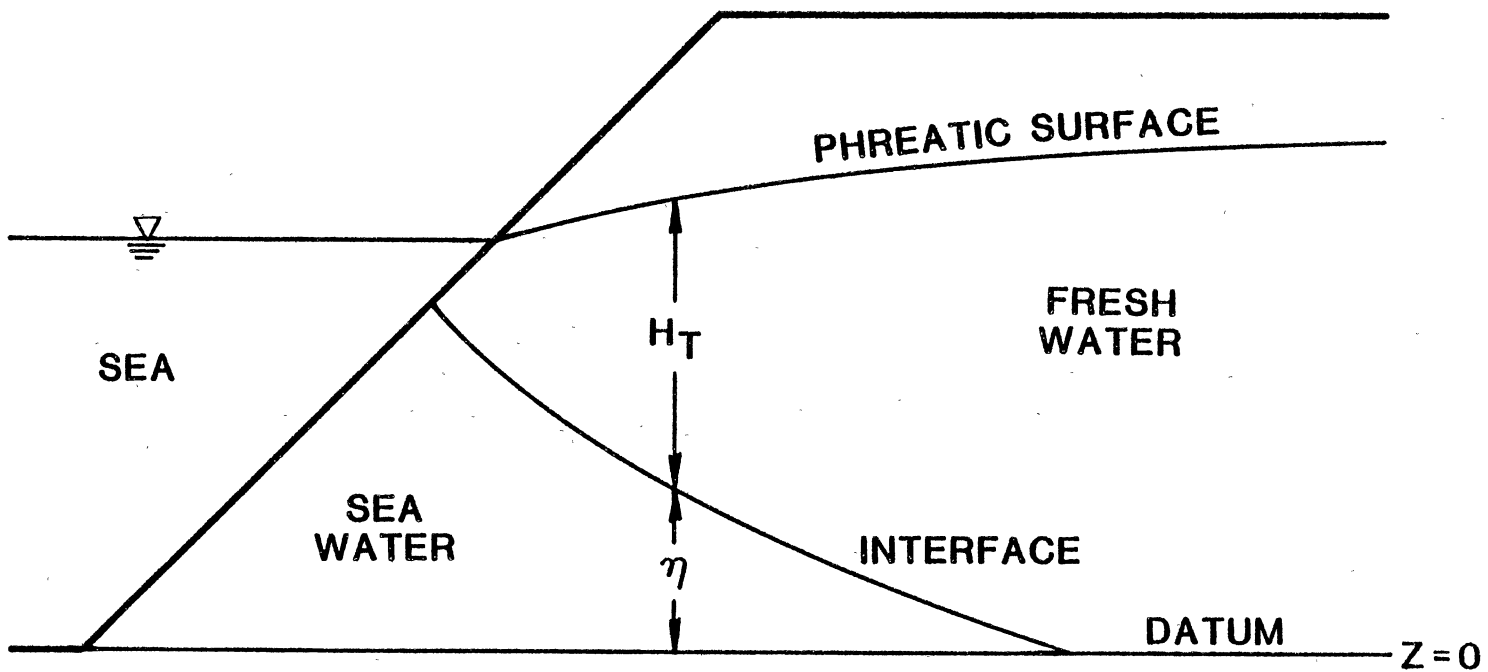


Figure 3. Vertical Cross-Section of an Unconfined Coastal Aquifer

where V_i = pore velocity $\approx q_i/\theta$,
 q_i = superficial velocity,
 θ = effective porosity, and
 i = fluid phase.

As the vertical gradients generally found in the field are relatively small an assumption can be made to the effect that

$$H_s = (H_s)_{z=0} = (H_s)_{z=n}$$

and

$$H_f = (H_f)_{z=H_t} = H_T.$$

Using these approximations, substituting Equation 9 into Equation 11, and expanding terms leads to

$$\theta \frac{DF}{Dt} = \theta \frac{\partial z}{\partial t} - \theta \frac{\partial H_f}{\partial t} - \theta \frac{\partial H_f}{\partial x} \frac{\partial x}{\partial t} - \theta \frac{\partial H_f}{\partial y} \frac{\partial y}{\partial t}. \quad (12)$$

In terms of the Darcy velocity at the phreatic surface,

$$(q_z)_{H_f} - \theta_f \frac{\partial H_f}{\partial t} = (q_x)_{H_f} \frac{\partial H_f}{\partial x} + (q_y)_{H_f} \frac{\partial H_f}{\partial y}. \quad (13)$$

Similarly, the salt-water/fresh-water interface equation is

$$(q_z)_n - \theta_s \frac{\partial \eta}{\partial t} = (q_x)_n \frac{\partial \eta}{\partial x} + (q_y)_n \frac{\partial \eta}{\partial y} \quad (14)$$

Assuming the fluids and the formation are incompressible, continuity requires

$$\frac{\partial q_x}{\partial x} + \frac{\partial q_y}{\partial y} + \frac{\partial q_z}{\partial z} = 0 \quad (15)$$

for the fresh-water, and

$$\frac{\partial q_x}{\partial x} + \frac{\partial q_y}{\partial y} + \frac{\partial q_z}{\partial z} = 0 \quad (16)$$

for the salt water.

Integrating Equation 15 with respect to z between the limits $z = n$ and $z = H_f$ and applying the Dupuit-Forchheimer principle for a mildly sloping free surface gives

$$\begin{aligned} & (q_z)_{H_f} - (q_z)_n + \frac{\partial}{\partial x} \int_n^{H_f} q_x dz + \frac{\partial}{\partial y} \int_n^{H_f} q_y dz + (q_x)_n \frac{\partial n}{\partial x} \\ & + (q_y)_n \frac{\partial n}{\partial y} - (q_x)_{H_f} \frac{\partial H_f}{\partial x} - (q_y)_{H_f} \frac{\partial H_f}{\partial y} = 0 \quad . \end{aligned} \quad (17)$$

Substituting Equations 13 and 14 into Equation 17 and expressing the velocity components, q_x and q_y , by Darcy's law, yields

$$\frac{\partial}{\partial x} \int_n^{H_f} K_x \left(\frac{\partial H_f}{\partial x} \right) dz + \frac{\partial}{\partial y} \int_n^{H_f} K_y \left(\frac{\partial H_f}{\partial y} \right) dz = \theta_f \frac{\partial H_f}{\partial t} - \theta_s \frac{\partial n}{\partial t} \quad . \quad (18)$$

Equation 18 can be expanded about the salt-water interface using a Taylor series. Accounting for capillarity by utilizing the concepts of equivalent permeable and equivalent saturated heights as defined by Duke (1973), yields:

$$\begin{aligned} & \frac{\partial}{\partial x} [K_x (H_f + H_k - n) \frac{\partial H_f}{\partial x}] + \frac{\partial}{\partial y} [K_y (H_f + H_k - n) \frac{\partial H_f}{\partial y}] + Q_f \\ & = \theta_f \left(1 + \frac{\partial H_e}{\partial H_f} \right) \frac{\partial H_f}{\partial t} - \theta_s \frac{\partial n}{\partial t} \end{aligned} \quad (19)$$

where

Q_f = fresh-water source or sink term,

H_k = equivalent permeable height, and

H_e = equivalent saturated height.

The equation for salt-water flow is obtained by integrating Equation 16 between $z = 0$ and $z = n$, or

$$(q_z)_n + \frac{\partial}{\partial x} \int_0^n q_x dz + \frac{\partial}{\partial y} \int_0^n q_y dz - (q_x)_n \frac{\partial n}{\partial x} - (q_y)_n \frac{\partial n}{\partial y} = 0. \quad (20)$$

Substituting Equation 14 into Equation 20 and expressing the velocity components, q_x and q_y , in terms of Darcy's law yields the salt-water flow equation:

$$\frac{\partial}{\partial x} [K_x n \left(\frac{\partial H_s}{\partial x}\right)] + \frac{\partial}{\partial y} [K_y n \left(\frac{\partial H_s}{\partial y}\right)] + Q_s = \theta_s \frac{\partial n}{\partial t} \quad (21)$$

where Q_s is included as a salt-water source or sink term.

Equations 19 and 21 can be solved simultaneously to yield values for the dynamic fresh-water and salt-water heads. The interface elevation can then be evaluated by using the boundary condition for continuity of pressure across the interface, or

$$\frac{\partial n}{\partial t} = \alpha_s \frac{\partial H_s}{\partial t} - \alpha_f \frac{\partial H_f}{\partial t}. \quad (22)$$

Equivalent Permeable Height

Duke (1973) defined the equivalent permeable height as a measure of the effectiveness of the partially saturated region for transmitting horizontal flow and presented the following relationship:

$$H_k = \frac{1}{K_m} \int_0^{H'} K(z) dz \quad (23)$$

where H_k = equivalent permeable height,

H' = distance from the water table to the soil surface,

K_m = saturated hydraulic conductivity, and

z = elevation above the water table.

According to Burdine (1952), the relative permeability of the wetting phase, K_{rw} , is given by

$$K_{rw} = \left(\frac{S - S_r}{1 - S_r} \right)^2 \frac{\int_0^S \frac{dS}{P_c^2}}{\int_0^1 \frac{dS}{P_c^2}} \quad (24)$$

where S_r = residual saturation,

S = saturation, and

P_c = capillary pressure.

Corey (1964) defined an effective saturation as

$$S_e = \frac{S - S_r}{1 - S_r} \quad (25)$$

By making a change of variable from S to S_e in the integrals of Equation 24, the relative wetting phase permeability becomes

$$K_{rw} = (S_e)^2 \frac{\int_0^{S_e} \frac{dS_e}{P_c^2}}{\int_0^1 \frac{dS_e}{P_c^2}} \quad (26)$$

Corey (1964) also found by experimentation that

$$S_e = \left(\frac{P_b}{P_c} \right)^\lambda \quad \text{for } P_c \geq P_b \quad (27)$$

and

$$S_e = 1.0 \quad \text{for } P_c < P_b \quad (28)$$

where λ = pore size distribution index, and

P_b = bubbling pressure.

Substituting Equation 27 into Equation 26 and performing the indicated integrations, the relative permeability of the wetting phase becomes

$$K_{rw} = \left[\frac{P_b}{P_c} \right]^n \quad \text{for } P_c > P_b \quad (29)$$

where $n = 2 + 3\lambda$. When the capillary pressure is less than the bubbling pressure, the relative permeability of the wetting phase is given by

$$K_{rw} = 1.0 \quad \text{for } P_c < P_b. \quad (30)$$

In terms of hydraulic conductivity, Equations 29 and 30 can be written as

$$K = K_m \left[\frac{P_b}{P_c} \right]^{2+3\lambda} \quad \text{for } P_c \geq P_b \quad (31)$$

and

$$K = K_m \quad \text{for } P_c < P_b. \quad (32)$$

The capillary pressure head is equivalent to the elevation, z (Figure 4), above the water table when the soil water profile is presumed to be in static equilibrium with the water table. Hence, Equations 31 and 32 transform to

$$K = K_m \left[\frac{P_b}{z} \right]^{2+3\lambda} \quad \text{for } z \geq P_b \quad (33)$$

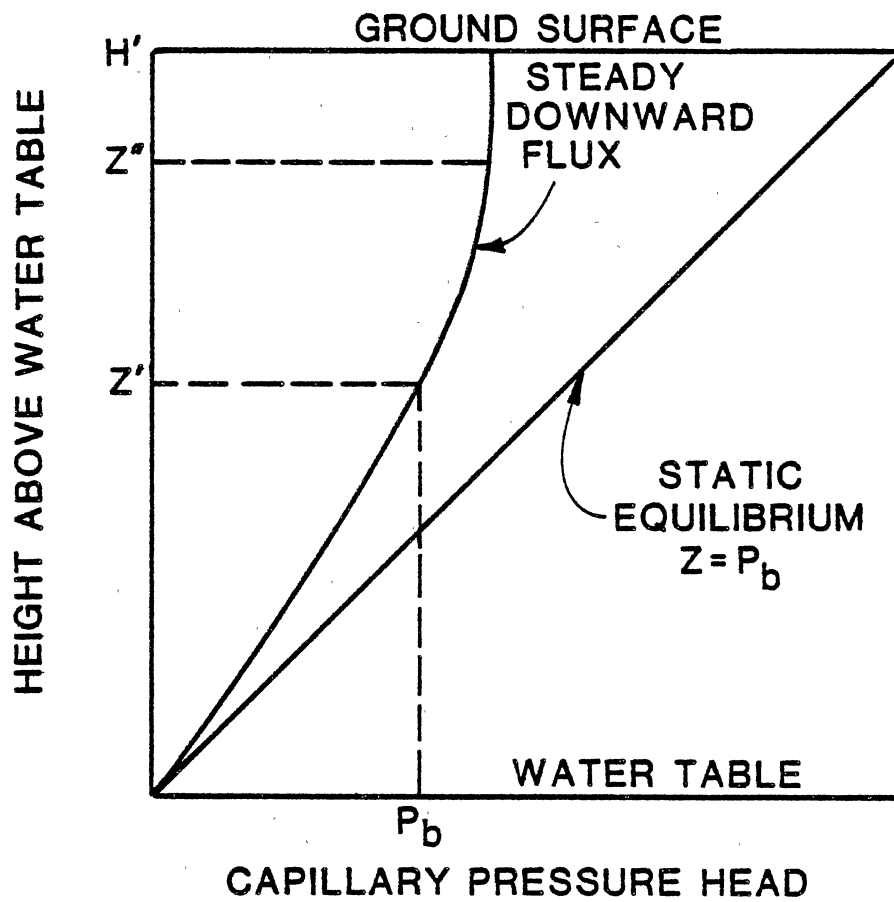


Figure 4. Capillary Pressure Profile in a Soil Column

$$K = K_m \quad \text{for } z < P_b \quad (34)$$

Substituting Equations 33 and 34 into Equation 23 yields

$$H_k = \frac{1}{K_m} \int_0^{P_b} K_m dz + \frac{1}{K_m P_b} \int_0^{H'} K_m \left[\frac{P_b}{z} \right]^{2+3\lambda} dz \quad (35)$$

where H' is the distance from the phreatic surface to the ground surface. Upon integration, the effective permeable height is

$$H_k = P_b \frac{(2+3\lambda) - \left(\frac{P_b}{H'}\right)^{1+3\lambda}}{1+3\lambda} \quad (36)$$

Equivalent Saturated Height

In saturated flow, the specific yield is identified with the porosity of the medium. However in unsaturated flow, the specific yield is defined as the volume of water per unit area of soil per unit lowering of the water table. Ortiz, et al. (1978) used the concept of an equivalent saturated height to illustrate this phenomenon. According to them, the equivalent saturated height is a measure of the influence of the partially saturated region upon the storage of water in unconfined aquifers. By definition,

$$H_e = \int_0^{H'} S_e(z) dz \quad (37)$$

where H_e is the equivalent saturated height and $S_e(z)$ is the effective saturation.

Brooks and Corey (1964) deduced from experimental data that

$$S_e = \left[\frac{P_b}{z} \right]^\lambda \quad \text{for } z \geq P_b \quad (38)$$

and

$$S_e = 1.0 \quad \text{for } z < P_b. \quad (39)$$

Substituting Equations 38 and 39 in Equation 37 yields

$$H_e = \int_0^{P_b} dz + \int_{P_b}^{H'} \left[\frac{P_b}{z} \right]^\lambda dz. \quad (40)$$

Upon integration,

$$H_e = P_b + P_b \frac{\left[\frac{P_b}{H'} \right]^{\lambda-1} - 1}{1 - \lambda}. \quad (41)$$

The relationship for the equivalent saturated height based on static conditions can be written as

$$H_e = P_b \left[\frac{\lambda - \left(\frac{P_b}{H'} \right)^{\lambda-1}}{\lambda - 1} \right] \quad (42)$$

Ortiz, et al. (1978) also presented the following relationship for the equivalent saturated height when steady downward flow conditions exist beneath a recharge site:

$$H_e = P_b \left[\frac{1 - \left(\frac{q}{K} \right)^{\lambda/n}}{1 - \left(\frac{q}{K} \right)} + \left(\frac{q}{K} \right)^{\lambda/n} \frac{H'}{P_b} + \int_1^{\hat{P}} \left(\frac{q}{K} \right)^{-\frac{1}{n}} \frac{\hat{P}^{-\lambda} - \left(\frac{q}{K} \right)^{\lambda/n}}{1 - \left(\frac{q}{K} \right) \hat{P}^n} d\hat{P} \right] \quad (43)$$

where q is the superficial recharge velocity and $\hat{P} = P_c/P_b$ is the scaled capillary pressure.

Following Tuma (1970), the integral appearing in Equation 43 can be evaluated as

$$\int \left(\frac{q}{K} \right)^{-1/n} \frac{\hat{p}^{-\lambda} - \left(\frac{q}{K} \right)^{\lambda/n}}{1 - \left(\frac{q}{K} \right) \hat{p}^n} d\hat{p} = \frac{1}{2n} \left[\frac{1+2n+\lambda}{1+\lambda} \left\{ \left(\frac{q}{K} \right)^{-(\lambda+1)/n} - 1 \right\} \right. \\ \left. + \left\{ 1 - \left(\frac{q}{K} \right)^2 \right\} \right] - \left[\left(\frac{q}{K} \right)^{(\lambda-1)/n} \left(1 + \frac{1}{2n} \right) + \frac{\left(\frac{q}{K} \right)^{\lambda/n}}{2n} \left\{ \left(\frac{q}{K} \right)^2 - 2 \left(\frac{q}{K} \right) - 2n \right\} \right]. \quad (44)$$

The equivalent saturated height then becomes

$$H_e = P_b \left[\frac{1 - \left(\frac{q}{K} \right)^{\lambda/n}}{1 - \left(\frac{q}{K} \right)} + \left(\frac{q}{K} \right)^{\lambda/n} \frac{H'}{P_b} + \frac{1}{2n} \left\{ \frac{1+2n+\lambda}{1+\lambda} \left(\frac{q}{K} \right)^{\frac{\lambda+1}{n}} - 1 \right\} \right. \\ \left. + \left\{ 1 - \left(\frac{q}{K} \right)^2 \right\} \right] - \left[\left(\frac{q}{K} \right)^{\frac{\lambda-1}{n}} \left(1 + \frac{1}{2n} \right) + \frac{\left(\frac{q}{K} \right)^{\lambda/n}}{2n} \left\{ \left(\frac{q}{K} \right)^2 - 2 \left(\frac{q}{K} \right) - 2n \right\} \right]. \quad (45)$$

The specific yield is evaluated by utilizing the appropriate equation for H_e ; depending on whether H_e is based on static conditions as beyond the recharge area, or steady downward flow conditions beneath the recharge site.

Confined Aquifers

Relationships for fluid surface elevations similar to Equations 13 and 14 can be written for a confined aquifer. At the top of the aquifer (Figure 5)

$$(q_z)_B - \theta \frac{\partial B}{\partial t} = (q_x)_B \frac{\partial B}{\partial x} + (q_y)_B \frac{\partial B}{\partial y}, \quad (46)$$

and at the interface

$$(q_z)_n - \theta \frac{\partial n}{\partial t} = (q_x)_n \frac{\partial n}{\partial x} + (q_y)_n \frac{\partial n}{\partial y} \quad (47)$$

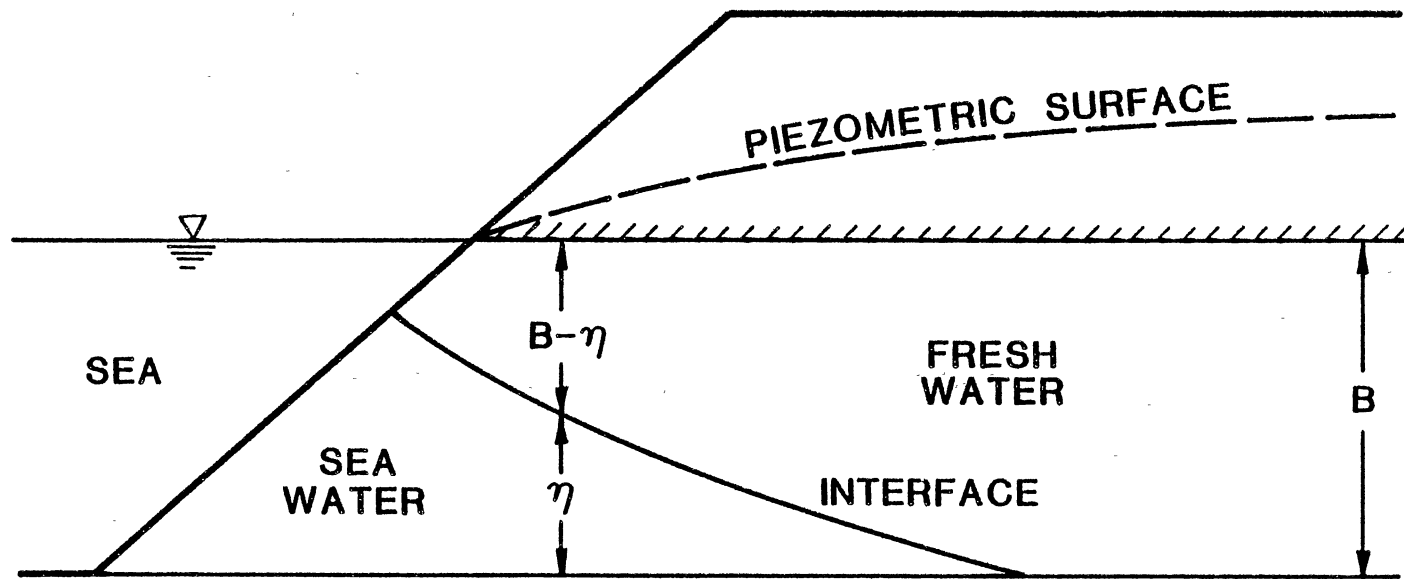


Figure 5. Vertical Cross-Section of a Confined Coastal Aquifer

where B is the saturated thickness of the aquifer. In a confined aquifer, continuity requires

$$\frac{\partial q_x}{\partial x} + \frac{\partial q_y}{\partial y} + \frac{\partial q_z}{\partial z} + S_s \frac{\partial H_f}{\partial t} = 0 \quad (48)$$

for the fresh-water, and

$$\frac{\partial q_x}{\partial x} + \frac{\partial q_y}{\partial y} + \frac{\partial q_z}{\partial z} + S_s \frac{\partial H_s}{\partial t} = 0 \quad (49)$$

for the salt water where S_s is the specific storage coefficient.

Integrating Equation 48 with respect to z between the limits $z = \eta$ and $z = B$ and changing the order of integration and differentiation for the first two terms yields

$$\begin{aligned} (q_z)_B - (q_z)_\eta + \frac{\partial}{\partial x} \int_\eta^B q_x dz + \frac{\partial}{\partial y} \int_\eta^B q_y dz + (q_x)_\eta \frac{\partial \eta}{\partial x} \\ + (q_y)_\eta \frac{\partial \eta}{\partial y} - (q_x)_B \frac{\partial B}{\partial x} - (q_y)_B \frac{\partial B}{\partial y} + S_s (B - \eta) \frac{\partial H_f}{\partial t} = 0 \end{aligned} \quad (50)$$

Substituting Equations 46 and 47 into Equation 50 and noting that $\partial B / \partial t = 0$ for constant saturated thickness gives

$$\frac{\partial}{\partial x} \int_\eta^B q_x dz + \frac{\partial}{\partial y} \int_\eta^B q_y dz - \theta \frac{\partial \eta}{\partial t} + S \frac{\partial H_f}{\partial t} + Q_f = 0 \quad (51)$$

where S is the storativity and is equal to $S_s(H_f - \eta)$.

Expressing the velocity components in terms of Darcy's law, the fresh-water flow equation becomes

$$\frac{\partial}{\partial x} [K_x (B - \eta) \frac{\partial H_f}{\partial x}] + \frac{\partial}{\partial y} [K_y (B - \eta) \frac{\partial H_f}{\partial y}] + Q_f = S \frac{\partial H_f}{\partial t} - \theta \frac{\partial \eta}{\partial t} \quad (52)$$

Similarly, integrating Equation 45 between $z = 0$ and $z = \eta$ and simplifying after substitutions yields

$$\frac{\partial}{\partial x} \left[K_x \eta \frac{\partial H_s}{\partial x} \right] + \frac{\partial}{\partial y} \left[K_y \eta \frac{\partial H_s}{\partial y} \right] + Q_s = S \frac{\partial H_s}{\partial t} + \theta \frac{\partial \eta}{\partial t} \quad (53)$$

for the salt water region where $S = S_s \eta$ for salt water.

Equations 51 and 53 describe the flow of fresh-water and salt-water, respectively, in a confined aquifer. They can be solved simultaneously, and the interface elevation can be evaluated from Equation 22 which describes the continuity of pressure across the interface.

CHAPTER IV

FINITE-ELEMENT MODEL

The Galerkin finite-element method is applied to solve the flow equations developed in the preceding chapter. The Galerkin method is a means of obtaining an approximate solution to a differential equation by requiring that the error between the approximate solution and the true solution be orthogonal to the functions used in the approximation. The finite-element technique uses the following procedure.

1. The flow domain is divided into elements and nodes.
2. An arbitrary trial solution is assumed to describe the partial differential equation to be solved.
3. Suitable basis functions are chosen which satisfy the boundary conditions imposed on the appropriate partial differential equation.
4. The appropriate integrations are performed to yield coefficients.
5. The weighted integrals of the residual are set equal to zero to obtain a set of simultaneous equations which can be solved to yield values of the dependent variables at all nodes.

The resulting set of algebraic equations are integrated with respect to time to yield values of the dependent variable at different time levels. The formulation of the finite-element approximations for flow in unconfined aquifers are developed in the following paragraphs.

Unconfined Aquifers

The finite-element approximation for the fresh-water flow equation described by Equation 19 can be rewritten using Equation 22 to yield:

$$\frac{\partial}{\partial x} [C_1 \frac{\partial H_f}{\partial x}] + \frac{\partial}{\partial y} [C_2 \frac{\partial H_f}{\partial y}] + Q_f - C_3 \frac{\partial H_f}{\partial t} + C_4 \frac{\partial H_s}{\partial t} = 0 = L(H_f) \quad (54)$$

where

$$C_1 = K_x (H_f + H_k - \eta),$$

$$C_2 = K_y (H_f + H_k - \eta),$$

$$C_3 = \theta_f (1 + \frac{\partial H_e}{\partial H_f}) + \theta_s \alpha_f, \text{ and}$$

$$C_4 = \theta_s \alpha_s.$$

The term $L(H_f)$ is the differential equation governing H_f . To solve $L(H_f) = 0$ by the Galerkin method, a trial solution

$$H_f(x,y,t) = \sum_{i=1}^n N_i(x,y) H_i(t) = [N]\{H_f\} \quad (55)$$

is assumed where

n = the number of nodal points,

N_i = the shape function, and

H_i = an $n \times 1$ column matrix denoting the nodal values of H_f .

The approximating function, $H_f(x,y,t)$, will be an exact solution of Equation (19) only if $L(H_f) = 0$. Orthogonality of $L(H_f)$ to all the shape functions $N_i(x,y)$ requires that

$$\int L [H_f(x,y,t)] N_i(x,y) dx dy = 0 \quad i = 1, 2, \dots, n \quad (56)$$

Substituting for $L(H_f)$ from Equation 54 and Equation 55 into Equation 56 and integrating by parts using Green's formula yields

$$\begin{aligned}
& \iint [N]Q_f dx dy + \iint C_4[N][N]\left(\frac{\partial H_s}{\partial t}\right) dx dy - \iint C_3[N][N]\left(\frac{\partial H_f}{\partial t}\right) dx dy \\
& + \iint [N_s](C_1\frac{\partial H_f}{\partial x})l_x dS - \iint \frac{\partial}{\partial x} [N] \frac{\partial}{\partial x} (C_1 H_f) dx dy \\
& + \iint [N_s](C_2\frac{\partial H_f}{\partial y})l_y - \iint \frac{\partial}{\partial y} [N] \frac{\partial}{\partial y} (C_2 H_f) dx dy = 0
\end{aligned} \tag{57}$$

where l_x and l_y are directional cosines. From Equation 55,

$$\frac{\partial H_f}{\partial x} = \{H_f\} \frac{\partial [N]}{\partial x} \tag{58}$$

and

$$\frac{\partial H_f}{\partial y} = \{H_f\} \frac{\partial [N]}{\partial y} \tag{59}$$

Replacing $\partial H_f/\partial x$ and $\partial H_f/\partial y$ in Equation 57 gives

$$\begin{aligned}
& \iint (C_1\{H_f\} \frac{\partial}{\partial x} [N] \frac{\partial}{\partial x} [N]) dx dy + \iint (C_2\{H_f\} \frac{\partial}{\partial y} [N] \frac{\partial}{\partial y} [N]) dx dy \\
& + \iint C_3[N][N]\left(\frac{\partial H_f}{\partial t}\right) dx dy - \iint C_4[N][N]\left(\frac{\partial H_s}{\partial t}\right) dx dy \\
& - \iint Q_f [N] dx dy - \iint q [N_s] dS = 0
\end{aligned} \tag{60}$$

Equation 60 can be written in matrix form as

$$[S]\{H_f\} + [BK]\left\{\frac{\partial H_f}{\partial t}\right\} - [BS]\left\{\frac{\partial H_s}{\partial t}\right\} - \{F\} = 0 \tag{61}$$

where

$$[S]_e = \iint (C_1 [N_x^i]^2 + C_2 [N_y^i]^2) dx dy \quad (62)$$

$$[BK]_e = \iint (C_3 [N][N]) dx dy \quad (63)$$

and

$$[BS]_e = \iint (C_4 [N][N]) dx dy \quad (64)$$

are $n \times n$ matrices; and

$$[F]_e = \iint (Q_f [N]) dx dy + \iint q [N_s] ds \quad (65)$$

is a vector.

In Equation 62,

$$N_x^i = \frac{\partial [N]}{\partial x} \quad \text{and} \quad N_y^i = \frac{\partial [N]}{\partial y}$$

The last term in Equation 65 takes care of the natural boundary conditions. This term incorporates the Neumann boundary condition for fresh-water seepage into the aquifer. This term disappears when the fresh-water flux per unit length of a boundary element is zero.

Equation 21 describing the salt-water flow can be rewritten with the aid of Equation 22 to give

$$\frac{\partial}{\partial x} [C_5 \frac{\partial H_s}{\partial x}] + \frac{\partial}{\partial y} [C_6 \frac{\partial H_s}{\partial y}] + Q_s - C_7 \frac{\partial H_s}{\partial t} + C_8 \frac{\partial H_f}{\partial t} = 0 \quad (66)$$

where

$$C_5 = K_x n,$$

$$C_6 = K_y n,$$

$$C_7 = \theta_s \alpha_s, \text{ and}$$

$$C_8 = \theta_s \alpha_f.$$

Utilizing the procedure followed to arrive at Equation 61, the finite-element matrix equation for salt-water flow is

$$[S]\{H_S\} + [BK]\left\{\frac{\partial H_S}{\partial t}\right\} - [BS]\left\{\frac{\partial H_f}{\partial t}\right\} = \{F\} \quad (67)$$

where

$$[S]_e = \iint (C_5[N_x']^2 + C_6[N_y']^2) \, dx dy \quad (68)$$

$$[BK]_e = \iint C_7[N][N] \, dx dy \quad (69)$$

and

$$[BS]_e = \iint C_8[N][N] \, dx dy \quad (70)$$

are $n \times n$ matrices; and

$$[F]_e = \iint Q_s[N] \, dx dy + \iint q[N_s] \, ds \quad (71)$$

is a vector. The last term in Equation 71 goes to zero when there is no salt-water flux at the boundary.

Equations 61 and 67 must be integrated with respect to time to achieve the unsteady state head distributions in an unconfined aquifer. The time derivative can be approximated using either finite-difference or finite-element methods.

Convergence to a reasonable solution can result only if a stable numerical integration scheme is chosen to approximate the time derivative. It has been observed that implicit finite-difference approximations lead to stable, accurate results. The coefficient matrices in Equations 61 and 67 are dependent on the unknown hydraulic heads. An iterative solution scheme is introduced to take care of the non-linearity.

Following Pinder and Page (1976), Equation 61 can be written in time to yield

$$\begin{aligned}
 & (1-\theta)[S]_{n+1/2} \{H_f\}_n + \theta [S]_{n+1/2}^m \{H_f\}_{n+1}^{m+1} \\
 & + \frac{1}{\Delta t} [BK]_{n+1}^m (\{H_f\}_{n+1}^{m+1} - \{H_f\}_n) - \frac{1}{\Delta t} [BS]_{n+1}^m (\{H_s\}_{n+1}^{m+1} - \{H_s\}_n) \\
 & - \{F\} = 0
 \end{aligned} \tag{72}$$

where θ is the time weighting parameter. For $\theta = 0$, Equation 72 is solved explicitly in time. With $\theta = 1$, a fully implicit solution is achieved, whereas $\theta = 0.5$ yields a Crank-Nicholson formulation. The indices m and n are the iteration level and the time step respectively.

Rearrangement of Equation 72 gives

$$\begin{aligned}
 & ((1-\theta)[S]_{n+1/2} - \frac{1}{\Delta t} [BK]_{n+1}^m) \{H_f\}_n + (\theta[S]_{n+1/2}^m + \frac{1}{\Delta t} [BK]_{n+1}^m) \\
 & \{H_f\}_{n+1}^{m+1} - \frac{1}{\Delta t} [BS]_{n+1}^m (\{H_s\}_{n+1}^{m+1} - \{H_s\}_n) - \{F\} = 0.
 \end{aligned} \tag{73}$$

Following a similar procedure, Equation 67 can be approximated to give

$$\begin{aligned}
 & ((1-\theta)[S]_{n+1/2} - \frac{1}{\Delta t} [BK]_{n+1}^m) \{H_s\}_n + (\theta[S]_{n+1/2}^m + \frac{1}{\Delta t} [BK]_{n+1}^m) \\
 & \{H_s\}_{n+1}^{m+1} - \frac{1}{\Delta t} [BS]_{n+1}^m (\{H_f\}_{n+1}^{m+1} - \{H_f\}_n) - \{F\} = 0.
 \end{aligned} \tag{74}$$

Equations 73 and 74 are solved simultaneously at a time step, and at each iteration the coefficient matrices are recomputed. Iterations

terminate when the changes in heads for two successive iterations are within a prescribed tolerance.

The freshwater and saltwater head distributions in an unconfined aquifer are described by Equations 73 and 74. The elevation of the interface can be computed from Equation 22 at the end of each time step.

Confined Aquifers

The fresh-water flow equation for confined aquifers, Equation 52, can be rewritten with the aid of Equation 22 to yield

$$\frac{\partial}{\partial x} \left[C_1 \frac{\partial H_f}{\partial x} \right] + \frac{\partial}{\partial y} \left[C_2 \frac{\partial H_f}{\partial y} \right] + Q_f - S_1 \frac{\partial H_f}{\partial t} + S_2 \frac{\partial H_s}{\partial t} = 0 \quad (75)$$

where

$$C_1 = K_x(B - \eta),$$

$$C_2 = K_y(B - \eta),$$

$$S_1 = S_s(B - \eta) + \theta \alpha_f, \text{ and}$$

$$S_2 = \theta \alpha_s.$$

Proceeding in a manner similar to that for unconfined aquifers, the finite-element matrix equation for fresh-water flow in a confined aquifer is

$$[S] \{H_f\} + [B] \left\{ \frac{\partial H_f}{\partial t} \right\} - [B1] \left\{ \frac{\partial H_s}{\partial t} \right\} - [F] = 0 \quad (76)$$

where

$$[S]_e = \iint (C_1 [N'_x]^2 + C_2 [N'_y]^2) dx dy \quad (77)$$

$$[B]_e = \iint S_1 [N][N] dx dy \quad (78)$$

and

$$[B1]_e = \iint S_2 [N][N] \, dx dy \quad (79)$$

are $n \times n$ matrices; and

$$\{F\}_e = \iint Q_f [N] \, dx dy + \iint q [N_s] \, dS \quad (80)$$

is a vector. In Equation 77,

$$N'_x = \frac{\partial [N]}{\partial x} \quad \text{and} \quad N'_y = \frac{\partial [N]}{\partial y} .$$

By making use of Equation 22, the salt-water flow equation for confined aquifers (Equation 53) becomes

$$\frac{\partial}{\partial x} [C_3 \frac{\partial H_s}{\partial x}] + \frac{\partial}{\partial y} [C_4 \frac{\partial H_s}{\partial y}] + Q_s - S_1 \frac{\partial H_s}{\partial t} + S_2 \frac{\partial H_f}{\partial t} = 0 \quad (81)$$

where

$$C_3 = K_{xn},$$

$$C_4 = K_{yn},$$

$$S_1 = S_{sn} + \theta \alpha_s, \text{ and}$$

$$S_2 = \theta \alpha_f.$$

The finite-element matrix equation for salt-water flow in a confined aquifer is

$$[S] \{H_s\} + [B] \left\{ \frac{\partial H_s}{\partial t} \right\} - [B1] \left\{ \frac{\partial H_f}{\partial t} \right\} - [F] = 0 \quad (82)$$

where

$$[S]_e = \iint (C_3 [N'_x]^2 + C_4 [N'_y]^2) \, dx dy \quad (83)$$

$$[B]_e = \iint S_1 [N][N] \, dx dy \quad (84)$$

and

$$[B1]_e = \iint S_2 [N][N] \, dx dy \quad (85)$$

are $n \times n$ matrices; and

$$[F]_e = \iint Q_S [N] \, dx dy + \iint q [N_S] \, dS \quad (86)$$

is a vector.

Approximation of the time derivative in Equation 76 yields

$$\begin{aligned} & ((1-\theta)[S]_{n+1/2} - \frac{1}{\Delta t} [B]_{n+1}^m) \{H_f\}_n \\ & + (\theta[S]_{n+1/2}^m + \frac{1}{\Delta t} [B]_{n+1}^m) \{H_f\}_{n+1}^{m+1} - \frac{1}{\Delta t} [B1]_{n+1}^m \\ & (\{H_s\}_{n+1}^{m+1} - \{H_s\}_m) - \{F\} = 0. \end{aligned} \quad (87)$$

The time derivative in Equation 82 can also be approximated to yield

$$\begin{aligned} & ((1-\theta)[S]_{n+1/2} - \frac{1}{\Delta t} [B]_{n+1}^m) \{H_s\}_n + (\theta[S]_{n+1/2}^m + \frac{1}{\Delta t} [B]_{n+1}^m) \\ & \{H_s\}_{n+1}^{m+1} - \frac{1}{\Delta t} [B1]_{n+1}^m (\{H_f\}_{n+1}^{m+1} - \{H_f\}_n) - \{F\} = 0 \end{aligned} \quad (88)$$

Equations 87 and 88 can be solved simultaneously to yield the head distributions in a confined aquifer. The change in interface elevation can be computed from Equation 22 at the end of every time increment.

Other Aspects of the Finite-Element Technique

According to Pinder and Frind (1972), implementation of the Galerkin finite-element approximation is heavily dependent on the weighting functions. The functions are continuous polynomials and are defined at each node. The polynomial to be chosen depends on the shape of the boundaries.

The flow domain, in this model, is divided into quadratic, triangular elements with six nodes per element. An appropriate polynomial is chosen to define the weighting functions. The shape functions and derivatives of the shape functions are given by Segerlind (1976) and Zienkiewicz (1971).

The element matrices arising in the finite-element equations have to be evaluated numerically using an integration scheme. A Gaussian quadrature integration technique is employed to integrate the elemental matrices and obtain the coefficients. The integrated element matrices are inserted into a global matrix. The force vector, F , is computed if a source or sink exists.

The resulting system of equations is solved by a backward Gauss elimination method to yield the change in the dependent variable at each node for each time interval. The new interface elevation is evaluated at the end of every time step. The computations are terminated when either

- a. the change of head between two successive time intervals is less than a predetermined tolerance, or
- b. the sum of the time increments equals the maximum time specified.

Finite-Element Computer Model

The computer program is capable of predicting the interface elevations in confined or unconfined aquifers. The program solves the fresh-water and salt-water flow equations and then updates the hydraulic heads and the interface elevation.

The program has been developed to handle steady-state or transient variations of the head distributions in an aquifer. In the case of an unconfined aquifer, the program can also incorporate the effects of capillarity on the specific yield and the water table elevation.

The programming language used in the development of this program is FORTRAN IV. Input data requirements and formats are described in Appendix A and the computer program is summarized in Appendix B. A listing of the source codes is included in Appendix C.

CHAPTER V

TESTING OF THE NUMERICAL MODEL

The numerical model developed in the preceding chapter has to be verified against existing analytical or experimental models before it can be used to simulate field conditions. The computer program has to be tested for 1) its ability to simulate the movement of the fresh-water/salt-water interface, 2) its effectiveness in accounting for capillary flow effects in the unsaturated zone, and 3) its capability in tracking the movement of the salt-water wedge in a coastal aquifer.

The first part of the model can be verified using Sahni's (1972) observations for salt-water coning below a fresh-water discharge well in a phreatic aquifer. The physical model was constructed to study the effects of discharge and well geometry on the critical rise in upconing. By using the numerical model to simulate the physical experiment, the ability of the model to predict the shape and position of the dynamic interface can be established.

The effect of capillarity on the water table and specific yield will be investigated on the basis of experimental observations made by Ortiz, et al. (1978). Their physical model was developed to study the effects of capillarity and specific storage on the growth of ground-water mounds beneath a surface recharge area. The experimental data will be used to demonstrate the ability of the numerical model to account for the capillary fringe in phreatic aquifers.

The above two applications will fulfill the primary objectives of this research. The versatility of the model can be demonstrated if it can track the transient sea-water wedge in a coastal aquifer. This part of the model will be tested against Henry's (1959) analytical model for salt-water intrusion into a confined coastal aquifer.

Upconing in an Unconfined Aquifer

Sahni (1972) simulated salt-water coning beneath a well discharging fresh-water using a pie-shaped model (Figure 6). The model was constructed in such a way as to preserve radial symmetry in the homogeneous, isotropic medium. The radial walls of the pie-shaped sector formed an included angle of 15° . The radius of the sector was 122 cm and it was 61 cm high. The radius of the fresh-water well was 2.38 cm and its base was 13.5 cm below the top of the model.

The fluids used to simulate fresh-water and salt-water were chosen so that a well defined interface existed between the two fluids. The homogeneous, isotropic medium was simulated by glass beads 2.5 mm in diameter.

The well radius and the outer perimeter of the pie-shaped sector were fixed and the hydraulic heads at the outer boundary held constant. After noting down the initial positions of the interface and the phreatic surface, fresh-water withdrawal was started. Finally, after allowing sufficient time for the system to attain steady state, the positions of the interface and free surface were recorded at several radial distances from the well axis.

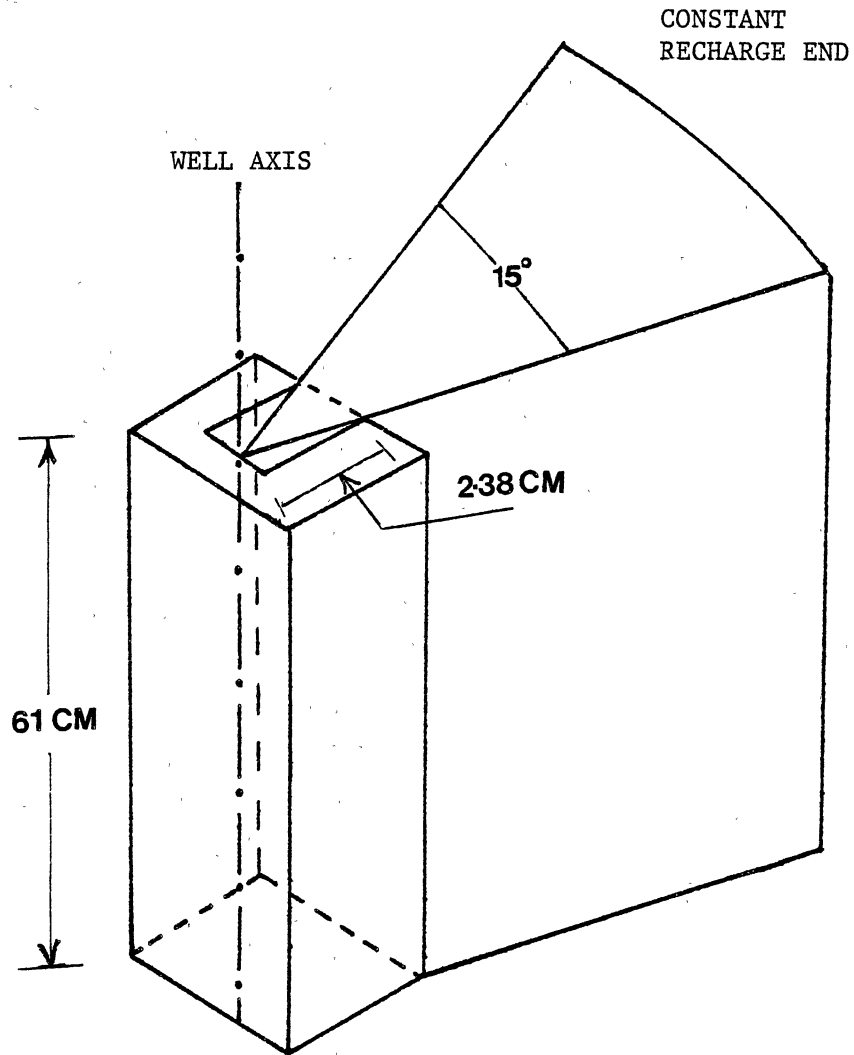


Figure 6. Sahni's Experimental Model for Salt-Water Upconing in a Phreatic Aquifer

Numerical Analysis of the Physical Model

In order to perform numerical simulation of Sahni's physical model, a finite-element mesh was constructed by Layla (1980) so that it closely resembled the physical model. The geometry and properties of the finite-element system and the physical model are shown in Figure 7.

The numerical model was first tested for three cases: (1) steady state flow with a nodal discharge, (2) steady state flow with an areal discharge, and (3) transient flow with an areal discharge. These cases were investigated using the finite-element mesh depicted in Figure 19 (Appendix F). The input data and the results of the numerical analyses for these three cases are listed in Tables I to III (Appendix D) and X to XII (Appendix E), respectively. The experimental observations made by Sahni are also listed in Table IX (Appendix E).

The results of Cases 1 and 2 are illustrated in Figure 8. The large errors near the well axis for a nodal sink can be attributed to the fact that in the numerical solution the fresh-water is discharged out from a point sink whereas in the experimental model the discharge is from a well of radius 2.38 cm. The reasoning is corroborated by the comparatively better results obtained by using an areal sink. The results would have more closely matched the physical model if the whole well could have been simulated instead of just a cross-section.

Figure 9 depicts the results from the numerical model for Case 3. The numerical model is accurate except within the area of the well radius where the head changes are extremely sensitive to the discharge velocities. Even so, the fresh-water elevations are essentially identical and the discrepancy in interface elevations is restricted to regions

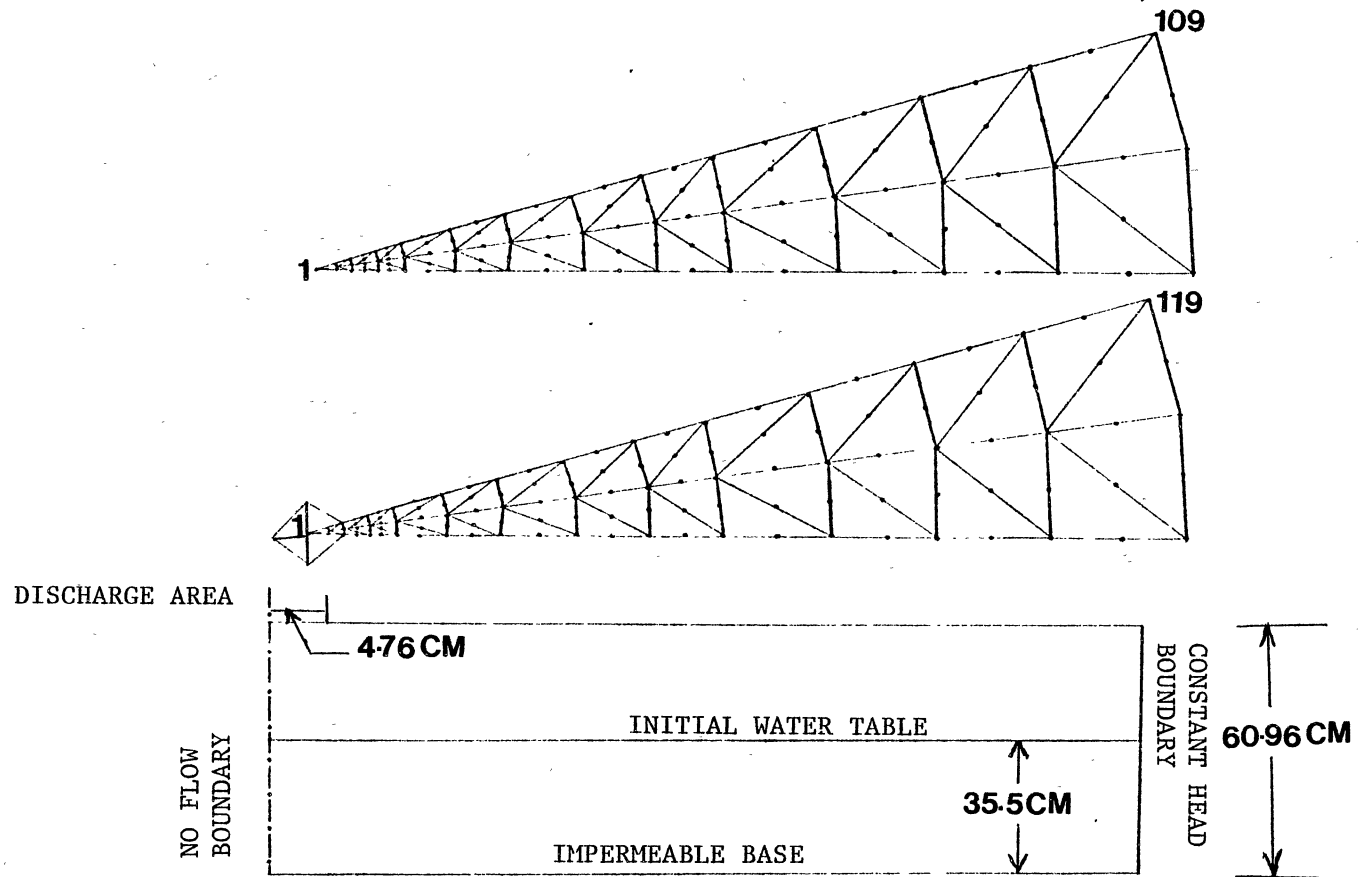


Figure 7. Finite Element Mesh Simulation of Sahni's Physical Model

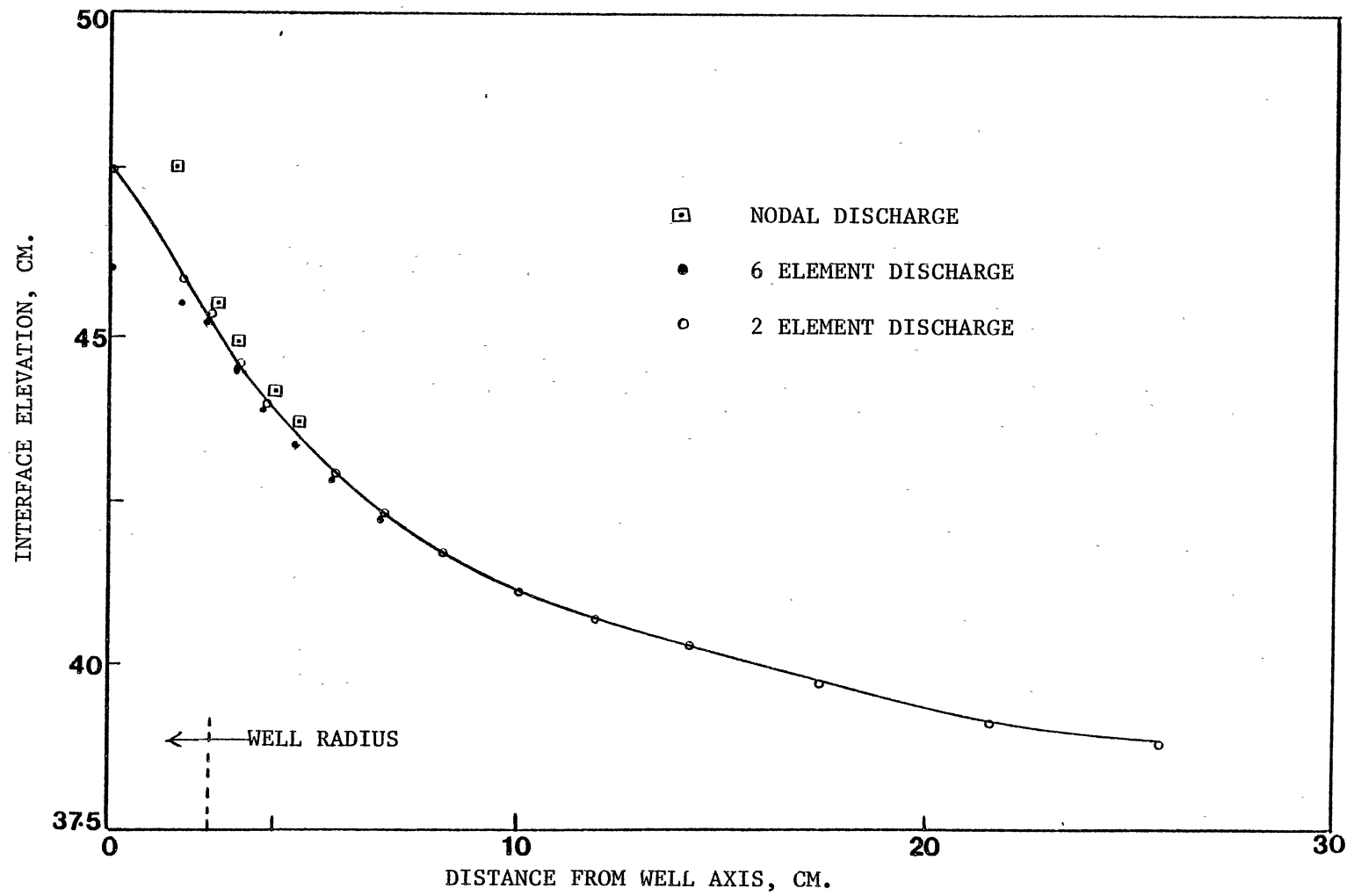


Figure 8. Steady State Solutions Employing Different Mesh Layouts

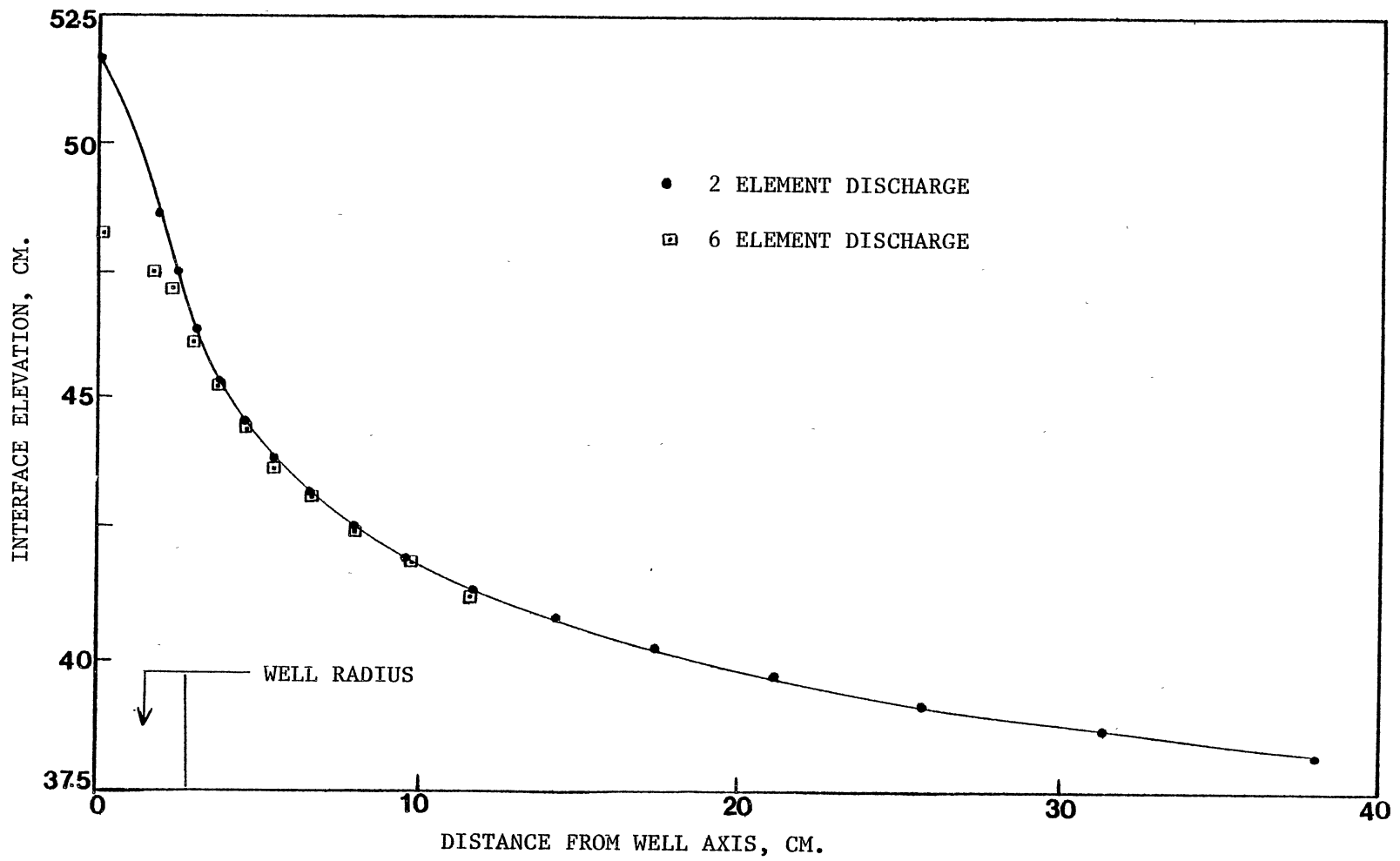


Figure 9. Transient Numerical Analyses Employing Different Mesh Layouts

near the well axis. This can be explained by the fact that, unlike the physical model, radial symmetry around the well axis is not preserved. In the physical model the well is 13.5 cm deep whereas the numerical model is built around the assumption of a well situated at ground-level. The Dupuit-Forchheimer assumptions are also not valid within the well radius as vertical flow components are not negligible.

The finite-element mesh configuration shown in Figure 19 (Appendix F) does not preserve radial symmetry around the well axis. The interface elevation, obtained from the numerical model, would have more closely matched the physical data if the mesh were to be reoriented to retain a certain amount of radial symmetry around the well axis. The finite-element mesh layout depicted in Figure 20 (Appendix F) is constructed so as to ensure a reasonable degree of radial symmetry around the well axis. Cases 4 and 5 are similar to Cases 2 and 3, respectively, except that they utilize the new mesh configuration to simulate Sahni's physical model. The corresponding input data and results for Cases 4 and 5 are given in Tables IV and V (Appendix D) and Tables XIII and XIV (Appendix E), respectively. Comparison of experimental results and the solution obtained from the steady state numerical analysis is presented in Figure 10. The transient numerical solution in Figure 11 matches the physical model very accurately except around the well axis where there is some deviation from the experimental results.

This new mesh layout could probably have given better results if 24 elements were situated in the discharge well area instead of the 6 elements which were used. However, the results obtained from the numerical model are accurate enough to suggest that this part of the numerical model was valid.

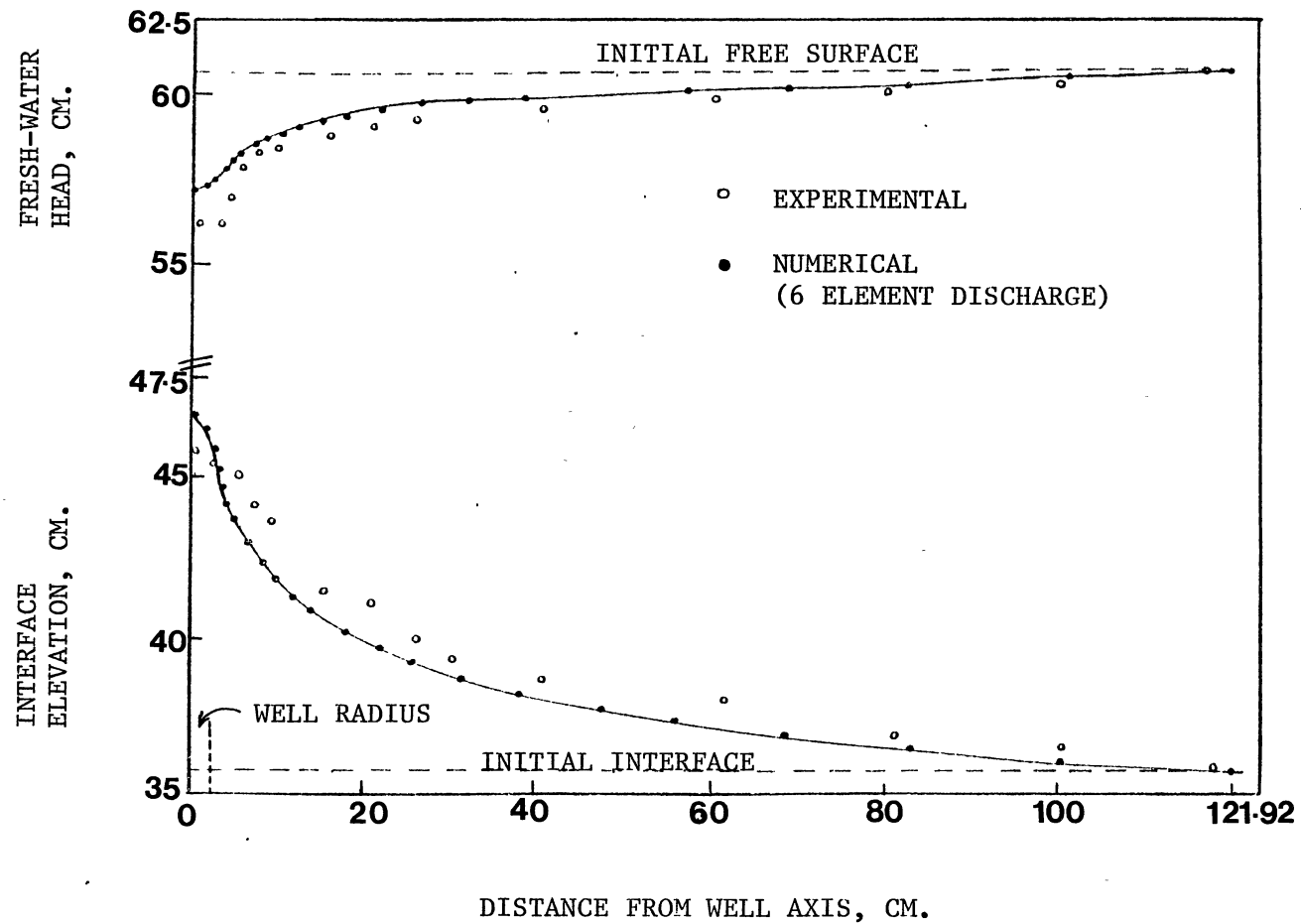


Figure 10. Experimental Observations versus Steady State Solution Obtained Using the Expanded Mesh

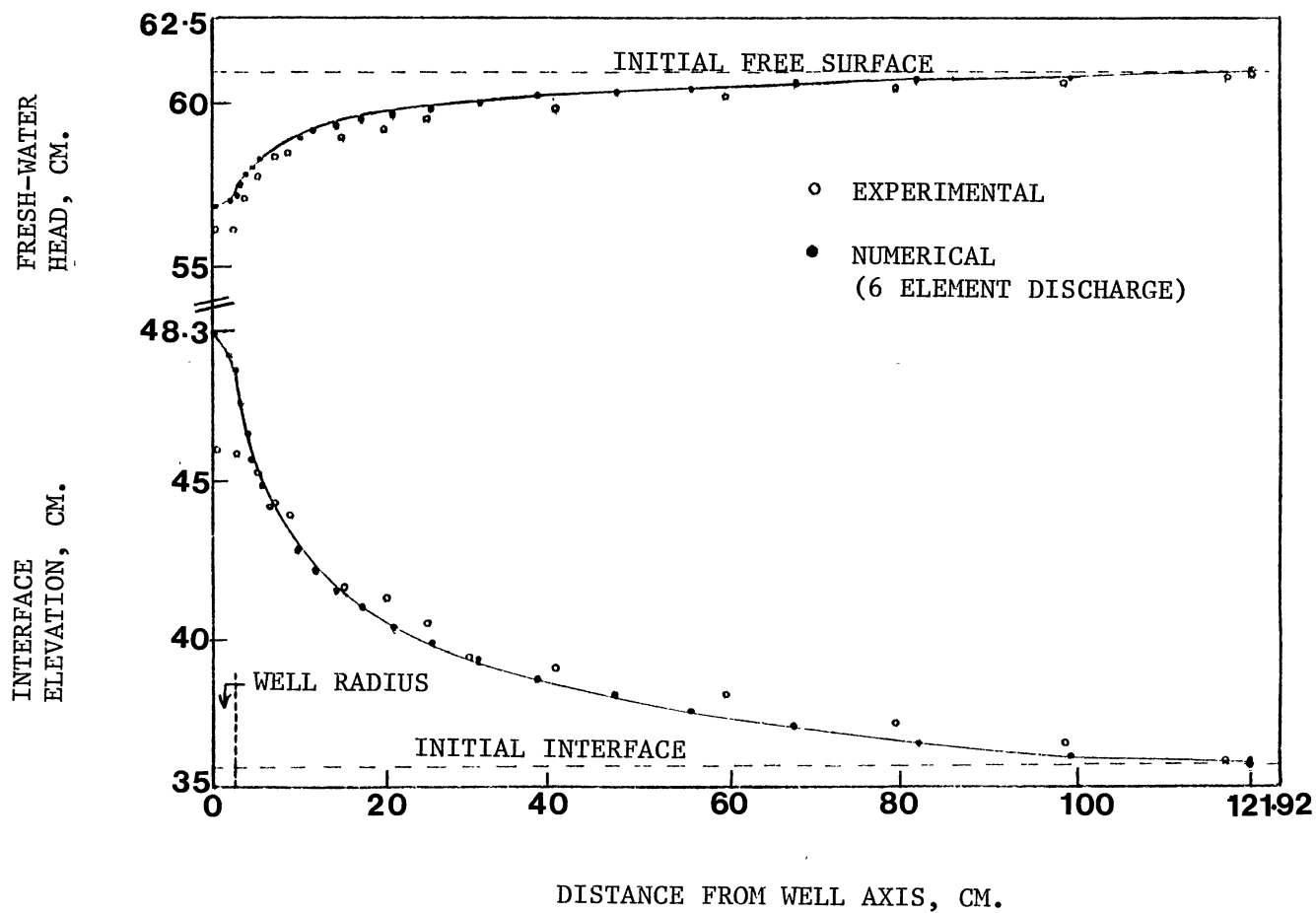


Figure 11. Experimental Results versus Transient Analysis of the Numerical Model Obtained Using the Expanded Mesh

Effect of Capillarity on Ground-Water Mounds

Earlier researchers have assumed that (1) the percolation rate is vertically downwards until it encounters the phreatic surface, (2) the water table encompasses the flow region, and (3) the fillable pore space is constant and equal to the drainable porosity, which amounts to neglecting the effects of capillarity.

In the 1978, Ortiz, et al. constructed a physical model to study the growth of ground-water mounds under artificial recharge areas in the presence of capillary pressure. The growth of ground-water mounds as a result of vertical percolation from surface recharge sites is illustrated in Figure 12. The physical model was a narrow flume approximately 365 cm long, 40 cm high and 5.1 cm wide, containing a porous medium. A constant recharge rate was established at the soil surface with the help of a recharge simulator. The initial condition for each recharge test was a horizontal water table elevation. After initiation of a constant recharge rate, Ortiz, et al. (1978) recorded the development of the ground water mound at pre-established time intervals.

Numerical Analysis of Physical Model

The finite-element mesh (Figure 13) was used to simulate the physical system used by Ortiz, et al, in their investigations on the effect of capillarity on ground-water mounds. It was possible to construct a very accurate mesh because of the way in which the physical model was constructed. The input data for the numerical analysis and the results are listed in Table VII (Appendix D) and Table XVII

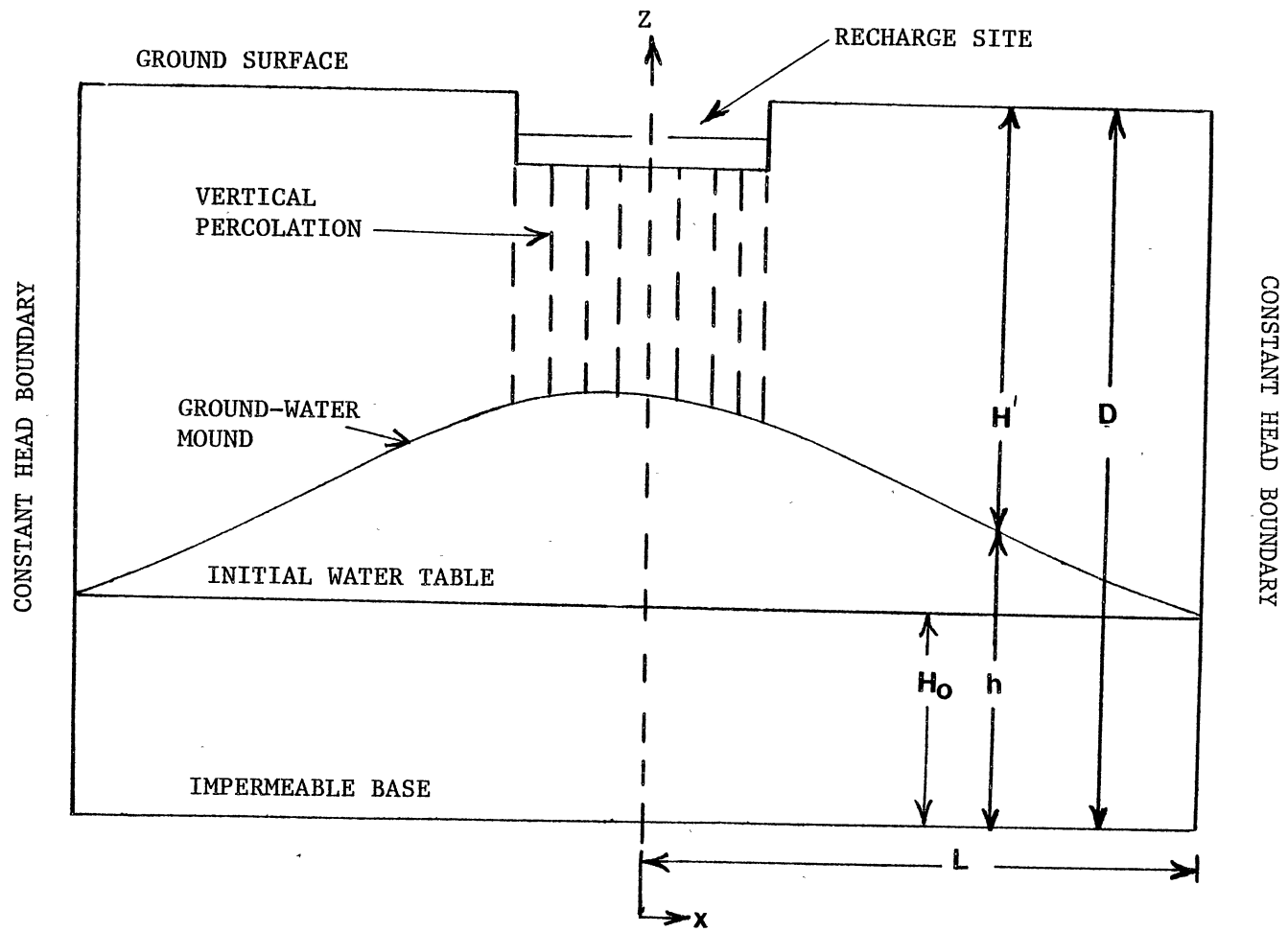


Figure 12. Ground-Water Mounding due to Vertical Percolation from Surface Recharge Areas

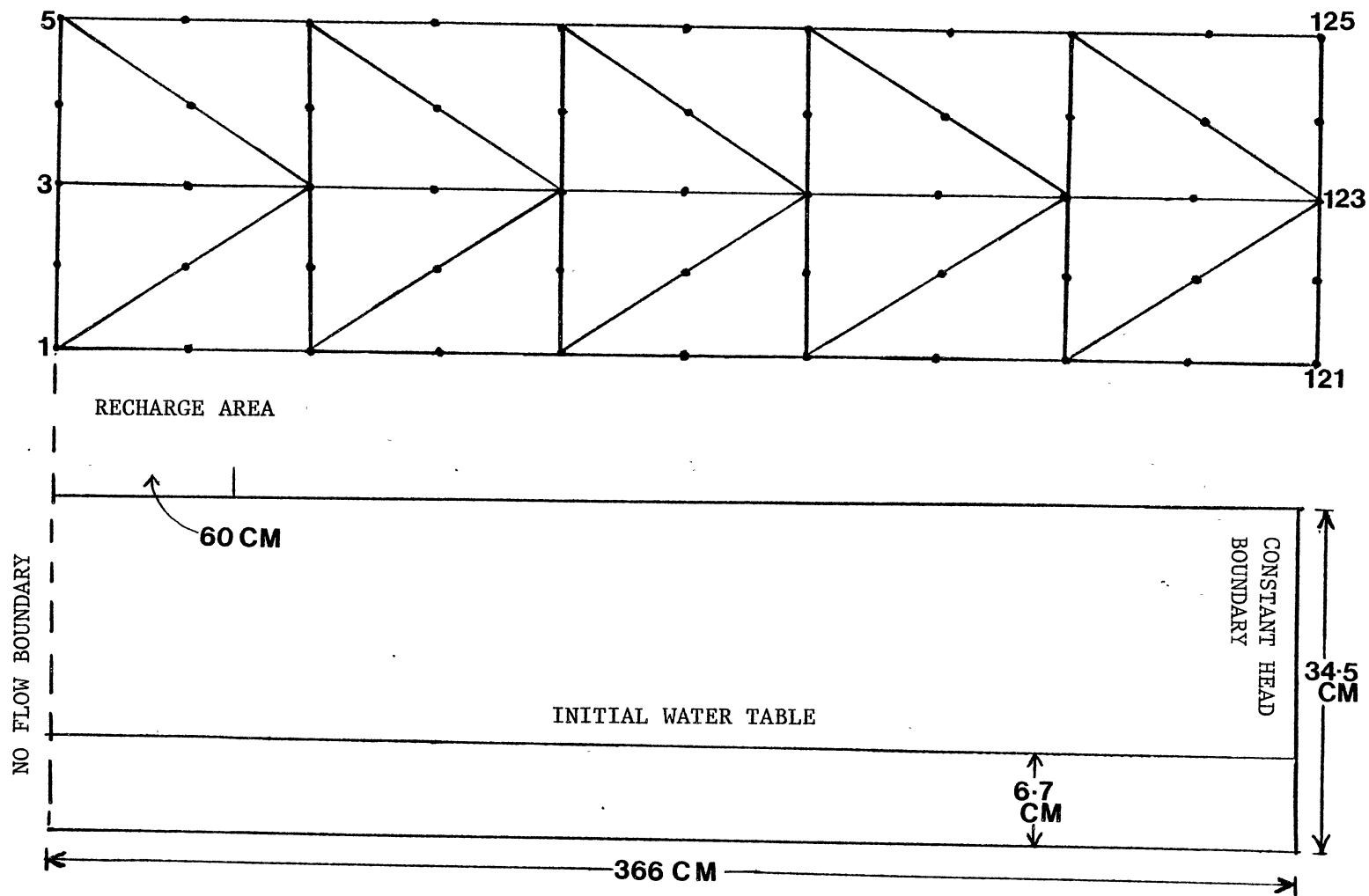


Figure 13. Finite Element Mesh Simulation of the Experimental Model of Ortiz, et al.

(Appendix E) respectively. A detailed sketch of the mesh layout used in the numerical simulation is shown in Figure 21 (Appendix F). The input data used in simulating the physical model, without the influence of capillarity, is shown in Table VIII (Appendix D) and the numerical solution is listed in Table XVIII (Appendix E).

The results of the physical and numerical models are shown in Figure 14. The results of the numerical model simulation are very good and the slight deviations from the experimental values can be attributed to the various simplifying assumptions which were incorporated into the numerical model. Comparison of the numerical solutions with and without the influence of capillarity on the ground-water mounds are shown in Figure 15 and demonstrated that the effects of capillarity significantly influence the development of ground-water mounds.

Salt-Water Intrusion in a Confined Coastal Aquifer

This case was investigated on the basis of Henry's (1959) analytical model and using Reddell and Sunada's (1970) numerical data. Sea-water intrudes into a confined, coastal aquifer (Figure 16) when fresh-water flows into the sea. Salt-water encroachment will be contained only when the fresh-water flow becomes steady.

Utilizing Darcy's law and the Dupuit-Forchheimer principle, the specific discharge of fresh-water per unit width of coast is given as

$$q = Ky \frac{dh^*}{dx} \quad (89)$$

where

K = hydraulic conductivity,

y = distance from impermeable confining layer to the interface and

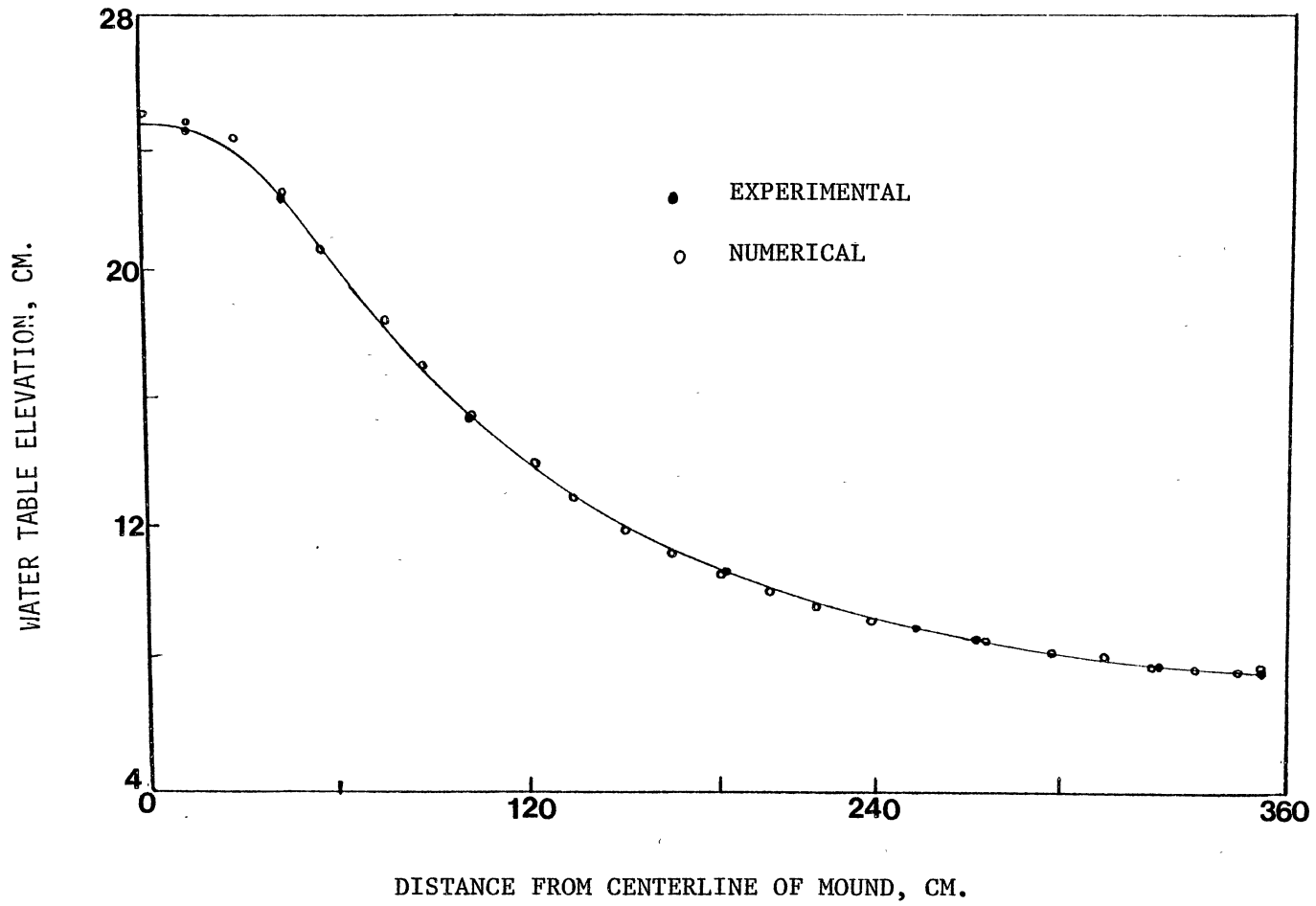


Figure 14. Experimental Results versus Numerical Solution

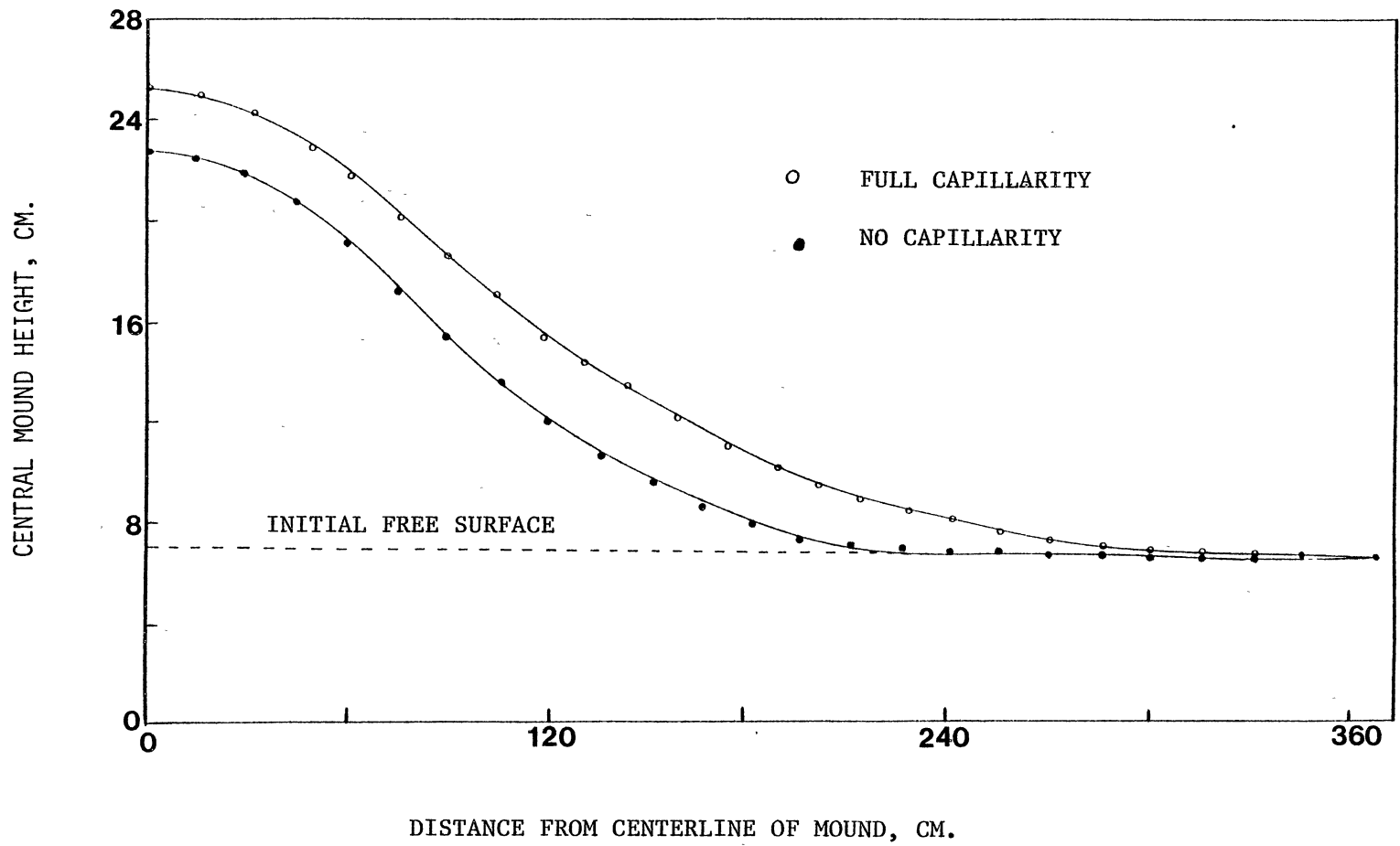


Figure 15. Comparison of Numerical Results with and without the Influence of Capillary Effects

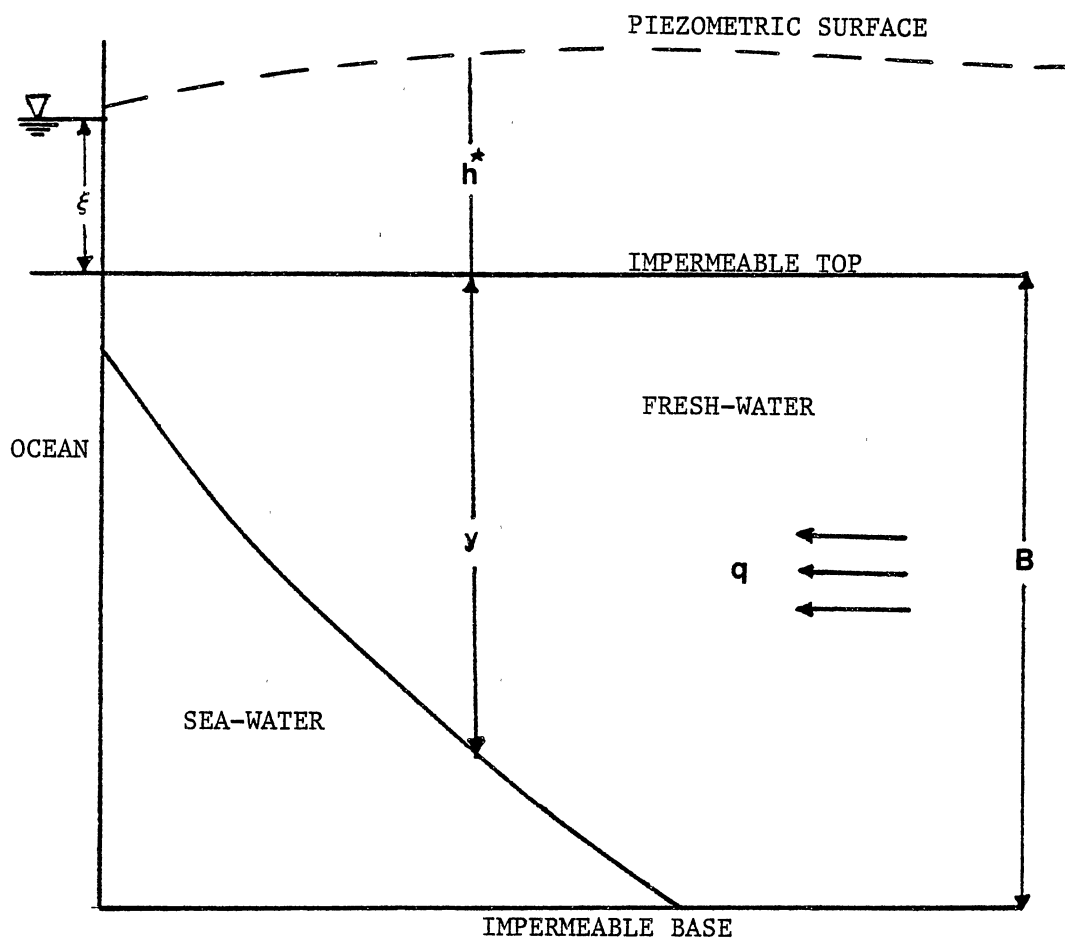


Figure 16. Sea-Water Wedge in a Confined Coastal Aquifer

h^* = piezometric head.

Pressure balance of the salt-water fresh-water interface, in the homogeneous, isotropic medium, requires that

$$y = \frac{\rho_f}{\Delta\rho} h^* - \frac{\rho_s}{\Delta\rho} \xi \quad (90)$$

where

ρ_f = density of fresh-water,

ρ_s = density of salt-water,

ξ = height of ocean above top of aquifer, and

$$\Delta\rho = \rho_s - \rho_f. \quad (91)$$

Substituting Equation 90 in Equation 89 yields

$$q = K \left(\frac{\rho_f}{\Delta\rho} h^* - \frac{\rho_s}{\Delta\rho} \xi \right) \frac{dh^*}{dx} \quad (92)$$

which can be rearranged to

$$\left(h^* - \frac{\rho_s}{\rho_f} \xi \right) dh^* = \frac{q\Delta\rho}{\rho_f K} dx. \quad (93)$$

Upon integration,

$$\frac{(h^*)^2}{2} - \frac{\rho_s}{\rho_f} \xi h^* = \frac{q\Delta\rho}{\rho_f K} x + C \quad (94)$$

where C is a constant of integration.

Henry (1959) found that for a vertical outflow face

$$y(x=0) = \frac{0.741 q \rho_f}{K\Delta\rho} \quad (95)$$

Substituting Equation 95 in Equation 90 gives

$$h^*(x = 0) = \frac{0.741q}{K} + \frac{\rho_s}{\rho_f} \xi \quad (96)$$

Equation 96 can be placed in Equation 94 to yield the constant of integration, or

$$C = \frac{\left(\frac{0.741q}{K} + \frac{\rho_s}{\rho_f} \xi\right)^2}{2} - \frac{\rho_s}{\rho_f} \xi \left(\frac{0.741q}{K} + \frac{\rho_s}{\rho_f} \xi\right) \quad (97)$$

After simplification,

$$C = \frac{\left(\frac{0.741q}{K}\right)^2 - \left(\frac{\rho_s}{\rho_f} \xi\right)^2}{2} \quad (98)$$

Equations 98 and Equation 94 can be combined to yield

$$h^* = \left[\frac{2q\Delta\rho}{K\rho_f} x + \left(\frac{0.741q}{K}\right)^2 \right]^{1/2} + \frac{\rho_s}{\rho_f} \xi \quad (99)$$

Finally, substituting Equation 99 in Equation 90 gives

$$y^2 = \frac{2q\rho_f}{K\Delta\rho} x + \left(\frac{0.741 q \rho_f}{K\Delta\rho}\right)^2 \quad (100)$$

Equations 99 and 100 were solved analytically using Reddell and Sunada's (1970) data, and the results are listed in Table XV (Appendix E). The finite-element mesh representation of the analytical model is shown in Figure 17. The mesh is divided into 20 elements with 63 nodes so that it can simulate a confined aquifer, 160 cm long and 1 cm wide. The input data and the results of numerical analysis using Figure 22 (Appendix F) are listed in Table VI (Appendix D) and Table XVI (Appendix E) respectively. The analytical and numerical results are plotted in Figure 18. It is evident that at steady state, the agreement between the numerical and analytical solutions is very good, except in the

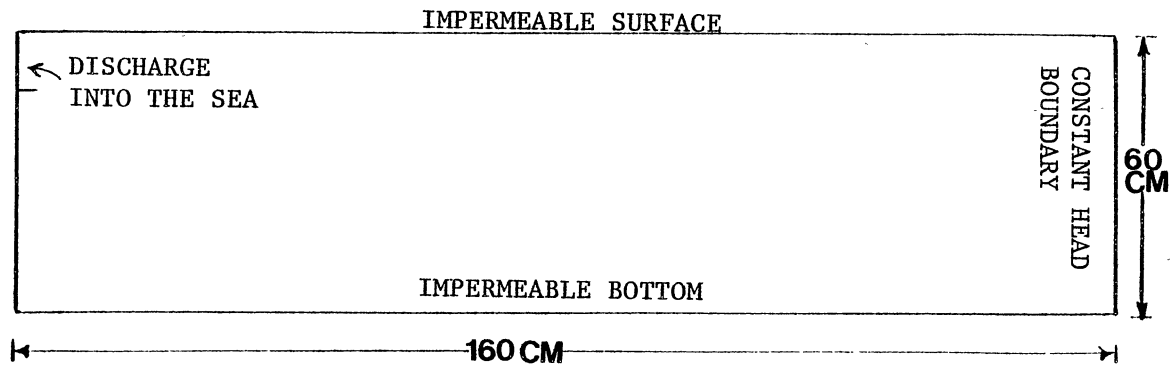
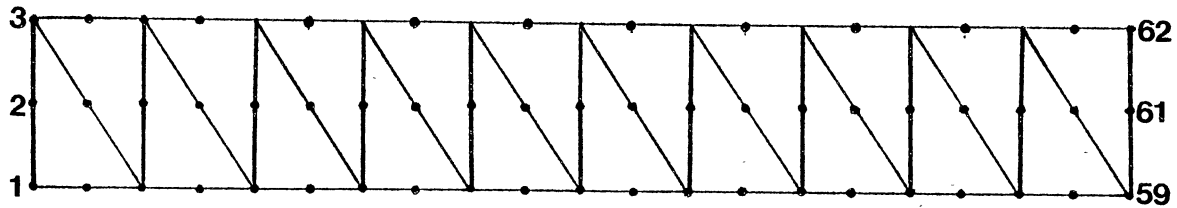


Figure 17. Finite Element Mesh Simulation of the Analytical Model

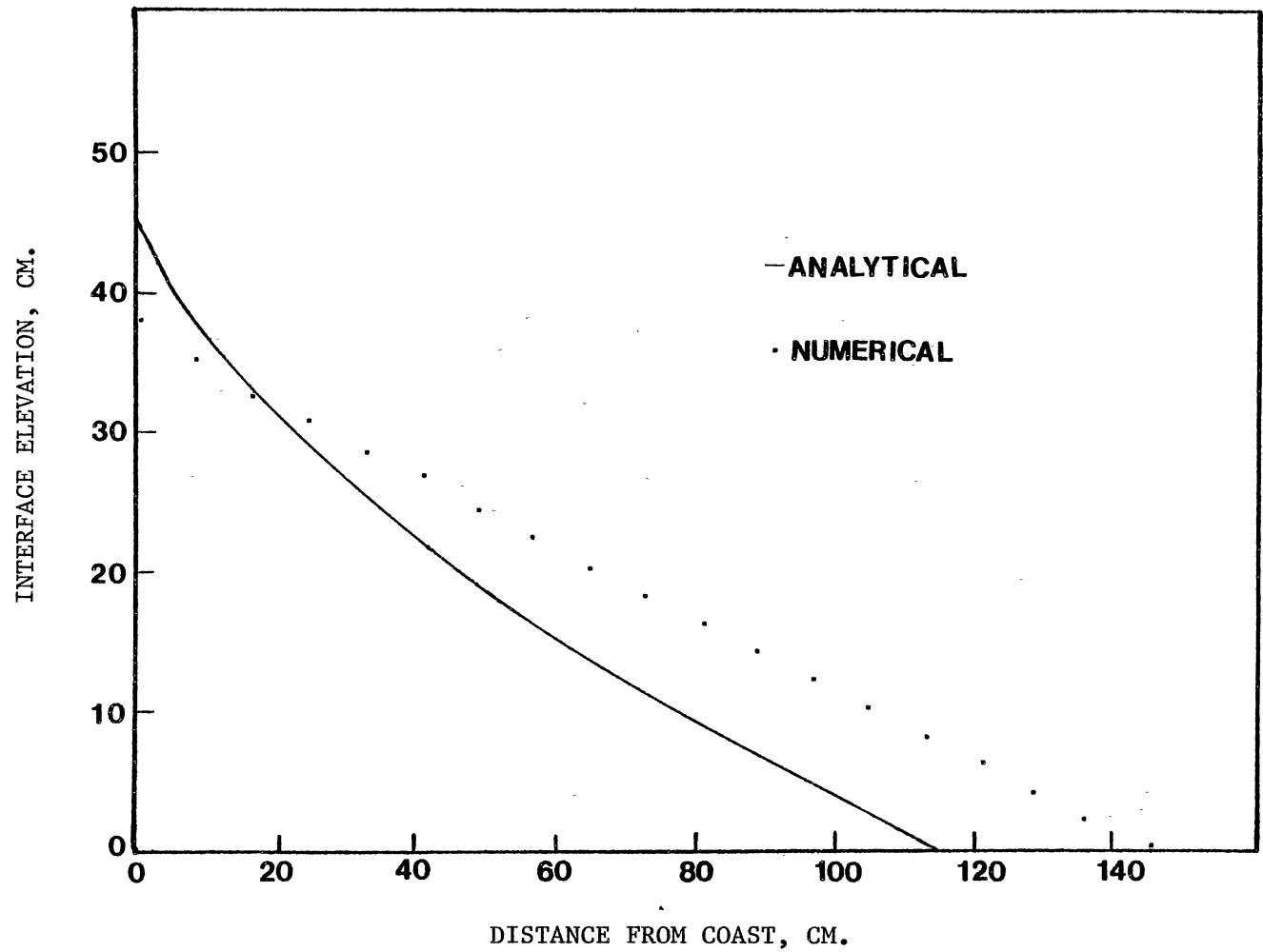


Figure 18. Analytical Solution versus Numerical Results

vicinity of the sea. In the analytical model, the fresh-water discharges into the ocean through a vertical outflow face. This boundary condition cannot be simulated in the numerical model. Hence, large deviations of interface elevation result at the coastline.

The finite-element mesh (Appendix F) used for this problem is not symmetrical along the longitudinal axis and could be an explanation for the discrepancy observed in Figure 18. Better results would be obtained if a symmetrical mesh were used and the spatial distances reduced in the vicinity of the coast. This would thereby establish a relatively smooth gradient, and the interface elevations would approach the analytical model. The boundary condition at the coast where the fresh-water discharges into the sea is extremely difficult to handle numerically due to the presence of an infinite gradient. This can be overcome by placing very small spatial grids near the coast but this would lead to enhanced computational costs.

CHAPTER VI

CONCLUSIONS AND RECOMMENDATIONS

The finite element model, developed and verified in the preceding chapters, has been found to be extremely accurate in its ability to predict the location of the dynamic fresh-water/salt-water interface. Unlike some earlier models, a few simplifying assumptions have been circumvented so as to ensure greater accuracy. For instance, instead of neglecting to consider salt-water hydrodynamics, the simultaneous movement of both fresh water and salt water has been incorporated into the model. Also, the effects of capillary flow and capillary storage on the water table and the specific yield have been taken into account. The contribution of these effects, as shown in the last chapter, significantly influence the growth of ground-water mounds under surface recharge.

An advantage of a two-dimensional areal model is that it can easily accommodate surface sources and/or sinks. Other useful features of the model include the ability to simulate single phase flow or immiscible displacement processes under steady-state or transient conditions and the capacity to include nodal sources and/or sinks.

The transient simulation of the salt-water wedge produced oscillations which showed no indication of dampening out. Mercer and Faust (1977) report that this problem persists even if the element and/or time step sizes are reduced. They suggest a collocation finite element

solution or a finite element approximation of the time derivative to effectively control oscillations in the numerical solution. The finite element approximation uses weighted averages of the time derivatives over the elements to simulate the intrusion of the salt-water wedge. The implementation of either of these techniques is impractical in this research, as it would involve restructuring the whole model from a fundamental basis.

Efficient use of the numerical model can be accomplished if the following guidelines are followed. One important consideration is the need to construct a refined mesh near discontinuities in the physical system to be simulated. Also, the numbering of nodes and elements should be done to minimize band width in the matrix equations. This can be accomplished by utilizing one of the many mesh-generation computer programs available in literature.

The finite element model is not restricted to salt-water/fresh-water systems but can be used to simulate other immiscible displacement problems as well. For example, the numerical model can be used to predict the formation of plumes for light or heavy hydrocarbon systems. The model also might be used to predict the formation of a water cone beneath a producing oil well with a natural water drive. Recovery of oil by water injection can also be simulated. Finally, liquid waste disposal by deep well injection can be modeled if the liquid waste-water system can be assumed to be immiscible.

The computer model was tested for homogeneous, isotropic aquifers. If field and/or laboratory data become available, future work could be directed toward analyzing the performance of the model for heterogeneous, anisotropic aquifers.

REFERENCES

- Bear, J., Hydraulics of Ground Water, McGraw-Hill, New York, 567 p., 1979.
- Bredehoeft, J. D. and G. F. Pinder, "Digital Analysis of Areal Flow in Multiaquifer Groundwater Systems: A Quasi Three-Dimensional Model," *Water Resources Research*, Vol. 6. No. 3, pp. 883-888, June, 1970.
- Brooks, R. H. and A. T. Corey, "Hydraulic Properties of Porous Media," *Hydrology Paper No. 3*, Colorado State University, Fort Collins, Colorado, March, 1964.
- Burdine, N. T., "Relative Permeability Calculations from Pore Size Distribution Data," *Petroleum Trans., AIME*, Vol. 198. pp. 71-78, March, 1953.
- Corey, A. T., "Measurement of Water and Air Permeability in Unsaturated Soil," *Soil Science Society of America Proceedings*, Vol. 21. No. 1, Jan.-Feb., 1957.
- Duke, H. R., "Capillary Properties of Soils-Influence Upon Specific Yield," *Trans. ASAE*, pp. 688-691, 1972.
- Glover, R. E., "The Pattern of Fresh-Water Flow in a Coastal Aquifer," *Journal of Geophysical Research*, Vol. 64. No. 4, pp. 457-459, April, 1959.
- Henry, H. R., "Salt Intrusion into Fresh-Water Aquifers," *Journal of Geophysical Research*, Vol. 64. No. 11. pp. 1911-1919, Nov., 1959.
- Layla, I. R., "Numerical Analysis of Transient Salt/Fresh-Water Interface in Coast Aquifers," Ph.D. Dissertation, Colorado State University, Fort Collins, p. 188, Spring, 1980.
- Mercer, J. W. and C. R. Faust, "The Application of Finite-Element Techniques to Immiscible Flow in Porous Media," *Finite Elements in Water Resources* (Gray et al. ed.), Princeton, N.J., pp. 1.21-1.57, July, 1977.
- Neuman, S. P. and P. A. Witherspoon, "Finite Element Method for Analyzing Steady State Seepage With a Free Surface," *Water Resources Research*, pp. 889-897, June, 1970.

- Ortiz, N. V., Duke, H. R., Sunada, D. K. and D. B. McWhorter, "Artificial Ground-Water Recharge with Capillarity," AACE, Irrigation and Drainage Division, IRI, pp. 78-93, March, 1978.
- Pinder, G. F., "A Galerkin-Finite Element Simulation of Groundwater Contamination on Long Island, New York," Water Resources Research, Vol. 9. No. 6, pp. 1657-1669, December, 1973.
- Pinder, G. F. and H. H. Cooper, Jr., "A Numerical Technique for Calculating the Transient Position of the Saltwater Front," Water Resources Research, Vol. 6. No. 3, pp. 875-882, June, 1970.
- Pinder, G. F. and E. O'Frind, "Application of Galerkin Procedure to Aquifer Analysis," Water Resources Research, Vol. 8. No. 1, pp. 108-120, Feb., 1972.
- Pinder, G. F. and R. H. Page, "Finite Element Simulation of Salt Water Intrusion on the South Fork of Long Island," Proc. Intern. Conf. on Finite Elements, Princeton, N.J., pp. 2.51-2.69, 1976.
- Reddell, D. L. and D. K. Sunada, "Numerical Simulation of Dispersion in Groundwater Aquifers," Hydrology Paper No. 4, Colorado State University, Fort Collins, p. 79, June, 1970.
- Sahni, B. M., "Salt Water Coning Beneath Fresh Water Wells," Ph.D. Dissertation, Colorado State University, Fort Collins, p. 168, April, 1972.
- Seegerlind, L. J., Applied Finite Element Analysis, John Wiley and Sons, Inc., New York, 1976.
- Segol, G., Pinder, G. F. and W. G. Gray, "A Galerkin-Finite Element Technique for Calculating the Transient Position of the Saltwater Front," Water Resources Research, Vol. II. No. 2, pp. 343-347, April, 1975.
- Zienkiewicz, O. C., The Finite Element Method in Engineering Science, McGraw-Hill, New York, p. 521, 1971.

APPENDIXES

APPENDIX A

INPUT CODES FOR PROGRAM

CARD SET 1

No: of cards = 1

NAQTYP = 0 ----- unconfined aquifer
 = 1 ----- confined aquifer

 NSS = 0 ----- transient flow
 = 1 ----- steady flow

 NCAP = 0 ----- no capillarity exists
 = 1 ----- capillarity exists

 NPHASE = 1 ----- single fluid present
 = 2 ----- two fluids present

 FORMAT ----- 4I3

CARD SET 2

No: of cards = 1

NUMEL = No: of elements
 NUMNP = No: of nodal points
 NNPE = No: of nodes per element
 IBWDTH = Band width
 NUMAT = No: of materials of varying permeabilities
 NCS = No: of cross sections

 FORMAT ----- 6I5

CARD SET 3

No: of cards = 1

NQF = No: of fresh water nodal sinks and/or sources
 NQS = No: of salt water nodal sinks and/or sources
 NQXYF = No: of fresh water areal sinks and/or sources

NQXYS = No: of salt water areal sinks and/or sources
 FORMAT ----- 4I5

CARD SET 4

No: of cards = NCS

NCS = Nodal points of cross section(s)
 FORMAT ----- 25I3

CARD SET 5

No: of cards - 1

GAMAF = Density of fresh water
 GAMAS = Density of salt water
 LAMDA = Pore size distribution index
 BUBPH = Bubbling pressure head
 (Ignore LAMDA and BUBPH if NCAP = 0)
 SPS = Specific storage of confined aquifer
 (Ignore if NAQTYP = 0)
 DHST = Tolerable change in head
 ITER = No: of time increments
 FORMAT ----- 6F10.5, I2

CARD SET 6

No: of cards = NUMAT

I = Element no:
 K_x = Hydraulic conductivity of element I in the x-
 direction
 K_y = Hydraulic conductivity of element I in the y-
 direction
 S_y = Specific yield of element I
 FORMAT ----- I5, 3F10.5

CARD SET 7

No: of cards = 1

FTIME = Initial time
 TMAX = Maximum time
 THETA = Numerical time integration parameter
 0.0 - Explicit
 0.5 - Crank-Nicholson
 1.0 - Implicit
 FORMAT ----- 3F10.3, F5.3

CARD SET 8

No: of cards = NUMNP

I = Nodal number
 NPBC = Boundary condition at node I
 0 ----- no flow
 1 ----- constant head
 XORD = x-ordinate of node I
 YORD = y-ordinate of note I
 HF = Total head at node I
 HS = Salt water head at node I
 PSI = Interface elevation at node I
 FORMAT ----- 2I10, 5F10.5
 (If NPHASE = 1: HS=PSI=0)

CARD SET 9

No: of cards = NUMEL

I = Element no:
 NP = Nodal no: of element I read counter clockwise
 FORMAT ----- 7I10

CARD SET 10

No: of cards = NUMEL

I = Element no:
 MAT = Material no: of I
 FORMAT ----- 42I1
 Skip this card if NUMAT = 1

CARD SET 11

No: of cards = NQF

I = Node no:
 QNODF = Discharge or recharge of fresh water at node(s) I
 - ve for discharge
 + ve for recharge
 FORMAT -----I5, F10.5
 Skip this card if NQF = 0

CARD SET 12

No: of cards = NQS

I = NQS
 QNODS = Discharge or recharge of salt water at node(s) I
 - ve for discharge
 + ve for recharge
 FORMAT ----- I5, F10.5
 Skip this card if NQS = 0

CARD SET 13

No: of cards = NQXYF

I = Element No:
 QXYF = Areal Discharge or recharge of fresh water on
 element(s) I
 - ve for discharge
 + ve for recharge
 FORMAT ----- I5, F10.f
 Skip this card if NQXYF = 0

CARD SET 14

No: of cards = NQXYS

I = Element No:

QXYS = Areal discharge or recharge of salt water on
element(s) I.
- for discharge
+ for recharge

FORMAT ----- I5, F10.5
Skip this card if NQXYS = 0

CARD SET 15

No: of cards = NUMNP/8

I = Node No:

B = Thickness of confined Aquifer

FORMAT ----- 8F8.4
Skip this card if NAQTYP = 1

CARD SET 16

No: of cards = NUMNP/8

I = Node No:

DGS = Distance from soil surface to aquifer bottom

FORMAT ----- 8F8.4
Skip this card if NCAP = 0

NOTE: The format statements may need modification for specific types of problems. Dimensions of input variables are given in the nomenclature as well as in the program. All units should be dimensionally consistent.

APPENDIX B

SUMMARY OF COMPUTER PROGRAM

The main program formulates element matrices, transmissivities, and applies the necessary boundary conditions for each time step. The nodal force vector is also computed if a nodal or areal source or sink exists.

SUBROUTINE IODAT

The input data consisting of control parameters, mesh and flow parameters, numerical parameters, and source and/or sink locations is read in by this subroutine. This subroutine also initializes various arrays.

SUBROUTINE SHAPFN

Quadrature points and weighting functions are defined so that the shape functions can be computed in subprogram SFN.

SUBPROGRAM SFN

Evaluates shape functions and returns them to SHAPFN.

SUBPROGRAM SFNXI

Computes the derivatives of the shape functions with respect to one global coordinate and returns them to SHAPFN.

SUBPROGRAM SFNETA

Computes the derivatives of the shape functions with respect to the other global coordinate and returns them to SHAPFN.

SUBROUTINE CHECK

This subroutine terminates execution of the program if the maximum change of interface elevation at any node, for successive time intervals, is less than a specified tolerance.

SUBROUTINE COEFFS

The coefficients appearing in the finite element matrix equations are computed and then averaged over an element.

SUBROUTINE GQINT

The matrices appearing in the finite element equations are integrated using a Gaussian quadrature integration scheme. The Jacobian and its inverse are computed to enable the shape functions to be derived with respect to cartesian coordinates.

The elemental matrices are pieced together and the force vector computed if areal sources and/or sinks exist.

SUBROUTINE GLOBAL

The global matrix is assembled using the elemental matrices computed in GQINT. Due to symmetry, the assembly is limited in the upper half of the global matrix.

SUBROUTINE GAUSOL

Gausol solves the resultant system of algebraic equations by an upper diagonal-upper Gaussian elimination. The output is the change in head for a particular time step.

SUBROUTINE INTELV

INTELV updates the interface elevation by utilizing the computed values of the head changes in both; fresh and salt water regions; at the end of each time step.

SUBROUTINE OUTDAT

This subroutine prints the new elevations after each time step.

SUBROUTINE CAPRES

This part of the program computes the saturated and permeable heights and also calculates the resulting specific yield.

SUBROUTINE HEADCH

The maximum changes in the fresh-water and salt-water heads, between iterations within a given time step, are evaluated in this routine. If convergence is reached, computations progress to the next time step.

SUBROUTINE TSTEP

This routine establishes optimum time step sizes with the aid of an acceleration factor.

APPENDIX C

SOURCE CODES FOR COMPUTER PROGRAM

```

C*****GROUN001
C*****GROUN002
C ***** PROGRAM GROUNDWATER COMPUTES THE FRESH AND SALT WATER *****GROUN003
C ***** HEAD DISTRIBUTIONS IN CONFINED OR UNCONFINED AQUIFERS *****GROUN004
C ***** THE PROGRAM IS BUILT TO HANDLE STEADY STATE AS WELL *****GROUN005
C ***** AS TRANSIENT VARIATIONS OF FLOW OF THE FLUIDS . THE *****GROUN006
C ***** INTERFACE ELEVATIONS ARE EVALUATED AT THE END OF A *****GROUN007
C ***** SPECIFIC YIELD IN UNCONFINED AQUIFERS IS INCORPORATED *****GROUN008
C ***** IN A SPECIFIC SUBROUTINE . *****GROUN009
C*****GROUN010
C*****GROUN011
C *****GROUN012
C *****GROUN013
C ***** DEFINITIONS OF VARIABLES *****GROUN014
C *****GROUN015
C *****GROUN016
C *** BETA --- AREAL AVERAGE OF THE SPECIFIC YIELD OF AN ELEMENT... *****GROUN017
C *** BETAS -- AREAL AVERAGE OF THE STORATIVITY OF AN ELEMENT..... *****GROUN018
C *** BUBPHD - BUBBLING PRESSURE HEAD (L) ..... *****GROUN019
C *** DETJ --- DETERMINANT OF THE JACOBIAN MATRIX..... *****GROUN020
C *** DGS ---- DISTANCE FROM AQUIFER BOTTOM TO SOIL SURFACE (L) ... *****GROUN021
C *** DHF ---- NODAL CHANGE OF THE FRESH WATER HEAD (L) ..... *****GROUN022
C *** DHS ---- NODAL CHANGE OF THE SALT WATER HEAD (L) ..... *****GROUN023
C *** DHST --- STEADY STATE TOLERANCE (L) ..... *****GROUN024
C *** DMAX --- MAXIMUM CHANGE OF INTERFACE ELEVATION AMONG ALL *****GROUN025
C ***          NODES AT THE END OF A TIME INTERVAL (L) ..... *****GROUN026
C *** DNDX --- DERIVATIVE OF THE SHAPE FUNCTION WITH RESPECT TO X.. *****GROUN027
C *** DNDY --- DERIVATIVE OF THE SHAPE FUNCTION WITH RESPECT TO Y.. *****GROUN028
C *** DTIME -- TIME INCREMENT (T) ..... *****GROUN029
C *** EPSX --- TIME INCREMENT ACCELERATION PARAMETER..... *****GROUN030
C *** FTIME -- INITIAL TIME (T) ..... *****GROUN031
C *** GAMAF -- DENSITY OF FRESH WATER (M/L**3) ..... *****GROUN032
C *** GAMAS -- DENSITY OF SALT WATER (M/L**3) ..... *****GROUN033
C *** H ----- HEAD AT A NODE (L) ..... *****GROUN034
C *** HE ----- EQUIVALENT SATURATED HEIGHT (L) ..... *****GROUN035
C *** HELD --- ARRAY FOR STORING THE SATURATED HEIGHT FROM A *****GROUN036
C ***          PREVIOUS TIME INCREMENT (L) ..... *****GROUN037
C *** HF ----- TOTAL HEAD IN THE AQUIFER (L) ..... *****GROUN038
C *** HK ----- EQUIVALENT PERMEABLE HEIGHT (L) ..... *****GROUN039
C *** HS ----- SALT WATER HEAD (L) ..... *****GROUN040
C *** IBAND -- BAND WIDTH PLUS ONE..... *****GROUN041
C *** IBWOTH - BAND WIDTH. THE LARGEST DIFFERENCE BETWEEN TWO NODES *****GROUN042
C ***          IN ANY GIVEN ELEMENT..... *****GROUN043
C *** IDIAG -- COLUMN LOCATION OF THE ROTATED SK MATRIX DIAGONAL... *****GROUN044
C *** INCR --- TIME INCREMENT COUNTER..... *****GROUN045
C *** ITER --- NUMBER OF TIME INCREMENTS..... *****GROUN046
C *** KX ----- HYDRAULIC CONDUCTIVITY OF AN ELEMENT IN THE X DIREC- *****GROUN047
C ***          TION (L/T) ..... *****GROUN048
C *** KY ----- HYDRAULIC CONDUCTIVITY OF AN ELEMENT IN THE Y DIREC- *****GROUN049
C ***          TION (L/T) ..... *****GROUN050
C *** LAMDA -- PORE SIZE DISTRIBUTION INDEX..... *****GROUN051
C *** MAT ---- MATERIAL PROPERTY OF ELEMENT I ..... *****GROUN052
C *** NAQTYP - TYPE OF AQUIFER *****GROUN053
C ***          0 -- UNCONFINED *****GROUN054
C ***          1 -- CONFINED *****GROUN055
C *** NCAP --- PRESENCE OF CAPILLARITY *****GROUN056
C ***          0 -- NO CAPILLARY FLOW AND STORAGE *****GROUN057
C ***          1 -- CAPILLARY FLOW AND STORAGE EXISTS *****GROUN058
C *** NPHASE --- NUMBER OF FLUIDS PRESENT IN AQUIFER *****GROUN059
C ***          1 -- SINGLE FLUID PRESENT *****GROUN060
C ***          2 -- TWO FLUIDS PRESENT *****GROUN061
C *** NCS ---- NUMBER OF HORIZONTAL CROSS SECTIONS..... *****GROUN062
C *** NNPE --- NUMBER OF NODES PER ELEMENT..... *****GROUN063
C *** NP ---- NODAL POINT OF AN ELEMENT..... *****GROUN064
C *** NPBC --- TYPE OF BOUNDARY CONDITION *****GROUN065
C ***          0 -- INTERIOR NODE OR VARIABLE HEAD *****GROUN066
C ***          1 -- CONSTANT HEAD *****GROUN067
C *** NPCS --- NODAL POINTS OF HORIZONTAL CROSS SECTIONS..... *****GROUN068
C *** NQF ---- NUMBER OF FRESH WATER SOURCE(S) AND/OR SINK(S)..... *****GROUN069
C *** NQS ---- NUMBER OF SALT WATER SOURCE(S) AND/OR SINK(S)..... *****GROUN070

```

```

C *** NQXYF -- NUMBER OF FRESH WATER SOURCE(S) AND/OR SINK(S)..... *****GROUN071
C *** NQXYS -- NUMBER OF SALT WATER SOURCE(S) AND/OR SINK(S)..... *****GROUN072
C *** NSS ---- TYPE OF FLOW *****GROUN073
C ***      0 -- TRANSIENT *****GROUN074
C ***      1 -- STEADY *****GROUN075
C *** NUMAT -- NUMBER OF MATERIALS WITH DIFFERING PERMEABILITIES... *****GROUN076
C *** NUMEL -- NUMBER OF ELEMENTS..... *****GROUN077
C *** NUMNP -- NUMBER OF NODES..... *****GROUN078
C *** NUMQPT - NUMBER OF QUADRATURE POINTS IN AN ELEMENT..... *****GROUN079
C *** PHIJ --- AREAL AVERAGE OF THE FRESH WATER OVER AN ELEMENT (L) *****GROUN080
C *** PSI ---- INTERFACE ELEVATION (L) ..... *****GROUN081
C *** QNOD --- NODAL DISCHARGE OR RECHARGE OF A FLUID (L**3/T) .... *****GROUN082
C *** QNODF -- FRESH WATER NODAL DISCHARGE OR RECHARGE (L**3/T) *****GROUN083
C ***      NEGATIVE SIGN FOR DISCHARGE *****GROUN084
C ***      POSITIVE SIGN FOR RECHARGE *****GROUN085
C *** QNODS -- SALT WATER NODAL DISCHARGE OR RECHARGE (L**3/T) *****GROUN086
C ***      NEGATIVE SIGN FOR DISCHARGE *****GROUN087
C ***      POSITIVE SIGN FOR RECHARGE *****GROUN088
C *** QPT ---- QUADRATURE POINT OF AN ELEMENT..... *****GROUN089
C *** QXY ---- AREAL DISCHARGE OR RECHARGE OF A FLUID (L/T) ..... *****GROUN090
C *** QXYF --- AREAL FRESH WATER DISCHARGE OR RECHARGE (L/T) ..... *****GROUN091
C ***      NEGATIVE SIGN FOR DISCHARGE *****GROUN092
C ***      POSITIVE SIGN FOR RECHARGE *****GROUN093
C *** QXYS --- AREAL SALT WATER DISCHARGE OR RECHARGE (LT) ..... *****GROUN094
C ***      NEGATIVE SIGN FOR DISCHARGE *****GROUN095
C ***      POSITIVE SIGN FOR RECHARGE *****GROUN096
C *** RJAC --- JACOBIAN MATRIX..... *****GROUN097
C *** RJACI -- INVERSE OF THE JACOBIAN MATRIX..... *****GROUN098
C *** SF ---- SHAPE FUNCTION OR ITS DERIVATIVES..... *****GROUN099
C *** SK ---- GLOBAL STIFFNESS MATRIX..... *****GROUN100
C *** SPB ---- MATRIX S MINUS MATRIX B1..... *****GROUN101
C *** SMB --- MATRIX S MINUS MATRIX B..... *****GROUN102
C *** BHS ---- MATRIX B PLUS MATRIX S..... *****GROUN103
C *** SPS ---- SPECIFIC STORATIVITY OF CONFINED AQUIFER..... *****GROUN104
C *** SY ---- SPECIFIC YIELD OR POROSITY..... *****GROUN105
C *** SYIJ --- AREAL AVERAGE OF THE SPECIFIC YIELD OVER AN ELEMANT. *****GROUN106
C *** THETA -- NUMERICAL TIME INTEGRATION PARAMETER *****GROUN107
C ***      0.0 -- EXPLICIT *****GROUN108
C ***      0.5 -- CRANK-NICOLSON *****GROUN109
C ***      1.0 -- IMPLICIT *****GROUN110
C *** TIME --- TIME AT THE END OF A TIME INCREMENT (T) ..... *****GROUN111
C *** TKX ---- TRANSMISSIVITY IN X DIRECTION (L**2/T) ..... *****GROUN112
C *** TKY ---- TRANSMISSIVITY IN Y DIRECTION (L**2/T) ..... *****GROUN113
C *** TMAX --- MAXIMUM TIME (T) ..... *****GROUN114
C *** WT ---- WEIGHTING FACTORS FOR QUADRATURE INTEGRATION..... *****GROUN115
C *** XORD --- X ORDINATE OF A NODAL POINT (L) ..... *****GROUN116
C *** YORD --- Y ORDINATE OF A NODAL POINT (L) ..... *****GROUN117
C *****GROUN118
C *****GROUN119
C *****GROUN120
C *****GROUN121
C *****GROUN122
COMMON /C1 / HF (160), HS (160), PSI (160), DHS (160), DHF (160), R (160)
COMMON /C2 / QNODF (160), QNODS (160), QXYF (62), QXYS (62), QNOD, QXY
COMMON /C3 / XORD (160), YORD (160), NPBC (160), B (160), MAT (62)
COMMON /C4 / BETA, ZETA, TKX, TKY, KX (62), KY (62)
COMMON /C5 / PHIJ (62), SYIJ (62), SY (160), SYS (160)
COMMON /C6 / SF (3, 6, 7), WT (7), QPT (7, 3), NPCS (3, 35), NP (160, 6)
COMMON /C7 / SPB (6, 6), SMB (6, 6), BHS (6, 6), SK (160, 25)
COMMON /C8 / DNDX (6), DNDY (6), RJAC (2, 2), RJACI (2, 2)
COMMON /C9 / IBAND, IDIAG, NUMNP, NUMEL, NNPE, NUMQPT, ISST
COMMON /C10 / INCR, NAQTYP, NSS, NCAP, NCS, NPHASE
COMMON /C11 / TIME (31), DTIME (31), TMAX, THETA, ITER, DMAX, EPSX, FTIME
COMMON /C12 / GAMAF, GAMAS, BUBPH, LAMDA, SPS, DHST, DFMAX, DSMAX
COMMON /C13 / DGS (160), HE (160), HK (160), HELD (160), H (160), F (160)
COMMON /C14 / SPIJ (60), GS, GF, DLTG, NQXYF, NQXYS
COMMON /C15 / HFST (160), HSST (160), PSS (160), HKLD (160)
REAL KX, KY, LAMDA
C ***** INPUT DATA AND INITIALIZE ARRAYS IN IODAT *****
C *****
C *****
C *****

```



```

CALL IODAT
C
C ***** COMPUTE TIME INCREMENTS FOR UNSTEADY STATE SOLUTION *****
C
C IF (NSS.EQ.0) CALL TSTEP
C ***** EVALUATION OF SHAPE FUNCTIONS AND THEIR DERIVATIVES *****
CALL SHAPFN
C ***** TIME STEP ITERATION STARTS FOR TRANSIENT SOLUTION *****
C
C DO 230 IT = 1,ITER
C
C ICDOUNT = 1
C
C 10 DO 200 LD = 1,2
C
C ***** COMPUTE THE EFFECT OF CAPILLARITY ON THE FRESH WATER *****
C ***** HEAD AND SPECIFIC YIELD IN UNCONFINED AQUIFERS . *****
DO 20 IK = 1,NUMNP
F(IK) = 0.0
20 CONTINUE
C
C IF (NAQTYP.EQ.0.AND.NCAP.EQ.1.AND.LO.EQ.1) CALL CAPRES(IT,ICOUNT)
ICOUNT = 2
C ***** AVERAGE THE COEFFICIENTS OVER THE ELEMENTS *****
C
CALL COEFFS (LO)
C
C ISST = ISST + 1
DO 60 I = 1,NUMNP
GO TO (30,40),LO
30 H(I) = HFST(I)
GO TO 50
40 H(I) = HSST(I)
50 DO 60 J = 1,IBAND
SK(I,J) = 0.0
60 CONTINUE
C
C
C FORMULATE ELEMENT MATRICES
DO 140 I = 1,NUMEL
DO 70 J = 1,NNPE
DO 70 K = 1,NNPE
SPB(J,K) = 0.0
BHS(J,K) = 0.0
SMB(J,K) = 0.0
70 CONTINUE
C EVALUATE TRANSMISSIVITY COEFFICIENTS
BETA = SYIJ(I)
ZETA = SPIJ(I)
TKX = KX(MAT(I)) * PHIJ(I)
TKY = KY(MAT(I)) * PHIJ(I)
C
C BEGIN QUADRATURE INTEGRATION
CALL GQINT (I,LO,IT)
C END OF QUADRATURE INTEGRATION
C
C IF (NSS.EQ.1) GO TO 110
C SUBTRACT SMB*PHI AND BHS*DHS FROM F
DO 100 J = 1,NNPE
NPJ = NP(I,J)
DO 100 K = 1,NNPE
NPK = NP(I,K)
GO TO (80,90),LO
80 F(NPJ) = F(NPJ) - (SPB(J,K) + SMB(J,K)) * HFST(NPK) + BHS(J,K)
1 * (HS(NPK) - HSST(NPK))
GO TO 100
90 F(NPJ) = F(NPJ) - (SPB(J,K) + SMB(J,K)) * HSST(NPK) + BHS(J,K)

```

```

      1 * (HF(NPK) - HFST(NPK))
100   CONTINUE
      GO TO 130
110   CONTINUE
C
      DO 120 J = 1, NNPE
      NPJ = NP(I, J)
      DO 120 K = 1, NNPE
      NPK = NP(I, K)
      F(NPJ) = F(NPJ) - SPB(J, K) * H(NPK)
120   CONTINUE
130   CONTINUE
C
C GLOBAL SUBROUTINE WILL FORMULATE THE LARGE SK MATRIX
      CALL GLOBAL (I, LO)
140   CONTINUE
C
C
C BOUNDARY CONDITIONS
      DO 150 I = 1, NUMNP
      IF (NPBC(I).EQ.O) GO TO 150
      F(I) = O.O
      SK(I, IDIAG) = 1.OE + 50
150   CONTINUE
C
C
C GAUSOL SOLVES FOR F(I)
      CALL GAUSOL
      DO 160 I = 1, NUMNP
      H(I) = H(I) + F(I)
C
      IF (H(I).LT.O.O) GO TO 240
160   CONTINUE
      CALL HEADCH(LO)
C
      DO 190 I = 1, NUMNP
      GO TO (170, 180), LO
170   DHF(I) = F(I)
      HF(I) = H(I)
      GO TO 190
180   DHS(I) = F(I)
      HS(I) = H(I)
190   CONTINUE
200   CONTINUE
      IF (NPHASE.EQ.2) CALL INTELV
      IF (DFMAX.GT.DHST.OR.DSMAX.GT.DHST) GO TO 10
      IF (NSS.EQ.1) GO TO 220
      DO 210 I=1, NUMNP
      HFST(I) = HF(I)
      HSST(I) = HS(I)
      HKLD(I) = HK(I)
      HELD(I) = HE(I)
      R(I) = PSI(I) - PSS(I)
210   CONTINUE
C INCREMENT VARIABLES
      TIME(IT) = TIME(IT) + DTIME(IT)
      INCR = INCR + 1
C
C
      IF (NPHASE.EQ.2) CALL CHECK
220   CALL OUTDAT(IT)
C
C ***** STEADY STATE CHECK ENFORCED AT THIS POINT *****
C
      IF ( NPHASE.EQ.1) GO TO 230
      IF ( DMAX .LE. DHST ) GO TO 260
C
230   CONTINUE
C
C

```

```

GROUN211
GROUN212
GROUN213
GROUN214
GROUN215
GROUN216
GROUN217
GROUN218
GROUN219
GROUN220
GROUN221
GROUN222
GROUN223
GROUN224
GROUN225
GROUN226
GROUN227
GROUN228
GROUN229
GROUN230
GROUN231
GROUN232
GROUN233
GROUN234
GROUN235
GROUN236
GROUN237
GROUN238
GROUN239
GROUN240
GROUN241
GROUN242
GROUN243
GROUN244
GROUN245
GROUN246
GROUN247
GROUN248
GROUN249
GROUN250
GROUN251
GROUN252
GROUN253
GROUN254
GROUN255
GROUN256
GROUN257
GROUN258
GROUN259
GROUN260
GROUN261
GROUN262
GROUN263
GROUN264
GROUN265
GROUN266
GROUN267
GROUN268
GROUN269
GROUN270
GROUN271
GROUN272
GROUN273
GROUN274
GROUN275
GROUN276
GROUN277
GROUN278
GROUN279
GROUN280

```

```

      GO TO 280
240  IF (NSS.EQ.1) GO TO 250
      TIME(IT) = TIME(IT) + DTIME(IT)
C
C
C ..... E R R O R   M E S S A G E
      WRITE (6,300) TIME(IT)
      GO TO 290
250  ISST = ISST / 2
      WRITE(6,310) ISST
      GO TO 290
260  IF (NSS.EQ.1) GO TO 270
      WRITE (6,320) TIME(IT)
      GO TO 290
270  ISST = ISST / 2
      WRITE (6,330) ISST
      GO TO 290
280  WRITE(6,340) ITER
C
290  STOP
300  FORMAT (///10X,24HNEGATIVE HEADS AT TIME =,F10.5/)
310  FORMAT (///10X,28HNEGATIVE HEADS AT ITERATION ,I2///)
320  FORMAT (///10X,30HSTEADY STATE REACHED AT TIME =,F8.3,
1     9H SECONDS/////////)
330  FORMAT (///10X,24HSTEADY STATE REACHED IN ,I3,13H ITERATIONS.)
340  FORMAT (///10X,18HNO CONVERGENCE IN ,I3,12H ITERATIONS)
C
      END
      SUBROUTINE IODAT
C
C * THIS SUBROUTINE READS THE INPUT DATA . IT ALSO INTIALIZES CONTROL *
C * PARAMETERS AND ECHO PRINTS THE INPUT DATA . *
C
      COMMON/C1/HF(160),HS(160),PSI(160),DHS(160),DHF(160),R(160)
      COMMON /C2/ QNODF(160),QNODS(160),QXYF(62),QXYS(62),QNOD,QXY
      COMMON /C3 / XORD(160),YORD(160),NPBC(160),B(160),MAT(62)
      COMMON /C4 / BETA,ZETA,TKX,TKY,KX(62),KY(62)
      COMMON /C5 / PHIJ(62),SYIJ(62),SY(160),SYS(160)
      COMMON /C6 / SF(3,6,7),WT(7),QPT(7,3),NPCS(3,35),NP(160,6)
      COMMON /C9 / IBAND,IDIAG,NUMNP,NUMEL,NNPE,NUMQPT,ISST
      COMMON /C10 / INCR,NAQTYP,NSS,NCAP,NCS,NPHASE
      COMMON /C11 / TIME(31),DTIME(31),TMAX,THETA,ITER,DMAX,EPSX,FTIME
      COMMON /C12 / GAMAF,GAMAS,BUBPH,LAMDA,SPS,DHST,DFMAX,DSMAX
      COMMON /C13 / DGS(160),HE(160),HK(160),HELD(160),H(160),F(160)
      COMMON /C14 /SPIJ(60),GS,GF,DLTG,NQXYF,NQXYS
      COMMON /C15 /HFST(160),HSST(160),PSS(160),HKLD(160)
      REAL KX,KY,LAMDA
C
C
C READ CONTROL PARAMETERS
      READ (5,50) NAQTYP,NSS,NCAP,NPHASE
C
C READ MESH AND FLOW DATA
      READ (5,60) NUMEL,NUMNP,NNPE,IBWDTH,NUMAT,NCS
      READ(5,70) NQF,NQXYF,NQS,NQXYS
      READ (5,80) ((NPCS(I,J),J = 1,25),I = 1,NCS)
      READ (5,90) GAMAF,GAMAS,LAMDA,BUBPH,SPS,DHST,ITER
      READ (5,100) (I,KX(I),KY(I),SY(I),IO = 1,NUMAT)
C
C READ NUMERICAL CONTROL DATA
      IF (NSS.EQ.0) READ (5,110) FTIME,TMAX,THETA,EPSX
C
C INCREMENTAL INITIALIZATION
      NUMQPT = 7
      IBAND = IBWDTH + 1
      INCR = 0
      ISST = 0
      IDIAG = 1
      IF (NPHASE.EQ.1) DMAX = 1.0
      IF (NPHASE.EQ.2) DMAX = 0.0

```

```

GROUN281
GROUN282
GROUN283
GROUN284
GROUN285
GROUN286
GROUN287
GROUN288
GROUN289
GROUN290
GROUN291
GROUN292
GROUN293
GROUN294
GROUN295
GROUN296
GROUN297
GROUN298
GROUN299
GROUN300
GROUN301
GROUN302
GROUN303
GROUN304
GROUN305
GROUN306
IODATO01
IODATO02
IODATO03
IODATO04
IODATO05
IODATO06
IODATO07
IODATO08
IODATO09
IODATO10
IODATO11
IODATO12
IODATO13
IODATO14
IODATO15
IODATO16
IODATO17
IODATO18
IODATO19
IODATO20
IODATO21
IODATO22
IODATO23
IODATO24
IODATO25
IODATO26
IODATO27
IODATO28
IODATO29
IODATO30
IODATO31
IODATO32
IODATO33
IODATO34
IODATO35
IODATO36
IODATO37
IODATO38
IODATO39
IODATO40
IODATO41
IODATO42
IODATO43
IODATO44

```

```

DFMAX = 0.0
DSMAX = 0.0
DLTG = GAMAS - GAMAF
IF (DLTG.EQ.0.0) DLTG = 1.0
GS = GAMAS/DLTG
GF = GAMAF/DLTG
C
C READ MESH PHYSICAL DIMENSIONS
READ (5,120) (I,NPBC(I),XORD(I),YORD(I),HF(I),HS(I),PSI(I),IO = 1,
1NUMNP)
READ (5,130) (I,(NP(I,J),J = 1,NNPE),I1 = 1,NUMEL)
IF (NUMAT.NE.1) READ (5,140) (MAT(I),I = 1,NUMEL)
DO 10 I = 1,NUMEL
  QXYF(I) = 0.0
  QXYS(I) = 0.0
  PHIJ(I) = 0.0
  SYIJ(I) = 0.0
  SPIJ(I) = 0.0
  IF (NUMAT.EQ.1) MAT(I) = 1
DO 10 J = 1,NNPE
  NPJ = NP(I,J)
  SY(NPJ) = SY(MAT(I))
  SYS(NPJ) = SY(MAT(I))
  HELD(NPJ) = 0.0
  HKLD(NPJ) = 0.0
  HE(NPJ) = 0.0
  HK(NPJ) = 0.0
  DHF(NPJ) = 0.0
  R(NPJ) = 0.0
  DHS(NPJ) = 0.0
  QNODF(NPJ) = 0.0
  QNODS(NPJ) = 0.0
  F(NPJ) = 0.0
  HFST(NPJ)=HF(NPJ)
  HSST(NPJ)=HS(NPJ)
  PSS(NPJ)=PSI(NPJ)
10 CONTINUE
C
C READ SOURCE AND/OR SINK AND THEIR NODAL AND/OR AREAL LOCATIONS
IF (NQF.GT.0) READ (5,150) (I,QNODF(I),IO = 1,NQF)
IF (NQS.GT.0) READ (5,150) (I,QNODS(I),IO = 1,NQS)
IF (NQXYF.GT.0) READ (5,150) (I,QXYF(I),IO = 1,NQXYF)
IF (NQXYS.GT.0) READ (5,150) (I,QXYS(I),IO = 1,NQXYS)
IF (NAQTYP.EQ.1) READ (5,160) (B(I),I = 1,NUMNP)
IF (NAQTYP.EQ.0.AND.NCAP.EQ.1) READ (5,160) (DGS(I),I = 1,NUMNP)
C
C PRINT THE PHYSICAL AND FLOW DATA
WRITE (6,170)
WRITE (6,180) NAQTYP,NSS,IBAND,NUMAT,NUMEL,NUMNP,NNPE
WRITE(6,190)GAMAF,GAMAS,BUBPH,LAMDA,SPS,DHST
IF (NSS.EQ.1) GO TO 20
WRITE(6,200) FTIME,TMAX,THETA,EPSX
20 WRITE (6,210) NCS,NQF,NQS,NQXYF,NQXYS,ITER
WRITE (6,170)
WRITE (6,220)
DO 30 I = 1,NUMNP
  WRITE (6,230) I,NPBC(I),XORD(I),YORD(I),HF(I),HS(I),PSI(I),
1 QNODF(I),QNODS(I),SY(I),SYS(I)
30 CONTINUE
WRITE (6,170)
WRITE (6,240)
DO 40 I = 1,NUMEL
  WRITE (6,250) I,(NP(I,J),J = 1,NNPE),MAT(I),KX(MAT(I)),KY(MAT(I)
1 ),QXYF(I),QXYS(I)
40 CONTINUE
RETURN
C
50 FORMAT (4I3)
60 FORMAT (6I5)
70 FORMAT (4I5)

```

IODAT114

```

80 FORMAT (25I3) IODAT115
90 FORMAT (6F10.5,I2) IODAT116
100 FORMAT (I5,3F10.5) IODAT117
110 FORMAT (3F10.3,F5.3) IODAT118
120 FORMAT (2I10,5F10.0) IODAT119
130 FORMAT (7I10) IODAT120
140 FORMAT (42I1) IODAT121
150 FORMAT (I5,F10.7) IODAT122
160 FORMAT (8F8.4) IODAT123
170 FORMAT (1H1) IODAT124
180 FORMAT (/////40X,27HAQUIFER AND MESH PARAMETERS//40X,6HNAQTYP,1X,I IODAT125
13/40X,3HNSS,3X,I4/40X,5HIBAND,I5/40X,5HNUMAT,I5/40X,5HNUMEL,I5/40X IODAT126
2,5HNUMNP,I5/40X,5HNNPE,I5/) IODAT127
190 FORMAT (///40X,25HFLUID AND SOIL PARAMETERS//40X,5HGAMAF,E12.4/40X IODAT128
1,5HGAMAS,E12.4/40X,5HBUBPH,E12.4/40X,5HLAMDA,E12.4/40X,5HSPS,E12 IODAT129
2.4/40X,5HDHST,E12.4/) IODAT130
200 FORMAT (///40X,20HNUMERICAL PARAMETERS//40X,5HFTIME,E12.4/40X IODAT131
1,5HTMAX,E12.4/40X,5HTHETA,E12.4/40X,5HEPSX,E12.4/) IODAT132
210 FORMAT (///40X,18HCONTROL PARAMETERS/40X,8HNCS,I3/40X,8HNQF IODAT133
1,I3/40X,8HNQS,I3/40X,8HNQXYF,I3/40X,8HNQXYS,I3/40X, IODAT134
2 8HITER,I3/) IODAT135
220 FORMAT (2X,11HNODAL DATA,//48X,7HINITIAL,9X,7HINITIAL,9X,7HINITIAL IODAT136
1,6X,18HDISCHARGE/RECHARGE,3X,14HSPECIFIC YIELD/8X,2HNP,36X, IODAT137
2 11HFRESH-WATER,6X,10HSALT-WATER,6X,9HINTERFACE,6X,5HFRESH,5X, IODAT138
3 4HSALT,6X,5HFRESH,5X,4HSALT/2X,4HNODE,2X,2HBC,3X,12HX-COORDINATE, IODAT139
4 4X,12HY-COORDINATE,8X,4HHEAD,12X,4HHEAD,10X,9HELEVATION,6X,5HWATE IODAT140
5R,5X,5HWATER,5X,5HWATER,5X,5HWATER/) IODAT141
230 FORMAT (3X,I3,3X,I1,5(3X,E13.6),4(3X,F7.3)) IODAT142
240 FORMAT (3X,11HAREAL DATA,//72X,18HDISCHARGE/RECHARGE/38X,4HMAT, IODAT143
14X,22HHYDRAULIC CONDUCTIVITY,5X,5HFRESH,4X,4HSALT/2X,4HELEM,2X, IODAT144
23HNPI,2X,3HNPJ,2X,3HNPK,2X,3HNPL,2X,3HNPM,2X,3HNPN,2X,4HPROP,3X, IODAT145
311HX-DIRECTION,3X,11HY-DIRECTION,3X,7HWATER,4X,5HWATER/) IODAT146
250 FORMAT (2X,I3,3X,I3,6I5,4X,E11.4,3X,E11.4,2X,F8.4,3X,F8.4) IODAT147
END OUTDAO01
C SUBROUTINE OUTDAT(IT) OUTDAO02
C OUTDAO03
C * THIS SUBROUTINE PRINTS OUT THE COMPUTED HEADS AND ELEVATIONS AT * OUTDAO05
C * THE END OF EVERY TIME INCREMENT ..... * OUTDAO06
C OUTDAO07
COMMON/C1/HF(160),HS(160),PSI(160),DHS(160),DHF(160),R(160) OUTDAO08
COMMON /C3 / XORD(160),YORD(160),NPBC(160),B(160),MAT(62) OUTDAO09
COMMON /C5 / PHIJ(62),SYIJ(62),SY(160),SYS(160) OUTDAO10
COMMON /C6 / SF(3,6,7),WT(7),QPT(7,3),NPCS(3,35),NP(160,6) OUTDAO11
COMMON /C9 / IBAND,IDIAG,NUMNP,NUMEL,NNPE,NUMQPT,ISST OUTDAO12
COMMON /C10 / INCR,NAQTYP,NSS,NCAP,NCS,NPHASE OUTDAO13
COMMON /C11 / TIME(31),DTIME(31),TMAX,THETA,ITER,DMAX,EPSX,FTIME OUTDAO14
COMMON /C12 / GAMAF,GAMAS,BUBPH,LAMDA,SPS,DHST,DFMAX,DSMAX OUTDAO15
COMMON /C13 / DGS(160),HE(160),HK(160),HELD(160),H(160),F(160) OUTDAO16
C OUTDAO17
C PRINT OUT THE COMPUTED VALUES OUTDAO18
WRITE (6,60) OUTDAO19
IF (NSS.EQ.0) WRITE (6,70) INCR,TIME(IT+1) OUTDAO20
WRITE (6,100) OUTDAO21
DO 10 I = 1,NUMNP OUTDAO22
WRITE (6,110) I,NPBC(I),HF(I),HS(I),PSI(I),HK(I),HE(I), OUTDAO23
1 SY(I),SYS(I) OUTDAO24
10 CONTINUE OUTDAO25
WRITE (6,60) OUTDAO26
IF (NSS.EQ.0) WRITE (6,120) INCR,TIME(IT+1) OUTDAO27
C PRINT OUT THE RESULTS BY CROSS SECTION OUTDAO28
IF (NCS.EQ.0) GO TO 40 OUTDAO29
DO 30 I = 1,NCS OUTDAO30
WRITE (6,130) I OUTDAO31
WRITE (6,100) OUTDAO32
DO 20 J = 1,23 OUTDAO33
M = NPCS(I,J) OUTDAO34
WRITE (6,110) M,NPBC(M),HF(M),HS(M),PSI(M),HK(M),HE(M), OUTDAO35
1 SY(M),SYS(M) OUTDAO36
20 CONTINUE OUTDAO37

```

```

30 CONTINUE
40 WRITE (6,80) DFMAX,DSMAX
    IF (NSS.EQ.1) GO TO 50
    WRITE (6,90) DMAX
50 WRITE (6,60)
    RETURN
60 FORMAT (1H1)
70 FORMAT (//1X,4HINCR,I10,/1X,4HTIME,E10.3/)
80 FORMAT (////10X,48HTHE MAXIMUM CHANGE IN THE FRESH-WATER HEAD =,
    1 ,F6.3,14H CENTIMETERS./10X,48HTHE MAXIMUM CHANGE IN THE SALT-WAT
    2ER HEAD = ,F6.3,14H CENTIMETERS./)
90 FORMAT (10X,48HTHE MAXIMUM CHANGE IN THE INTERFACE-ELEVATION = ,
    1F6.3,14H CENTIMETERS.)
100 FORMAT (95X,14HSPECIFIC YIELD/8X,2HNP,4X,11HFRESH-WATER,5X,
    110HSALT-WATER,6X,9HINTERFACE,7X,9HSATURATED,7X,9HPERMEABLE,8X,
    25HFRESH,5X,4HSALT/2X,4HNODE,2X,2HBC,8X,4HHEAD,12X,4HHEAD,8X,
    39HELEVATION,10X,6HHEIGHT,10X,6HHEIGHT,8X,5HWATER,5X,5HWATER/)
110 FORMAT (3X,I3,3X,I1,5(3X,E13.6),2(3X,F7.3))
120 FORMAT (//1X,23HOUTPUT BY CROSS SECTION//1X,4HINCR,I10,/1X,4HTIME,
    1E10.3/)
130 FORMAT (//18H CROSS SECTION NO.,I2/)
    END
C
C SUBROUTINE GQINT(I,LO,IT)
C
C * THIS SUBROUTINES MAIN FUNCTION IS TO INTEGRATE THE MATRIX EQUATION *GQINT005
C * USING A GAUSSIAN QUADRATURE SCHEME . AT EACH QUADRATURE POINT IN *GQINT006
C * AN ELEMENT ,THE CORRESPONDING JACOBIAN RJAC ,ITS DTERMINANT DETJ *GQINT007
C * AND ITS INVERSE RJACI ARE GENERATED AND USED TO COMPUTE THE * GQINT008
C * DERIVATIVES OF THE SHAPE FUNCTIONS WITH RESPECT TO THE LOCAL *GQINT009
C * COORDINATE SYSTEM. THE OTHER FUNCTION OF THIS SUBPROGRAM IS THE *GQINT010
C * FORMULATION OF THE FORCE MATRIX F AND MATRICES SMB ,SPB AND BHS TO *GQINT011
C * BE USED LATER AS ELEMENTS OF THE GLOBAL MATRIX SK ..... *GQINT012
C
COMMON /C2/ QNODF(160),QNODS(160),QXYF(62),QXYS(62),QNOD,QXY
COMMON /C3 / XORD(160),YORD(160),NPBC(160),B(160),MAT(62)
COMMON /C4 / BETA,ZETA,TKX,TKY,KX(62),KY(62)
COMMON /C6 / SF(3,6,7),WT(7),QPT(7,3),NPCS(3,35),NP(160,6)
COMMON /C7 / SPB(6,6),SMB(6,6),BHS(6,6),SK(160,25)
COMMON /C8 / DNDX(6),DNDY(6),RJAC(2,2),RJACI(2,2)
COMMON /C9 / IBAND,IDIAG,NUMNP,NUMEL,NNPE,NUMQPT,ISST
COMMON /C10 / INCR,NAQTYP,NSS,NCAP,NCS,NPHASE
COMMON /C11 / TIME(31),DTIME(31),TMAX,THETA,ITER,DMAX,EPSX,FTIME
COMMON /C13 / DGS(160),HE(160),HK(160),HELD(160),H(160),F(160)
COMMON /C14 /SPIJ(60),GS,GF,DLTG,NQXYF,NQXYS
C
REAL KX,KY,LAMDA
C
C FORMULATE JACOBIAN RJAC
DO 90 J = 1,NUMQPT
    RJAC(1,1) = 0.0
    RJAC(1,2) = 0.0
    RJAC(2,1) = 0.0
    RJAC(2,2) = 0.0
    DO 10 K = 1,NNPE
        NPK = NP(I,K)
        RJAC(1,1) = RJAC(1,1) + SF(2,K,J) * XORD(NPK)
        RJAC(1,2) = RJAC(1,2) + SF(3,K,J) * XORD(NPK)
        RJAC(2,1) = RJAC(2,1) + SF(2,K,J) * YORD(NPK)
        RJAC(2,2) = RJAC(2,2) + SF(3,K,J) * YORD(NPK)
    10 CONTINUE
C
C FORMULATE ITS DETERMINANT
DETJ = RJAC(1,1) * RJAC(2,2) - RJAC(1,2) * RJAC(2,1)
IF (DETJ.LE.0.0) GO TO 150
C
C FORMULATE ITS INVERSE
RJACI(1,1) = RJAC(2,2)/DETJ
RJACI(1,2) = - RJAC(1,2)/DETJ
RJACI(2,1) = - RJAC(2,1)/DETJ

```

```

      RJACI(2,2) = RJAC(1,1)/DETJ
C
C
C DETERMINE DNDX AND DNDY
      DO 20 K = 1,NNPE
          DNDX(K) = RJACI(1,1) * SF(2,K,J) + RJACI(2,1) * SF(3,K,J)
          DNDY(K) = RJACI(1,2) * SF(2,K,J) + RJACI(2,2) * SF(3,K,J)
      20 CONTINUE
C FORMULATE ELEMENTAL MATRICES SMB AND SPB
      DO 40 K = 1,NNPE
          DO 40 L = 1,NNPE
              ST = WT(J) * (DNDX(K) * TKX * DNDX(L) + DNDY(K) * TKY
          1 * DNDY(L)) * DETJ
              IF (NSS .EQ. 0) GO TO 30
              SPB(K,L) = SPB(K,L) + ST
              GO TO 40
          30 CONTINUE
              BK = WT(J) * SF(1,K,J) * BETA * SF(1,L,J) * DETJ
              BS = WT(J) * SF(1,K,J) * ZETA * SF(1,L,J) * DETJ
              SPB(K,L) = SPB(K,L) + THETA * ST + BK/DTIME(IT)
              SMB(K,L) = SMB(K,L) + (1.0-THETA) * ST - BK/DTIME(IT)
              BHS(K,L) = BHS(K,L) + BS/DTIME(IT)
          40 CONTINUE
C
          IF (NQXYF.EQ.O.AND.NQXYS.EQ.O) GO TO 90
C
          GO TO ( 50,60 ), LO
          50 QXY = QXYF(I)
              GO TO 70
          60 QXY = QXYS(I)
          70 CONTINUE
C FORMULATE FORCE MATRIX
          DO 80 K = 1,NNPE
              K1 = NP(I,K)
              DO 80 L = 1,NNPE
                  F(K1) = F(K1) + WT(J) * SF(1,K,J) * QXY * SF(1,L,J) * DETJ
          80 CONTINUE
          90 CONTINUE
C
          IF (NQXYF.EQ.O.AND.NQXYS.EQ.O) GO TO 100
          GO TO 160
C
          100 CONTINUE
              DO 140 K=1,NNPE
                  K1 = NP(I,K)
                  GO TO (110,120), LO
          110 QNOD = QNODF(K1)
                  GO TO 130
          120 QNOD = QNODS(K1)
          130 CONTINUE
                  F(K1) = QNOD
          140 CONTINUE
                  GO TO 160
C
C ..... E R R O R M E S S A G E
          150 WRITE (6,170) I
          160 CONTINUE
              RETURN
C
          170 FORMAT (//36H ERROR IN JACOBIAN CHECK ELEMENT NO.,I4/)
              END
              SUBROUTINE COEFFS(LO)
C
C * THIS SUBROUTINE EVALUATES THE AREAL AVERAGE OF THE NODAL VALUES OF *COEFF005
C * THE TRANSMISSIVITY, INTERFACE ELEVATION, THICKNESS OF AQUIFER AND *COEFF006
C * THE SPECIFIC YIELD USING THE CONCEPT OF SHAPE FUNCTIONS ..... *COEFF007
C
          COMMON/C1/HF(160),HS(160),PSI(160),DHS(160),DHF(160),R(160)
          COMMON /C3 / XORD(160),YORD(160),NPBC(160),B(160),MAT(62)
          COMMON /C5 / PHIJ(62),SYIJ(62),SY(160),SYS(160)

```

```

COMMON /C6 / SF(3,6,7),WT(7),QPT(7,3),NPCS(3,35),NP(160,6)
COMMON /C9 / IBAND,IDIAG,NUMNP,NUMEL,NNPE,NUMQPT,ISST
COMMON /C10 / INCR,NAQTYP,NSS,NCAP,NCS,NPHASE
COMMON /C12 / GAMAF,GAMAS,BUBPH,LAMDA,SPS,DHST,DFMAX,DSMAX
COMMON /C13 / DGS(160),HE(160),HK(160),HELD(160),H(160),F(160)
COMMON /C14 / SPIJ(60),GS,GF,DLTG,NQXYF,NQXYS
COMMON /C15 / HFST(160),HSST(160),PSS(160),HKLD(160)
DO 160 I = 1,NUMEL
C
IF (NAQTYP.EQ.1) GO TO 80
IF (NSS.EQ.0) GO TO 40
C
C
C PSIJ IS THE SAME FOR CONFINED AND UNCONFINED AQUIFERS
IF (LO.EQ.1) GO TO 20
PHIJ(I) = 0.0
DO 10 J = 1,NUMQPT
DO 10 K = 1,NNPE
PHIJ(I) = PHIJ(I) + SF(1,K,J) * (PSI(NP(I,K)))
10 CONTINUE
PHIJ(I) = PHIJ(I)/NUMQPT
GO TO 160
20 CONTINUE
PHIJ(I) = 0.0
DO 30 J = 1,NUMQPT
DO 30 K = 1,NNPE
PHIJ(I) = PHIJ(I) + SF(1,K,J) * (HFST(NP(I,K))+HKLD(NP(I,K))
- PSI(NP(I,K)))
30 CONTINUE
PHIJ(I) = PHIJ(I)/NUMQPT
GO TO 160
40 CONTINUE
C
IF (LO.EQ.1) GO TO 60
PHIJ(I) = 0.0
SYIJ(I) = 0.0
SPIJ(I) = 0.0
DO 50 J = 1,NUMQPT
DO 50 K = 1,NNPE
PHIJ(I) = PHIJ(I) + SF(1,K,J) * (PSS(NP(I,K))+PSI(NP(I,K)))/2.0
SYIJ(I) = SYIJ(I) + SF(1,K,J) * (SYS(NP(I,K))*GS)
SPIJ(I) = SPIJ(I) + SF(1,K,J) * (SYS(NP(I,K))*GF)
50 CONTINUE
PHIJ(I) = PHIJ(I)/NUMQPT
SYIJ(I) = SYIJ(I)/NUMQPT
SPIJ(I) = SPIJ(I)/NUMQPT
GO TO 160
60 CONTINUE
PHIJ(I) = 0.0
SYIJ(I) = 0.0
SPIJ(I) = 0.0
DO 70 J = 1,NUMQPT
DO 70 K = 1,NNPE
PHIJ(I) = PHIJ(I) + SF(1,K,J) * ((HFST(NP(I,K)) + HKLD(NP(I,K))
- PSS(NP(I,K))) + (HF(NP(I,K)) + HK(NP(I,K)) -
PSI(NP(I,K))))/2.0
SYIJ(I) = SYIJ(I) + SF(1,K,J) * (SY(NP(I,K)) + (SYS(NP(I,K))
* GF))
SPIJ(I) = SPIJ(I) + SF(1,K,J) * (SYS(NP(I,K)) * GS)
70 CONTINUE
PHIJ(I) = PHIJ(I)/NUMQPT
SYIJ(I) = SYIJ(I)/NUMQPT
SPIJ(I) = SPIJ(I)/NUMQPT
GO TO 160
80 CONTINUE
IF (NSS.EQ.0) GO TO 120
IF (LO.EQ.1) GO TO 100
PHIJ(I) = 0.0
DO 90 J = 1,NUMQPT
DO 90 K = 1,NNPE

```

COEFF012
COEFF013
COEFF014
COEFF015
COEFF016
COEFF017
COEFF018
COEFF019
COEFF020
COEFF021
COEFF022
COEFF023
COEFF024
COEFF025
COEFF026
COEFF027
COEFF028
COEFF029
COEFF030
COEFF031
COEFF032
COEFF033
COEFF034
COEFF035
COEFF036
COEFF037
COEFF038
COEFF039
COEFF040
COEFF041
COEFF042
COEFF043
COEFF044
COEFF045
COEFF046
COEFF047
COEFF048
COEFF049
COEFF050
COEFF051
COEFF052
COEFF053
COEFF054
COEFF055
COEFF056
COEFF057
COEFF058
COEFF059
COEFF060
COEFF061
COEFF062
COEFF063
COEFF064
COEFF065
COEFF066
COEFF067
COEFF068
COEFF069
COEFF070
COEFF071
COEFF072
COEFF073
COEFF074
COEFF075
COEFF076
COEFF077
COEFF078
COEFF079
COEFF080
COEFF081


```

          PHIJ(I) = PHIJ(I) + SF(1,K,J) * (PSI(NP(I,K)))
90  CONTINUE
          PHIJ(I) = PHIJ(I)/NUMQPT
          GO TO 160
100  CONTINUE
          PHIJ(I) = 0.0
          DO 110 J = 1,NUMQPT
          DO 110 K = 1,NNPE
          PHIJ(I) = PHIJ(I) + SF(1,K,J) * (B(NP(I,K)) - PSI(NP(I,K)))
110  CONTINUE
          PHIJ(I) = PHIJ(I)/NUMQPT
          GO TO 160
120  CONTINUE
          IF (LO.EQ.1) GO TO 140
          PHIJ(I) = 0.0
          SYIJ(I) = 0.0
          SPIJ(I) = 0.0
          DO 130 J = 1,NUMQPT
          DO 130 K = 1,NNPE
          PHIJ(I) = PHIJ(I) + SF(1,K,J) * (PSS(NP(I,K)) + PSI(NP(I,K)))/2.0
          SYIJ(I) = SYIJ(I) + SF(1,K,J) * (SPS * PSI(NP(I,K)) + (SY(NP(I,K)
1  ) * GS))
          SPIJ(I) = SPIJ(I) + SF(1,K,J) * (SY(NP(I,K)) * GF)
130  CONTINUE
          PHIJ(I) = PHIJ(I)/NUMQPT
          SYIJ(I) = SYIJ(I)/NUMQPT
          SPIJ(I) = SPIJ(I)/NUMQPT
          GO TO 160
140  CONTINUE
          PHIJ(I) = 0.0
          SYIJ(I) = 0.0
          SPIJ(I) = 0.0
          DO 150 J = 1,NUMQPT
          DO 150 K = 1,NNPE
          PHIJ(I) = PHIJ(I) + SF(1,K,J) * ((B(NP(I,K)) - PSS(NP(I,K))) +
1  (B(NP(I,K)) - PSI(NP(I,K))))/2.0
          SYIJ(I) = SYIJ(I) + SF(1,K,J) * (SPS * (B(NP(I,K)) - PSI(NP(I,K)
1  ) + (SY(NP(I,K)) * GF)).
          SPIJ(I) = SPIJ(I) + SF(1,K,J) * (SY(NP(I,K)) * GS)
150  CONTINUE
          PHIJ(I) = PHIJ(I)/NUMQPT
          SYIJ(I) = SYIJ(I)/NUMQPT
          SPIJ(I) = SPIJ(I)/NUMQPT
160  CONTINUE
          RETURN
          END
C
          SUBROUTINE GLOBAL(I,LO)
C
C * THIS SUBROUTINE ASSEMBLES THE ELEMENTAL MATRIX SMB FORMED IN GQINT *
C * TO FORMULATE THE GLOBAL MATRIX SK . THE ASSEMBLY IS LIMITED TO THE *
C * UPPER HALF OF SK DUE TO THE EXISTENCE OF SYMMETRY ..... *
C
C
          COMMON /C6 / SF(3,6,7),WT(7),QPT(7,3),NPCS(3,35),NP(160,6)
          COMMON /C7 / SPB(6,6),SMB(6,6),BHS(6,6),SK(160,25)
          COMMON /C9 / IBAND,IDIAG,NUMNP,NUMEL,NNPE,NUMQPT,ISST
C
C PLACE IN LARGE SK MATRIX
          DO 10 J = 1,NNPE
          J1 = NP(I,J)
          DO 10 K = 1,NNPE
          K1 = NP(I,K)
          IF (K1.LT.J1) GO TO 10
          K2 = K1 - J1 + IDIAG
          SK(J1,K2) = SK(J1,K2) + SPB(J,K)
10  CONTINUE
          RETURN
          END
C

```

GAUS0001
GAUS0002

```

SUBROUTINE GAUSOL
C
C * THIS SUBROUTINE SOLVES A SYSTEM OF NUMEL ALGEBRAIC EQUATIONS BY
C * UPPER - DIAGONAL - UPPER GAUSSIAN ELIMINATION. THE INPUT MATRICES
C * FOR THE SUBPROGRAM ARE THE GLOBAL MATRIX SK AND THE FORCE VECTOR F
C * . THE OUTPUT SOLUTION IS THE CHANGE OF HEAD .....
C
COMMON /C7 / SPB(6,6),SMB(6,6),BHS(6,6),SK(160,25)
COMMON /C9 / IBAND,IDIAG,NUMNP,NUMEL,NNPE,NUMQPT,ISST
COMMON /C13 / DGS(160),HE(160),HK(160),HELD(160),H(160),F(160)
C
NEM1 = NUMNP - 1
DO 30 I = 1,NEM1
C * AN EXPONENT UNDERFLOW ERROR WILL OCCUR HERE IF AN ERROR RESETTING
C * ROUTINE IS NOT CALLED FROM THE SYSTEM LIBRARY .....
C
CALL TRAPS (100,100,100,100,100)
B = 1.0 / SK(I,1)
JEND = NUMNP - I + 1
IF (JEND.GT.IBAND) JEND = IBAND
DO 20 J = 2,JEND
J1 = I + J - 1
FAC = SK(I,J) * B
K1 = 0
DO 10 K = J,JEND
K1 = K1 + 1
C * AN EXPONENT UNDERFLOW ERROR WILL OCCUR HERE IF AN ERROR RESETTING
C * ROUTINE IS NOT CALLED FROM THE SYSTEM LIBRARY .....
CALL TRAPS (100,100,100,100,100)
SK(J1,K1) = SK(J1,K1) - SK(I,K) * FAC
10 CONTINUE
SK(I,J) = FAC
F(J1) = F(J1) - F(I) * SK(I,J)
20 CONTINUE
F(I) = F(I)/SK(I,1)
30 CONTINUE
F(NUMNP) = F(NUMNP)/SK(NUMNP,1)
C
C
C BACK SUBSTITUTION
DO 50 I = 1,NEM1
I1 = NUMNP - I
JEND = NUMNP - I1 + 1
IF (JEND.GT.IBAND) JEND = IBAND
RHS = F(I1)
DO 40 J = 2,JEND
J1 = I1 + J - 1
C * AN EXPONENT UNDERFLOW ERROR WILL OCCUR HERE IF AN ERROR RESETTING
C * ROUTINE IS NOT CALLED FROM THE SYSTEM LIBRARY .....
CALL TRAPS (100,100,100,100,100)
RHS = RHS - SK(I1,J) * F(J1)
40 CONTINUE
F(I1) = RHS
50 CONTINUE
RETURN
END
C
SUBROUTINE SHAPFN
C
C * THIS SUBROUTINE DEFINES THE QUADRATURE POINTS QPT WITH RESPECT TO
C * THE LOCAL COORDINATES X AND Y , THE MAGNITUDES OF THE WEIGHTING
C * FUNCTIONS WT AND SETS UP THE VALUES OF THE SHAPE FUNCTIONS N AND
C * THEIR DERIVATIVES WITH RESPECT TO LOCAL COORDINATE SYSTEM AT EACH
C * QUADRATURE LOCATION .....
C
COMMON /C6 / SF(3,6,7),WT(7),QPT(7,3),NPCS(3,35),NP(160,6)
COMMON /C9 / IBAND,IDIAG,NUMNP,NUMEL,NNPE,NUMQPT,ISST
C
C DEFINE QUADRATURE VALUES ... THERE ARE SEVEN QUADRATURE LOCATIONS IN
C THE TRIANGULAR ELEMENT

```

```

GAUS0003
GAUS0004
*GAUS0005
*GAUS0006
*GAUS0007
*GAUS0008
GAUS0009
GAUS0010
GAUS0011
GAUS0012
GAUS0013
GAUS0014
GAUS0015
*GAUS0016
*GAUS0017
GAUS0018
GAUS0019
GAUS0020
GAUS0021
GAUS0022
GAUS0023
GAUS0024
GAUS0025
GAUS0026
GAUS0027
GAUS0028
*GAUS0029
*GAUS0030
GAUS0031
GAUS0032
GAUS0033
GAUS0034
GAUS0035
GAUS0036
GAUS0037
GAUS0038
GAUS0039
GAUS0040
GAUS0041
GAUS0042
GAUS0043
GAUS0044
GAUS0045
GAUS0046
GAUS0047
GAUS0048
GAUS0049
*GAUS0050
*GAUS0051
GAUS0052
GAUS0053
GAUS0054
GAUS0055
GAUS0056
GAUS0057
SHAPF001
SHAPF002
SHAPF003
SHAPF004
*SHAPF005
*SHAPF006
*SHAPF007
*SHAPF008
*SHAPF009
SHAPF010
SHAPF011
SHAPF012
SHAPF013
SHAPF014
SHAPF015

```

```

C
QPT(1,1) = 1.0/3.0
QPT(1,2) = 1.0/3.0
QPT(2,1) = 0.5
QPT(2,2) = 0.5
QPT(3,1) = 0.0
QPT(3,2) = 0.5
QPT(4,1) = 0.5
QPT(4,2) = 0.0
QPT(5,1) = 1.0
QPT(5,2) = 0.0
QPT(6,1) = 0.0
QPT(6,2) = 1.0
QPT(7,1) = 0.0
QPT(7,2) = 0.0

C
C DEFINE WEIGHTING FUNCTIONS
C
WT(1) = 9.0/40.0
WT(2) = 1.0/15.0
WT(3) = WT(2)
WT(4) = WT(2)
WT(5) = 0.025
WT(6) = WT(5)
WT(7) = WT(5)

C
DO 10 I = 1, NUMQPT
  QPT(I,3) = 1.0 - QPT(I,1) - QPT(I,2)
10 CONTINUE

C
C DEFINE SHAPE FUNCTIONS AND THEIR DERIVATIVES
C
DO 30 J = 1, NUMQPT
  DO 20 I = 1, NNPE
    SF(1,I,J) = SFN(QPT(J,1), QPT(J,2), QPT(J,3), I)
    SF(2,I,J) = SFNXI(QPT(J,1), QPT(J,2), QPT(J,3), I)
    SF(3,I,J) = SFNETA(QPT(J,1), QPT(J,2), QPT(J,3), I)
20 CONTINUE
30 CONTINUE
RETURN
END

C
FUNCTION SFN(XI, ETA, ZETA, N)
C
C * THIS SUBPROGRAM EVALUATES THE SHAPE FUNCTION AT A GIVEN POINT.
C * INPUT PARAMETERS ARE THE QUADRATURE COORDINATES XI , ETA AND ZETA
C * OF THE NODAL POINT N .....
C
GO TO ( 10, 20, 30, 40, 50, 60 ), N
10 SFN = (2.0 * XI - 1.0) * XI
RETURN
20 SFN = 4.0 * ETA * XI
RETURN
30 SFN = (2.0 * ETA - 1.0) * ETA
RETURN
40 SFN = 4.0 * ETA * ZETA
RETURN
50 SFN = (2.0 * ZETA - 1.0) * ZETA
RETURN
60 SFN = 4.0 * XI * ZETA
RETURN
END

C
FUNCTION SFNETA(XI, ETA, ZETA, N)
C
C * THIS SUBPROGRAM EVALUATES THE DERIVATIVE OF THE SHAPE FUNCTION
C * WITH RESPECT TO ONE AXIS OF THE GLOBAL COORDINATE SYSTEM XI. INPUT
C * PARAMETERS ARE THE QUADRATURE COORDINATES XI, ETA AND ZETA OF THE
C * NODAL POINT N .....
C

```

```

SHAPFO16
SHAPFO17
SHAPFO18
SHAPFO19
SHAPFO20
SHAPFO21
SHAPFO22
SHAPFO23
SHAPFO24
SHAPFO25
SHAPFO26
SHAPFO27
SHAPFO28
SHAPFO29
SHAPFO30
SHAPFO31
SHAPFO32
SHAPFO33
SHAPFO34
SHAPFO35
SHAPFO36
SHAPFO37
SHAPFO38
SHAPFO39
SHAPFO40
SHAPFO41
SHAPFO42
SHAPFO43
SHAPFO44
SHAPFO45
SHAPFO46
SHAPFO47
SHAPFO48
SHAPFO49
SHAPFO50
SHAPFO51
SHAPFO52
SHAPFO53
SHAPFO54
SHAPFO55
FNSFN001
FNSFN002
FNSFN003
FNSFN004
FNSFN005
FNSFN006
FNSFN007
FNSFN008
FNSFN009
FNSFN010
FNSFN011
FNSFN012
FNSFN013
FNSFN014
FNSFN015
FNSFN016
FNSFN017
FNSFN018
FNSFN019
FNSFN020
FNSFN021
SFNETO01
SFNETO02
SFNETO03
SFNETO04
SFNETO05
SFNETO06
SFNETO07
SFNETO08
SFNETO09

```

```

      GO TO (10,20,30,40,50,60), N
10  SFNETA = 0.0
      RETURN
20  SFNETA = 4.0 * XI
      RETURN
30  SFNETA = 4.0 * ETA - 1.0
      RETURN
40  SFNETA = 4.0 * ZETA - 4.0 * ETA
      RETURN
50  SFNETA = - 4.0 * ZETA + 1.0
      RETURN
60  SFNETA = - 4.0 * XI
      RETURN
      END
C
      FUNCTION SFNXI(XI,ETA,ZETA,N)
C
C * THIS SUBPROGRAM EVALUATES THE DERIVATIVE OF THE SHAPE FUNCTION
C * WITH RESPECT TO ONE AXIS OF THE GLOBAL COORDINATE SYSTEM ETA.INPUT
C * PARAMETERS ARE THE QUADRATUE COORDINATES XI, ETA AND ZETA OF THE
C * NODAL POINT N .....
C
      GO TO (10, 20, 30, 40, 50, 60), N
10  SFNXI = 4.0 * XI - 1.0
      RETURN
20  SFNXI = 4.0 * ETA
      RETURN
30  SFNXI = 0.0
      RETURN
40  SFNXI = - 4.0 * ETA
      RETURN
50  SFNXI = - 4.0 * ZETA + 1.0
      RETURN
60  SFNXI = 4.0 * ZETA - 4.0 * XI
      RETURN
      END
C
      SUBROUTINE INTELV
C
C * THIS SUBROUTINE UPDATES THE ELEVATION OF THE INTERFACE BY APPLYING
C * THE DYNAMIC BOUNDARY CONDITION ACROSS THE INTERFACE .....
C
      COMMON/C1/HF(160),HS(160),PSI(160),DHS(160),DHF(160),R(160)
      COMMON /C3 / XORD(160),YORD(160),NPBC(160),B(160),MAT(62)
      COMMON /C9 / IBAND,IDIAG,NUMNP,NUMEL,NNPE,NUMQPT,ISST
      COMMON /C10 / INCR,NAQTYP,NSS,NCAP,NCS,NPHASE
      COMMON /C14 /SPIJ(60),GS,GF,DLTG,NQXYF,NQXYS
      COMMON /C15 /HFST(160),HSST(160),PSS(160),HKLD(160)
C
      IF (NAQTYP.EQ.0) GO TO 30
C
      DO 20 I = 1,NUMNP
        R(I) = (GS * DHS(I) - GF * DHF(I))
        PSI(I) = PSI(I) + R(I)
        IF (PSI(I).GE.0.0) GO TO 10
        PSI(I) = 0.0
C
C
      GO TO 20
10  CONTINUE
      IF (PSI(I).LT.B(I)) GO TO 20
      PSI(I) = B(I)
C
C
20  CONTINUE
      RETURN
C
30  CONTINUE
C
      DO 40 I = 1,NUMNP

```

```

SFNETO10
SFNETO11
SFNETO12
SFNETO13
SFNETO14
SFNETO15
SFNETO16
SFNETO17
SFNETO18
SFNETO19
SFNETO20
SFNETO21
SFNETO22
SFNXIO01
SFNXIO02
SFNXIO03
SFNXIO04
*SFNXIO05
*SFNXIO06
*SFNXIO07
*SFNXIO08
SFNXIO09
SFNXIO10
SFNXIO11
SFNXIO12
SFNXIO13
SFNXIO14
SFNXIO15
SFNXIO16
SFNXIO17
SFNXIO18
SFNXIO19
SFNXIO20
SFNXIO21
SFNXIO22
INTELO01
INTELO02
INTELO03
INTELO04
*INTELO05
*INTELO06
INTELO07
INTELO08
INTELO09
INTELO10
INTELO11
INTELO12
INTELO13
INTELO14
INTELO15
INTELO16
INTELO17
INTELO18
INTELO19
INTELO20
INTELO21
INTELO22
INTELO23
INTELO24
INTELO25
INTELO26
INTELO27
INTELO28
INTELO29
INTELO30
INTELO31
INTELO32
INTELO33
INTELO34
INTELO35

```

```

      PSI(I) = (GS * HS(I) - GF * HF(I))
      IF (PSI(I).LE.O.O) PSI(I) = O.O
40  CONTINUE
C
      RETURN
      END
C
      SUBROUTINE CAPRES(IT,ICOUNT)
C
C * SUBROUTINE CAPRES EVALUATES THE SATURATED AND PERMEABLE HEIGHTS AS
C * A FUNCTION OF THE ELEVATION WHEN THE INFILTRATION RATE IS NON-ZERO
C
      COMMON/C1/HF(160),HS(160),PSI(160),DHS(160),DHF(160),R(160)
      COMMON /C2/ QNODF(160),QNODS(160),QXYF(62),QXYS(62),QNOD,QXY
      COMMON /C3 / XORD(160),YORD(160),NPBC(160),B(160),MAT(62)
      COMMON /C4 / BETA,ZETA,TKX,TKY,KX(62),KY(62)
      COMMON /C5 / PHIJ(62),SYIJ(62),SY(160),SYS(160)
      COMMON /C6 / SF(3,6,7),WT(7),QPT(7,3),NPCS(3,35),NP(160,6)
      COMMON /C9 / IBAND,IDIAG,NUMNP,NUMEL,NNPE,NUMQPT,ISST
      COMMON /C10 / INCR,NAQTYP,NSS,NCAP,NCS,NPHASE
      COMMON /C11 / TIME(31),DTIME(31),TMAX,THETA,ITER,DMAX,EPSX,FTIME
      COMMON /C12 / GAMAF,GAMAS,BUBPH,LAMDA,SPS,DHST,DFMAX,DSMAX
      COMMON /C13 / DGS(160),HE(160),HK(160),HELD(160),H(160),F(160)
      COMMON /C15 /HFST(160),HSST(160),PSS(160),HKLD(160)
      REAL KX,KY,LAMDA
C
      PETA = 2.0 + 3.0 * LAMDA
      CONST1 = (1.0+2.0*PETA+LAMDA)/(LAMDA+1.0)
      CONST2 = LAMDA/PETA
      CONST3 = -1.0 *(LAMDA+1.0)/PETA
      CONST4 = 1.0 + 1.0/(2.0*PETA)
      CONST5 = (LAMDA - 1.0)/PETA
      DO 40 I = 1,NUMEL
      QSCALE = QXYF(I)/KX(MAT(I))
      DO 30 J = 1,NNPE
      NPJ = NP(I,J)
      DGSD = DGS(NPJ) - HF(NPJ)
      DWTD = DGSD/BUBPH
      IF(DWTD.LT.1.0) GO TO 20
      HK(NPJ) = BUBPH *(PETA-DWTD**((1.0-PETA)))/(PETA-1.0)
      IF(QSCALE.NE.O.O) GO TO 10
      HE(NPJ) = BUBPH *((DWTD**((1.0-LAMDA))-LAMDA)/(1.0-LAMDA)
      GO TO 30
10  CONTINUE
      HE(NPJ) = BUBPH *((1.0-QSCALE**CONST2)/(1.0-QSCALE)+(QSCALE**
      1CONST2)*DWTD+(1.0/(2.0*PETA))*(CONST1*((QSCALE**CONST3)-1.0)+
      2(1.0-QSCALE)**2.0)-((QSCALE**CONST5)*CONST4+((QSCALE**CONST2)/
      3(2.0*PETA))*(QSCALE**2.0-2.0*QSCALE-2.0*PETA)))
      GO TO 30
20  CONTINUE
      HK(NPJ) = DGSD
      HE(NPJ) = DGSD
30  CONTINUE
40  CONTINUE
      IF(IT.EQ.1.AND.NSS.EQ.O) GO TO 60
      DO 50 I=1,NUMNP
      DHE = HE(I) - HELD(I)
      SY(I) = SY(I) * (1.0+(DHE/DHF(I)))
50  CONTINUE
60  IF(IT.NE.1.AND.NSS.EQ.O) GO TO 80
      IF (ICOUNT.EQ.2) GO TO 80
      DO 70 I=1,NUMNP
      HELD(I) = HE(I)
      HKLD(I) = HK(I)
70  CONTINUE
80  RETURN
      END
C
      SUBROUTINE CHECK
C

```

INTELO36
INTELO37
INTELO38
INTELO39
INTELO40
CAPREO01
CAPREO02
CAPREO03
CAPREO04
CAPREO05
CAPREO06
CAPREO07
CAPREO08
CAPREO09
CAPREO10
CAPREO11
CAPREO12
CAPREO13
CAPREO14
CAPREO15
CAPREO16
CAPREO17
CAPREO18
CAPREO19
CAPREO20
CAPREO21
CAPREO22
CAPREO23
CAPREO24
CAPREO25
CAPREO26
CAPREO27
CAPREO28
CAPREO29
CAPREO30
CAPREO31
CAPREO32
CAPREO33
CAPREO34
CAPREO35
CAPREO36
CAPREO37
CAPREO38
CAPREO39
CAPREO40
CAPREO41
CAPREO42
CAPREO43
CAPREO44
CAPREO45
CAPREO46
CAPREO47
CAPREO48
CAPREO49
CAPREO50
CAPREO51
CAPREO52
CAPREO53
CAPREO54
CAPREO55
CAPREO56
CAPREO57
CAPREO58
CAPREO59
CAPREO60
CAPREO61
CHECKO01
CHECKO02
CHECKO03
CHECKO04

```

C * THIS ROUTINE COMPUTES THE CHANGE OF INTERFACE ELEVATION AT ALL *CHECKK005
C * AND COMPARES THEM TO RETAIN THE MAXIMUM CHANGE IN ORDER TO CHECK *CHECKK006
C * FOR STEADY STATE ..... *CHECKK007
C CHECKK008
COMMON/C1/HF(160),HS(160),PSI(160),DHS(160),DHF(160),R(160) CHECKK009
COMMON /C9 / IBAND,IDIAG,NUMNP,NUMEL,NNPE,NUMQPT,ISST CHECKK010
COMMON /C11 / TIME(31),DTIME(31),TMAX,THETA,ITER,DMAX,EPSX,FTIME CHECKK011
COMMON /C15 /HFST(160),HSST(160),PSS(160),HKLD(160) CHECKK012
C CHECKK013
DMAX = 0.0 CHECKK014
DO 20 I = 1,NUMNP CHECKK015
DHSS = ABS ( R(I) ) CHECKK016
IF (DHSS .LT. DMAX) GO TO 10 CHECKK017
DMAX = DHSS CHECKK018
10 PSS(I)=PSI(I) CHECKK019
20 CONTINUE CHECKK020
RETURN CHECKK021
END HEADCO01
C HEADCO02
SUBROUTINE HEADCH(LO) HEADCO03
C HEADCO04
C * THIS SUBROUTINE COMPUTES THE CHANGES OF THE FRESH-WATER HEAD AT *HEADCO05
C * ALL NODES AND COMPARES THEM TO RETAIN THE MAXIMUM CHANGE IN ORDER *HEADCO06
C * TO CHECK FOR CONVERGENCE WITHIN A TIME STEP . IF CONVERGENCE IS *HEADCO07
C * REACHED , THEN THE PROGRAM PROCEEDS TO THE NEXT TIME STEP . THE *HEADCO08
C * SAME PROCEDURE IS FOLLOWED FOR THE SALT-WATER REGION ALSO ..... *HEADCO09
COMMON/C1/HF(160),HS(160),PSI(160),DHS(160),DHF(160),R(160) HEADCO10
COMMON /C9 / IBAND,IDIAG,NUMNP,NUMEL,NNPE,NUMQPT,ISST HEADCO11
COMMON /C12 / GAMAF,GAMAS,BUBPH,LAMDA,SPS,DHST,DFMAX,DSMAX HEADCO12
COMMON /C13 / DGS(160),HE(160),HK(160),HELD(160),H(160),F(160) HEADCO13
C HEADCO14
GO TO (10,30), LO HEADCO15
10 DFMAX = 0.0 HEADCO16
DO 20 I = 1,NUMNP HEADCO17
DHSS = ABS ( H(I) - HF(I) ) HEADCO18
IF (DHSS .LT. DFMAX) GO TO 20 HEADCO19
DFMAX = DHSS HEADCO20
20 CONTINUE HEADCO21
C HEADCO22
GO TO 50 HEADCO23
30 DSMAX = 0.0 HEADCO24
DO 40 I=1,NUMNP HEADCO25
DHSS=ABS(H(I)-HS(I)) HEADCO26
IF(DHSS.LT.DSMAX) GO TO 40 HEADCO27
DSMAX=DHSS HEADCO28
40 CONTINUE HEADCO29
50 RETURN HEADCO30
END TSTEP001
C SUBROUTINE TSTEP TSTEP002
C TSTEP003
C * THIS SUBROUTINE ESTABLISHES OPTIMUM TIME INCREMENTS WITH THE HELP *TSTEP005
C * OF AN ACCELERATION FACTOR ..... *TSTEP006
C TSTEP007
COMMON /C11 / TIME(31),DTIME(31),TMAX,THETA,ITER,DMAX,EPSX,FTIME TSTEP008
C TSTEP009
IT = ITER +1 TSTEP010
DXAPP = TMAX / FLOAT(ITER) TSTEP011
TIME(1) = FTIME TSTEP012
DO 10 I=2,IT TSTEP013
TIME(I) = TIME(I-1) + DXAPP TSTEP014
DXAPP = DXAPP * EPSX TSTEP015
10 CONTINUE TSTEP016
FACT = TMAX / TIME(IT) TSTEP017
DO 20 I=2,IT TSTEP018
TIME(I) = TIME(I) * FACT TSTEP019
DTIME(I-1) = TIME(I) - TIME(I-1) TSTEP020
20 CONTINUE TSTEP021
C TSTEP022
RETURN TSTEP023

```

APPENDIX D

INPUT DATA FOR NUMERICAL SIMULATION

TABLE I (CONTD.)

57	0	17.3513	1.1373	60.96	54.7223	35.5
58	0	14.1890	1.8680	60.96	54.7223	35.5
59	0	17.2397	2.2697	60.96	54.7223	35.5
60	0	20.9465	-2.7577	60.96	54.7223	35.5
61	0	25.4504	-3.3506	60.96	54.7223	35.5
62	0	21.0821	-1.3818	60.96	54.7223	35.5
63	0	25.6150	-1.6789	60.96	54.7223	35.5
64	0	21.1273	0.0	60.96	54.7223	35.5
65	0	25.6699	0.0	60.96	54.7223	35.5
66	0	21.0821	1.3818	60.96	54.7223	35.5
67	0	25.6150	1.6789	60.96	54.7223	35.5
68	0	20.9465	2.7577	60.96	54.7223	35.5
69	0	25.4504	3.3506	60.96	54.7223	35.5
70	0	30.9226	-4.0710	60.96	54.7223	35.5
71	0	37.5713	-4.9464	60.96	54.7223	35.5
72	0	31.1226	-2.0399	60.96	54.7223	35.5
73	0	37.8143	-2.4785	60.96	54.7223	35.5
74	0	31.1894	0.0	60.96	54.7223	35.5
75	0	37.8955	0.0	60.96	54.7223	35.5
76	0	31.1226	2.0399	60.96	54.7223	35.5
77	0	37.8143	2.4785	60.96	54.7223	35.5
78	0	30.9226	4.0710	60.96	54.7223	35.5
79	0	37.5713	4.9464	60.96	54.7223	35.5
80	0	45.6497	-6.0099	60.96	54.7223	35.5
81	0	55.4650	-7.3021	60.96	54.7223	35.5
82	0	45.9450	-3.0114	60.96	54.7223	35.5
83	0	55.8238	-3.6589	60.96	54.7223	35.5
84	0	46.9436	0.0	60.96	54.7223	35.5
85	0	55.9436	0.0	60.96	54.7223	35.5
86	0	45.9450	3.0114	60.96	54.7223	35.5
87	0	55.8238	3.6589	60.96	54.7223	35.5
88	0	45.6497	6.0099	60.96	54.7223	35.5
89	0	55.4650	7.3021	60.96	54.7223	35.5
90	0	67.3907	-8.8722	60.96	54.7223	35.5
91	0	81.8806	-10.7798	60.96	54.7223	35.5
92	0	67.8267	-4.4456	60.96	54.7223	35.5
93	0	82.4104	-5.4015	60.96	54.7223	35.5
94	0	67.9722	0.0	60.96	54.7223	35.5
95	0	82.5872	0.0	60.96	54.7223	35.5
96	0	67.8267	4.4456	60.96	54.7223	35.5
97	0	82.4104	5.4015	60.96	54.7223	35.5
98	0	67.3907	8.8722	60.96	54.7223	35.5
99	0	81.8806	10.7798	60.96	54.7223	35.5
100	0	99.4861	-13.0976	60.96	54.7223	35.5
101	1	120.8769	-15.9138	60.96	54.7223	35.5
102	0	100.1297	-6.5629	60.96	54.7223	35.5
103	1	121.6589	-7.9740	60.96	54.7223	35.5
104	0	100.3446	0.0	60.96	54.7223	35.5
105	1	121.9200	0.0	60.96	54.7223	35.5
106	0	100.1297	6.5629	60.96	54.7223	35.5
107	1	121.6589	7.9740	60.96	54.7223	35.5
108	0	99.4861	13.0976	60.96	54.7223	35.5
109	1	120.8769	15.9138	60.96	54.7223	35.5
1	1	2	3	5	6	4
2	1	4	6	7	9	8
3	6	5	3	10	11	12
4	6	12	11	13	15	14
5	6	14	15	17	19	16
6	6	16	19	18	9	7
7	15	13	11	20	21	22
8	15	22	21	23	25	24
9	15	24	25	27	29	26
10	15	26	29	28	19	17
11	25	23	21	30	31	32
12	25	32	31	33	35	34

TABLE I (CONTD.)

13	25	34	35	37	39	36
14	25	36	39	38	29	27
15	35	33	31	40	41	42
16	35	42	41	43	45	44
17	35	44	45	47	49	46
18	35	46	49	48	39	37
19	45	43	41	50	51	52
20	45	52	51	53	55	54
21	45	54	55	57	59	56
22	45	56	59	58	49	47
23	55	53	51	60	61	62
24	55	62	61	63	65	64
25	55	64	65	67	69	66
26	55	66	69	68	59	57
27	65	63	61	70	71	72
28	65	72	71	73	75	74
29	65	74	75	77	79	76
30	65	76	79	78	69	67
31	75	73	71	80	81	82
32	75	82	81	83	85	84
33	75	84	85	87	89	86
34	75	86	89	88	79	77
35	85	83	81	90	91	92
36	85	92	91	93	95	94
37	85	94	95	97	99	96
38	85	96	99	98	89	87
39	95	93	91	100	101	102
40	95	102	101	103	105	104
41	95	104	105	107	109	106
42	95	106	109	108	99	97
1	-11.5					

TABLE II (CONTD.)

57	0	17.3513	1.1373	60.96	54.7223	35.5
58	0	14.1890	1.8680	60.96	54.7223	35.5
59	0	17.2397	2.2697	60.96	54.7223	35.5
60	0	20.9465	-2.7577	60.96	54.7223	35.5
61	0	25.4504	-3.3506	60.96	54.7223	35.5
62	0	21.0821	-1.3818	60.96	54.7223	35.5
63	0	25.6150	-1.6789	60.96	54.7223	35.5
64	0	21.1273	0.0	60.96	54.7223	35.5
65	0	25.6699	0.0	60.96	54.7223	35.5
66	0	21.0821	1.3818	60.96	54.7223	35.5
67	0	25.6150	1.6789	60.96	54.7223	35.5
68	0	20.9465	2.7577	60.96	54.7223	35.5
69	0	25.4504	3.3506	60.96	54.7223	35.5
70	0	30.9226	-4.0710	60.96	54.7223	35.5
71	0	37.5713	-4.9464	60.96	54.7223	35.5
72	0	31.1226	-2.0399	60.96	54.7223	35.5
73	0	37.8143	-2.4785	60.96	54.7223	35.5
74	0	31.1894	0.0	60.96	54.7223	35.5
75	0	37.8955	0.0	60.96	54.7223	35.5
76	0	31.1226	2.0399	60.96	54.7223	35.5
77	0	37.8143	2.4785	60.96	54.7223	35.5
78	0	30.9226	4.0710	60.96	54.7223	35.5
79	0	37.5713	4.9464	60.96	54.7223	35.5
80	0	45.6497	-6.0099	60.96	54.7223	35.5
81	0	55.4650	-7.3021	60.96	54.7223	35.5
82	0	45.9450	-3.0114	60.96	54.7223	35.5
83	0	55.8238	-3.6589	60.96	54.7223	35.5
84	0	46.9436	0.0	60.96	54.7223	35.5
85	0	55.9436	0.0	60.96	54.7223	35.5
86	0	45.9450	3.0114	60.96	54.7223	35.5
87	0	55.8238	3.6589	60.96	54.7223	35.5
88	0	45.6497	6.0099	60.96	54.7223	35.5
89	0	55.4650	7.3021	60.96	54.7223	35.5
90	0	67.3907	-8.8722	60.96	54.7223	35.5
91	0	81.8806	-10.7798	60.96	54.7223	35.5
92	0	67.8267	-4.4456	60.96	54.7223	35.5
93	0	82.4104	-5.4015	60.96	54.7223	35.5
94	0	67.9722	0.0	60.96	54.7223	35.5
95	0	82.5872	0.0	60.96	54.7223	35.5
96	0	67.8267	4.4456	60.96	54.7223	35.5
97	0	82.4104	5.4015	60.96	54.7223	35.5
98	0	67.3907	8.8722	60.96	54.7223	35.5
99	0	81.8806	10.7798	60.96	54.7223	35.5
100	0	99.4861	-13.0976	60.96	54.7223	35.5
101	1	120.8769	-15.9138	60.96	54.7223	35.5
102	0	100.1297	-6.5629	60.96	54.7223	35.5
103	1	121.6589	-7.9740	60.96	54.7223	35.5
104	0	100.3446	0.0	60.96	54.7223	35.5
105	1	121.9200	0.0	60.96	54.7223	35.5
106	0	100.1297	6.5629	60.96	54.7223	35.5
107	1	121.6589	7.9740	60.96	54.7223	35.5
108	0	99.4861	13.0976	60.96	54.7223	35.5
109	1	120.8769	15.9138	60.96	54.7223	35.5
1	1	2	3	5	6	4
2	1	4	6	7	9	8
3	6	5	3	10	11	12
4	6	12	11	13	15	14
5	6	14	15	17	19	16
6	6	16	19	18	9	7
7	15	13	11	20	21	22
8	15	22	21	23	25	24
9	15	24	25	27	29	26
10	15	26	29	28	19	17
11	25	23	21	30	31	32
12	25	32	31	33	35	34

TABLE II (CONTD.)

13	25	34	35	37	39	36
14	25	36	39	38	29	27
15	35	33	31	40	41	42
16	35	42	41	43	45	44
17	35	44	45	47	49	46
18	35	46	49	48	39	37
19	45	43	41	50	51	52
20	45	52	51	53	55	54
21	45	54	55	57	59	56
22	45	56	59	58	49	47
23	55	53	51	60	61	62
24	55	62	61	63	65	64
25	55	64	65	67	69	66
26	55	66	69	68	59	57
27	65	63	61	70	71	72
28	65	72	71	73	75	74
29	65	74	75	77	79	76
30	65	76	79	78	69	67
31	75	73	71	80	81	82
32	75	82	81	83	85	84
33	75	84	85	87	89	86
34	75	86	89	88	79	77
35	85	83	81	90	91	92
36	85	92	91	93	95	94
37	85	94	95	97	99	96
38	85	96	99	98	89	87
39	95	93	91	100	101	102
40	95	102	101	103	105	104
41	95	104	105	107	109	106
42	95	106	109	108	99	97
1	-15.51					
2	-15.51					

TABLE III (CONTD.)

56	0	14.2808	0.9360	60.96	54.7223	35.5
57	0	17.3513	1.1373	60.96	54.7223	35.5
58	0	14.1890	1.8680	60.96	54.7223	35.5
59	0	17.2397	2.2697	60.96	54.7223	35.5
60	0	20.9465	-2.7577	60.96	54.7223	35.5
61	0	25.4504	-3.3506	60.96	54.7223	35.5
62	0	21.0821	-1.3818	60.96	54.7223	35.5
63	0	25.6150	-1.6789	60.96	54.7223	35.5
64	0	21.1273	0.0	60.96	54.7223	35.5
65	0	25.6699	0.0	60.96	54.7223	35.5
66	0	21.0821	1.3818	60.96	54.7223	35.5
67	0	25.6150	1.6789	60.96	54.7223	35.5
68	0	20.9465	2.7577	60.96	54.7223	35.5
69	0	25.4504	3.3506	60.96	54.7223	35.5
70	0	30.9226	-4.0710	60.96	54.7223	35.5
71	0	37.5713	-4.9464	60.96	54.7223	35.5
72	0	31.1226	-2.0399	60.96	54.7223	35.5
73	0	37.8143	-2.4785	60.96	54.7223	35.5
74	0	31.1894	0.0	60.96	54.7223	35.5
75	0	37.8955	0.0	60.96	54.7223	35.5
76	0	31.1226	2.0399	60.96	54.7223	35.5
77	0	37.8143	2.4785	60.96	54.7223	35.5
78	0	30.9226	4.0710	60.96	54.7223	35.5
79	0	37.5713	4.9464	60.96	54.7223	35.5
80	0	45.6497	-6.0099	60.96	54.7223	35.5
81	0	55.4650	-7.3021	60.96	54.7223	35.5
82	0	45.9450	-3.0114	60.96	54.7223	35.5
83	0	55.8238	-3.6589	60.96	54.7223	35.5
84	0	46.9436	0.0	60.96	54.7223	35.5
85	0	55.9436	0.0	60.96	54.7223	35.5
86	0	45.9450	3.0114	60.96	54.7223	35.5
87	0	55.8238	3.6589	60.96	54.7223	35.5
88	0	45.6497	6.0099	60.96	54.7223	35.5
89	0	55.4650	7.3021	60.96	54.7223	35.5
90	0	67.3907	-8.8722	60.96	54.7223	35.5
91	0	81.8806	-10.7798	60.96	54.7223	35.5
92	0	67.8267	-4.4456	60.96	54.7223	35.5
93	0	82.4104	-5.4015	60.96	54.7223	35.5
94	0	67.9722	0.0	60.96	54.7223	35.5
95	0	82.5872	0.0	60.96	54.7223	35.5
96	0	67.8267	4.4456	60.96	54.7223	35.5
97	0	82.4104	5.4015	60.96	54.7223	35.5
98	0	67.3907	8.8722	60.96	54.7223	35.5
99	0	81.8806	10.7798	60.96	54.7223	35.5
100	0	99.4861	-13.0976	60.96	54.7223	35.5
101	1	120.8769	-15.9138	60.96	54.7223	35.5
102	0	100.1297	-6.5629	60.96	54.7223	35.5
103	1	121.6589	-7.9740	60.96	54.7223	35.5
104	0	100.3446	0.0	60.96	54.7223	35.5
105	1	121.9200	0.0	60.96	54.7223	35.5
106	0	100.1297	6.5629	60.96	54.7223	35.5
107	1	121.6589	7.9740	60.96	54.7223	35.5
108	0	99.4861	13.0976	60.96	54.7223	35.5
109	1	120.8769	15.9138	60.96	54.7223	35.5
1	1	2	3	5	6	4
2	1	4	6	7	9	8
3	6	5	3	10	11	12
4	6	12	11	13	15	14
5	6	14	15	17	19	16
6	6	16	19	18	9	7
7	15	13	11	20	21	22
8	15	22	21	23	25	24
9	15	24	25	27	29	26
10	15	26	29	28	19	17
11	25	23	21	30	31	32

TABLE III (CONTD.)

12	25	32	31	33	35	34
13	25	34	35	37	39	36
14	25	36	39	38	29	27
15	35	33	31	40	41	42
16	35	42	41	43	45	44
17	35	44	45	47	49	46
18	35	46	49	48	39	37
19	45	43	41	50	51	52
20	45	52	51	53	55	54
21	45	54	55	57	59	56
22	45	56	59	58	49	47
23	55	53	51	60	61	62
24	55	62	61	63	65	64
25	55	64	65	67	69	66
26	55	66	69	68	59	57
27	65	63	61	70	71	72
28	65	72	71	73	75	74
29	65	74	75	77	79	76
30	65	76	79	78	69	67
31	75	73	71	80	81	82
32	75	82	81	83	85	84
33	75	84	85	87	89	86
34	75	86	89	88	79	77
35	85	83	81	90	91	92
36	85	92	91	93	95	94
37	85	94	95	97	99	96
38	85	96	99	98	89	87
39	95	93	91	100	101	102
40	95	102	101	103	105	104
41	95	104	105	107	109	106
42	95	106	109	108	99	97
1	-15.51					
2	-15.51					

TABLE IV (CONTD.)

57	0	11.7536	0.7704	60.96	00.0000	00.0
58	0	9.6115	1.2654	60.96	00.0000	00.0
59	0	11.6780	1.5374	60.96	00.0000	00.0
60	0	14.1890	-1.8680	60.96	00.0000	00.0
61	0	17.2397	-2.2697	60.96	00.0000	00.0
62	0	14.2808	-0.9360	60.96	00.0000	00.0
63	0	17.3513	-1.1373	60.96	00.0000	00.0
64	0	14.3114	0.0	60.96	00.0000	00.0
65	0	17.3885	0.0	60.96	00.0000	00.0
66	0	14.2808	0.9360	60.96	00.0000	00.0
67	0	17.3513	1.1373	60.96	00.0000	00.0
68	0	14.1890	1.8680	60.96	00.0000	00.0
69	0	17.2397	2.2697	60.96	00.0000	00.0
70	0	20.9465	-2.7577	60.96	00.0000	00.0
71	0	25.4504	-3.3506	60.96	00.0000	00.0
72	0	21.0821	-1.3818	60.96	00.0000	00.0
73	0	25.6150	-1.6789	60.96	00.0000	00.0
74	0	21.1273	0.0	60.96	00.0000	00.0
75	0	25.6699	0.0	60.96	00.0000	00.0
76	0	21.0821	1.3818	60.96	00.0000	00.0
77	0	25.6150	1.6789	60.96	00.0000	00.0
78	0	20.9465	2.7577	60.96	00.0000	00.0
79	0	25.4504	3.3506	60.96	00.0000	00.0
80	0	30.9226	-4.0710	60.96	00.0000	00.0
81	0	37.5713	-4.9464	60.96	00.0000	00.0
82	0	31.1226	-2.0399	60.96	00.0000	00.0
83	0	37.8143	-2.4785	60.96	00.0000	00.0
84	0	31.1894	0.0	60.96	00.0000	00.0
85	0	37.8955	0.0	60.96	00.0000	00.0
86	0	31.1226	2.0399	60.96	00.0000	00.0
87	0	37.8143	2.4785	60.96	00.0000	00.0
88	0	30.9226	4.0710	60.96	00.0000	00.0
89	0	37.5713	4.9464	60.96	00.0000	00.0
90	0	45.6497	-6.0099	60.96	00.0000	00.0
91	0	55.4650	-7.3021	60.96	00.0000	00.0
92	0	45.9450	-3.0114	60.96	00.0000	00.0
93	0	55.8238	-3.6589	60.96	00.0000	00.0
94	0	46.9436	0.0	60.96	00.0000	00.0
95	0	55.9436	0.0	60.96	00.0000	00.0
96	0	45.9450	3.0114	60.96	00.0000	00.0
97	0	55.8238	3.6589	60.96	00.0000	00.0
98	0	45.6497	6.0099	60.96	00.0000	00.0
99	0	55.4650	7.3021	60.96	00.0000	00.0
100	0	67.3907	-8.8722	60.96	00.0000	00.0
101	0	81.8806	-10.7798	60.96	00.0000	00.0
102	0	67.8267	-4.4456	60.96	00.0000	00.0
103	0	82.4104	-5.4015	60.96	00.0000	00.0
104	0	67.9722	0.0	60.96	00.0000	00.0
105	0	82.5872	0.0	60.96	00.0000	00.0
106	0	67.8267	4.4456	60.96	00.0000	00.0
107	0	82.4104	5.4015	60.96	00.0000	00.0
108	0	67.3907	8.8722	60.96	00.0000	00.0
109	0	81.8806	10.7798	60.96	00.0000	00.0
110	0	99.4861	-13.0976	60.96	00.0000	00.0
111	1	120.8769	-15.9138	60.96	00.0000	00.0
112	0	100.1297	-6.5629	60.96	00.0000	00.0
113	1	121.6589	-7.9740	60.96	00.0000	00.0
114	0	100.3446	0.0	60.96	00.0000	00.0
115	1	121.9200	0.0	60.96	00.0000	00.0
116	0	100.1297	6.5629	60.96	00.0000	00.0
117	1	121.6589	7.9740	60.96	00.0000	00.0
118	0	99.4861	13.0976	60.96	00.0000	00.0
119	1	120.8769	15.9138	60.96	00.0000	00.0
1	1	2	3	5	6	4
2	1	4	6	7	9	8

TABLE IV (CONTD.)

3	1	8	9	10	11	12
4	1	12	11	13	14	15
5	1	15	14	16	17	18
6	1	18	17	19	3	2
7	3	20	21	22	6	5
8	6	22	21	23	25	24
9	6	24	25	27	29	26
10	6	26	29	28	9	7
11	25	23	21	30	31	32
12	25	32	31	33	35	34
13	25	34	35	37	39	36
14	25	36	39	38	29	27
15	35	33	31	40	41	42
16	35	42	41	43	45	44
17	35	44	45	47	49	46
18	35	46	49	48	39	37
19	45	43	41	50	51	52
20	45	52	51	53	55	54
21	45	54	55	57	59	56
22	45	56	59	58	49	47
23	55	53	51	60	61	62
24	55	62	61	63	65	64
25	55	64	65	67	69	66
26	55	66	69	68	59	57
27	65	63	61	70	71	72
28	65	72	71	73	75	74
29	65	74	75	77	79	76
30	65	76	79	78	69	67
31	75	73	71	80	81	82
32	75	82	81	83	85	84
33	75	84	85	87	89	86
34	75	86	89	88	79	77
35	85	83	81	90	91	92
36	85	92	91	93	95	94
37	85	94	95	97	99	96
38	85	96	99	98	89	87
39	95	93	91	100	101	102
40	95	102	101	103	105	104
41	95	104	105	107	109	106
42	95	106	109	108	99	97
43	105	103	101	110	111	112
44	105	112	111	113	115	114
45	105	114	115	117	119	116
46	105	116	119	118	109	107
1	-0.6462					
2	-0.6462					
3	-0.6462					
4	-0.6462					
5	-0.6462					
6	-0.6462					

TABLE V (CONTD.)

56	0	9.6736	0.6340	60.96	00.0000	00.0	
57	0	11.7536	0.7704	60.96	00.0000	00.0	
58	0	9.6115	1.2654	60.96	00.0000	00.0	
59	0	11.6780	1.5374	60.96	00.0000	00.0	
60	0	14.1890	-1.8680	60.96	00.0000	00.0	
61	0	17.2397	-2.2697	60.96	00.0000	00.0	
62	0	14.2808	0.9360	60.96	00.0000	00.0	
63	0	17.3513	-1.1373	60.96	00.0000	00.0	
64	0	14.3114	0.0	60.96	00.0000	00.0	
65	0	17.3885	0.0	60.96	00.0000	00.0	
66	0	14.2808	0.9360	60.96	00.0000	00.0	
67	0	17.3513	1.1373	60.96	00.0000	00.0	
68	0	14.1890	1.8680	60.96	00.0000	00.0	
69	0	17.2397	2.2697	60.96	00.0000	00.0	
70	0	20.9465	-2.7577	60.96	00.0000	00.0	
71	0	25.4504	-3.3506	60.96	00.0000	00.0	
72	0	21.0821	-1.3818	60.96	00.0000	00.0	
73	0	25.6150	-1.6789	60.96	00.0000	00.0	
74	0	21.1273	0.0	60.96	00.0000	00.0	
75	0	25.6699	0.0	60.96	00.0000	00.0	
76	0	21.0821	1.3818	60.96	00.0000	00.0	
77	0	25.6150	1.6789	60.96	00.0000	00.0	
78	0	20.9465	2.7577	60.96	00.0000	00.0	
79	0	25.4504	3.3506	60.96	00.0000	00.0	
80	0	30.9226	-4.0710	60.96	00.0000	00.0	
81	0	37.5713	-4.9464	60.96	00.0000	00.0	
82	0	31.1226	-2.0399	60.96	00.0000	00.0	
83	0	37.8143	-2.4785	60.96	00.0000	00.0	
84	0	31.1894	0.0	60.96	00.0000	00.0	
85	0	37.8955	0.0	60.96	00.0000	00.0	
86	0	31.1226	2.0399	60.96	00.0000	00.0	
87	0	37.8143	2.4785	60.96	00.0000	00.0	
88	0	30.9226	4.0710	60.96	00.0000	00.0	
89	0	37.5713	4.9464	60.96	00.0000	00.0	
90	0	45.6497	-6.0099	60.96	00.0000	00.0	
91	0	55.4650	-7.3021	60.96	00.0000	00.0	
92	0	45.9450	-3.0114	60.96	00.0000	00.0	
93	0	55.8238	-3.6589	60.96	00.0000	00.0	
94	0	46.9436	0.0	60.96	00.0000	00.0	
95	0	55.9436	0.0	60.96	00.0000	00.0	
96	0	45.9450	3.0114	60.96	00.0000	00.0	
97	0	55.8238	3.6589	60.96	00.0000	00.0	
98	0	45.6497	6.0099	60.96	00.0000	00.0	
99	0	55.4650	7.3021	60.96	00.0000	00.0	
100	0	67.3907	-8.8722	60.96	00.0000	00.0	
101	0	81.8806	-10.7798	60.96	00.0000	00.0	
102	0	67.8267	-4.4456	60.96	00.0000	00.0	
103	0	82.4104	-5.4015	60.96	00.0000	00.0	
104	0	67.9722	0.0	60.96	00.0000	00.0	
105	0	82.5872	0.0	60.96	00.0000	00.0	
106	0	67.8267	4.4456	60.96	00.0000	00.0	
107	0	82.4104	5.4015	60.96	00.0000	00.0	
108	0	67.3907	8.8722	60.96	00.0000	00.0	
109	0	81.8806	10.7798	60.96	00.0000	00.0	
110	0	99.4861	-13.0976	60.96	00.0000	00.0	
111	1	120.8769	-15.9138	60.96	00.0000	00.0	
112	0	100.1297	-6.5629	60.96	00.0000	00.0	
113	1	121.6589	-7.9740	60.96	00.0000	00.0	
114	0	100.3446	0.0	60.96	00.0000	00.0	
115	1	121.9200	0.0	60.96	00.0000	00.0	
116	0	100.1297	6.5629	60.96	00.0000	00.0	
117	1	121.6589	7.9740	60.96	00.0000	00.0	
118	0	99.4861	13.0976	60.96	00.0000	00.0	
119	1	120.8769	15.9138	60.96	00.0000	00.0	
1	1		2	3	5	6	4

TABLE V (CONTD.)

2	1	4	6	7	9	8
3	1	8	9	10	11	12
4	1	12	11	13	14	15
5	1	15	14	16	17	18
6	1	18	17	19	3	2
7	3	20	21	22	6	5
8	6	22	21	23	25	24
9	6	24	25	27	29	26
10	6	26	29	28	9	7
11	25	23	21	30	31	32
12	25	32	31	33	35	34
13	25	34	35	37	39	36
14	25	36	39	38	29	27
15	35	33	31	40	41	42
16	35	42	41	43	45	44
17	35	44	45	47	49	46
18	35	46	49	48	39	37
19	45	43	41	50	51	52
20	45	52	51	53	55	54
21	45	54	55	57	59	56
22	45	56	59	58	49	47
23	55	53	51	60	61	62
24	55	62	61	63	65	64
25	55	64	65	67	69	66
26	55	66	69	68	59	57
27	65	63	61	70	71	72
28	65	72	71	73	75	74
29	65	74	75	77	79	76
30	65	76	79	78	69	67
31	75	73	71	80	81	82
32	75	82	81	83	85	84
33	75	84	85	87	89	86
34	75	86	89	88	79	77
35	85	83	81	90	91	92
36	85	92	91	93	95	94
37	85	94	95	97	99	96
38	85	96	99	98	89	87
39	95	93	91	100	101	102
40	95	102	101	103	105	104
41	95	104	105	107	109	106
42	95	106	109	108	99	97
43	105	103	101	110	111	112
44	105	112	111	113	115	114
45	105	114	115	117	119	116
46	105	116	119	118	109	107

1 -0.6462
2 -0.6462
3 -0.6462
4 -0.6462
5 -0.6462
6 -0.6462

TABLE VII (CONTD.)

55	0	150.0	5.08	6.7	0.0	0.0
56	0	165.0	0.00	6.7	0.0	0.0
57	0	165.0	1.27	6.7	0.0	0.0
58	0	165.0	2.54	6.7	0.0	0.0
59	0	165.0	3.81	6.7	0.0	0.0
60	0	165.0	5.08	6.7	0.0	0.0
61	0	180.0	0.00	6.7	0.0	0.0
62	0	180.0	1.27	6.7	0.0	0.0
63	0	180.0	2.54	6.7	0.0	0.0
64	0	180.0	3.81	6.7	0.0	0.0
65	0	180.0	5.08	6.7	0.0	0.0
66	0	195.0	0.00	6.7	0.0	0.0
67	0	195.0	1.27	6.7	0.0	0.0
68	0	195.0	2.54	6.7	0.0	0.0
69	0	195.0	3.81	6.7	0.0	0.0
70	0	195.0	5.08	6.7	0.0	0.0
71	0	210.0	0.00	6.7	0.0	0.0
72	0	210.0	1.27	6.7	0.0	0.0
73	0	210.0	2.54	6.7	0.0	0.0
74	0	210.0	3.81	6.7	0.0	0.0
75	0	210.0	5.08	6.7	0.0	0.0
76	0	225.0	0.00	6.7	0.0	0.0
77	0	225.0	1.27	6.7	0.0	0.0
78	0	225.0	2.54	6.7	0.0	0.0
79	0	225.0	3.81	6.7	0.0	0.0
80	0	225.0	5.08	6.7	0.0	0.0
81	0	240.0	0.00	6.7	0.0	0.0
82	0	240.0	1.27	6.7	0.0	0.0
83	0	240.0	2.54	6.7	0.0	0.0
84	0	240.0	3.81	6.7	0.0	0.0
85	0	240.0	5.08	6.7	0.0	0.0
86	0	255.0	0.00	6.7	0.0	0.0
87	0	255.0	1.27	6.7	0.0	0.0
88	0	255.0	2.54	6.7	0.0	0.0
89	0	255.0	3.81	6.7	0.0	0.0
90	0	255.0	5.08	6.7	0.0	0.0
91	0	270.0	0.00	6.7	0.0	0.0
92	0	270.0	1.27	6.7	0.0	0.0
93	0	270.0	2.54	6.7	0.0	0.0
94	0	270.0	3.81	6.7	0.0	0.0
95	0	270.0	5.08	6.7	0.0	0.0
96	0	285.0	0.00	6.7	0.0	0.0
97	0	285.0	1.27	6.7	0.0	0.0
98	0	285.0	2.54	6.7	0.0	0.0
99	0	285.0	3.81	6.7	0.0	0.0
100	0	285.0	5.08	6.7	0.0	0.0
101	0	300.0	0.00	6.7	0.0	0.0
102	0	300.0	1.27	6.7	0.0	0.0
103	0	300.0	2.54	6.7	0.0	0.0
104	0	300.0	3.81	6.7	0.0	0.0
105	0	300.0	5.08	6.7	0.0	0.0
106	0	315.0	0.00	6.7	0.0	0.0
107	0	315.0	1.27	6.7	0.0	0.0
108	0	315.0	2.54	6.7	0.0	0.0
109	0	315.0	3.81	6.7	0.0	0.0
110	0	315.0	5.08	6.7	0.0	0.0
111	0	330.0	0.00	6.7	0.0	0.0
112	0	330.0	1.27	6.7	0.0	0.0
113	0	330.0	2.54	6.7	0.0	0.0
114	0	330.0	3.81	6.7	0.0	0.0
115	0	330.0	5.08	6.7	0.0	0.0
116	0	345.0	0.00	6.7	0.0	0.0
117	0	345.0	1.27	6.7	0.0	0.0
118	0	345.0	2.54	6.7	0.0	0.0
119	0	345.0	3.81	6.7	0.0	0.0

TABLE VIII (CONTD.)

55	0	150.0	5.08	6.7	0.0	0.0
56	0	165.0	0.00	6.7	0.0	0.0
57	0	165.0	1.27	6.7	0.0	0.0
58	0	165.0	2.54	6.7	0.0	0.0
59	0	165.0	3.81	6.7	0.0	0.0
60	0	165.0	5.08	6.7	0.0	0.0
61	0	180.0	0.00	6.7	0.0	0.0
62	0	180.0	1.27	6.7	0.0	0.0
63	0	180.0	2.54	6.7	0.0	0.0
64	0	180.0	3.81	6.7	0.0	0.0
65	0	180.0	5.08	6.7	0.0	0.0
66	0	195.0	0.00	6.7	0.0	0.0
67	0	195.0	1.27	6.7	0.0	0.0
68	0	195.0	2.54	6.7	0.0	0.0
69	0	195.0	3.81	6.7	0.0	0.0
70	0	195.0	5.08	6.7	0.0	0.0
71	0	210.0	0.00	6.7	0.0	0.0
72	0	210.0	1.27	6.7	0.0	0.0
73	0	210.0	2.54	6.7	0.0	0.0
74	0	210.0	3.81	6.7	0.0	0.0
75	0	210.0	5.08	6.7	0.0	0.0
76	0	225.0	0.00	6.7	0.0	0.0
77	0	225.0	1.27	6.7	0.0	0.0
78	0	225.0	2.54	6.7	0.0	0.0
79	0	225.0	3.81	6.7	0.0	0.0
80	0	225.0	5.08	6.7	0.0	0.0
81	0	240.0	0.00	6.7	0.0	0.0
82	0	240.0	1.27	6.7	0.0	0.0
83	0	240.0	2.54	6.7	0.0	0.0
84	0	240.0	3.81	6.7	0.0	0.0
85	0	240.0	5.08	6.7	0.0	0.0
86	0	255.0	0.00	6.7	0.0	0.0
87	0	255.0	1.27	6.7	0.0	0.0
88	0	255.0	2.54	6.7	0.0	0.0
89	0	255.0	3.81	6.7	0.0	0.0
90	0	255.0	5.08	6.7	0.0	0.0
91	0	270.0	0.00	6.7	0.0	0.0
92	0	270.0	1.27	6.7	0.0	0.0
93	0	270.0	2.54	6.7	0.0	0.0
94	0	270.0	3.81	6.7	0.0	0.0
95	0	270.0	5.08	6.7	0.0	0.0
96	0	285.0	0.00	6.7	0.0	0.0
97	0	285.0	1.27	6.7	0.0	0.0
98	0	285.0	2.54	6.7	0.0	0.0
99	0	285.0	3.81	6.7	0.0	0.0
100	0	285.0	5.08	6.7	0.0	0.0
101	0	300.0	0.00	6.7	0.0	0.0
102	0	300.0	1.27	6.7	0.0	0.0
103	0	300.0	2.54	6.7	0.0	0.0
104	0	300.0	3.81	6.7	0.0	0.0
105	0	300.0	5.08	6.7	0.0	0.0
106	0	315.0	0.00	6.7	0.0	0.0
107	0	315.0	1.27	6.7	0.0	0.0
108	0	315.0	2.54	6.7	0.0	0.0
109	0	315.0	3.81	6.7	0.0	0.0
110	0	315.0	5.08	6.7	0.0	0.0
111	0	330.0	0.00	6.7	0.0	0.0
112	0	330.0	1.27	6.7	0.0	0.0
113	0	330.0	2.54	6.7	0.0	0.0
114	0	330.0	3.81	6.7	0.0	0.0
115	0	330.0	5.08	6.7	0.0	0.0
116	0	345.0	0.00	6.7	0.0	0.0
117	0	345.0	1.27	6.7	0.0	0.0
118	0	345.0	2.54	6.7	0.0	0.0
119	0	345.0	3.81	6.7	0.0	0.0

APPENDIX E

RESULTS OF NUMERICAL SIMULATION

TABLE IX
SAMPLE OUTPUT FOR CASE 1

NODE NO.	FRESH-WATER HEAD (CM.)	INTERFACE ELEVATION (CM.)
1	55.1314	53.6484
4	57.0774	47.6523
6	57.7086	45.7076
14	57.9557	44.9476
15	58.1600	44.3193
24	58.3515	43.7289
25	58.5410	43.1433
34	58.7203	42.5894
35	58.8979	42.0395
44	59.0671	41.5138
45	59.2350	40.9917
54	59.3957	40.4906
55	59.5554	39.9908
64	59.7088	39.5086
65	59.8613	39.0276
74	60.0085	38.5607
75	60.1548	38.0947
84	60.3094	37.6007
85	60.4346	37.1996
94	60.5697	36.7641
95	60.7030	36.3342
104	60.8320	35.9164
105	60.9600	35.5000

TABLE X
SAMPLE OUTPUT FOR CASE 2

NODE NO.	FRESH-WATER HEAD (CM.)	INTERFACE ELEVATION (CM.)
1	57.0616	47.5451
4	57.5405	46.0710
6	57.7596	45.3965
14	58.0041	44.6429
15	58.2049	44.0240
24	58.3930	43.4432
25	58.5795	42.8683
34	58.7560	42.3243
35	58.9307	41.7854
44	59.0974	41.2713
45	59.2629	40.7605
54	59.4212	40.2707
55	59.5781	39.7843
64	59.7289	39.3172
65	59.8789	38.8529
74	60.0233	38.4052
75	60.1669	37.9598
84	60.3183	37.4889
85	60.4411	37.1068
94	60.5741	36.6944
95	60.7054	36.2870
104	60.8328	35.8933
105	60.9600	35.5000

TABLE XI
 SAMPLE OUTPUT FOR CASE 3

OUTPUT BY CROSS SECTION

INCR 1

TIME 0.569E 00

DMAX 0.30E 01

CROSS SECTION NO. 1

NODE NO.	FRESH-WATER HEAD (CM.)	INTERFACE ELEVATION (CM.)
1	59.7478	38.4790
4	60.0522	37.5999
6	60.1673	37.2666
14	60.3091	36.8552
15	60.4201	36.5419
24	60.5216	36.2657
25	60.6141	36.0278
34	60.6955	35.8330
35	60.7657	35.6804
44	60.8237	35.5716
45	60.8697	35.5036
54	60.9041	35.4694
55	60.9279	35.4612
64	60.9431	35.4663
65	60.9522	35.4770
74	60.9569	35.4878
75	60.9593	35.4949
84	60.9599	35.4988
85	60.9601	35.4999
94	60.9601	35.5003
95	60.9601	35.5002
104	60.9601	35.5001
105	60.9600	35.5000

TABLE XI (CONTD.)

 OUTPUT BY CROSS SECTION

INCR 12

TIME 0.308E 02

DMAX 0.54E 00

CROSS SECTION NO. 1

NODE NO.	FRESH-WATER HEAD (CM.)	INTERFACE ELEVATION (CM.)
1	57.5009	45.6316
4	58.0671	43.8860
6	58.2805	43.2283
14	58.5261	42.4713
15	58.7265	41.8533
24	58.9114	41.2807
25	59.0942	40.7138
34	59.2651	40.1831
35	59.4339	39.6588
44	59.5925	39.1652
45	59.7487	38.6793
54	59.8966	38.2166
55	60.0413	37.7658
64	60.1772	37.3441
65	60.3080	36.9429
74	60.4290	36.5804
75	60.5422	36.2551
84	60.6528	35.9577
85	60.7333	35.7631
94	60.8101	35.6053
95	60.8724	35.5160
104	60.9210	35.4881
105	60.9600	35.5000

TABLE XI (CONTD.)

OUTPUT BY CROSS SECTION

INCR 25

TIME 0.600E 03

DMAX 0.48E-01

CROSS SECTION NO. 1

NODE NO.	FRESH-WATER HEAD (CM.)	INTERFACE ELEVATION (CM.)
1	55.8003	51.7291
4	56.7962	48.6620
6	57.1719	47.5049
14	57.5374	46.3793
15	57.8298	45.4760
24	58.0783	44.7062
25	58.3213	43.9521
34	58.5383	43.2767
35	58.7518	42.6110
44	58.9472	41.9986
45	59.1398	41.3942
54	59.3186	40.8283
55	59.4954	40.2678
64	59.6614	39.7375
65	59.8258	39.2110
74	59.9816	38.7091
75	60.1360	38.2100
84	60.2965	37.6878
85	60.4263	37.2637
94	60.5647	36.8080
95	60.7008	36.3591
104	60.8309	35.9280
105	60.9600	35.5000

TABLE XII

SAMPLE OUTPUT FOR CASE 4

NODE NO.	FRESH-WATER HEAD (CM.)	INTERFACE ELEVATION (CM.)
1	57.5453	46.0344
4	57.6850	45.6043
6	57.7938	45.2698
24	58.0261	44.5547
25	58.2249	43.9434
34	58.4418	43.3675
35	58.5968	42.7976
44	58.7702	42.2566
45	58.9460	41.7207
54	59.1116	41.2095
55	59.2755	40.7035
64	59.4323	40.2196
65	59.5885	39.7370
74	59.7388	39.2721
75	59.8879	38.8114
84	60.0314	38.3688
85	60.1737	37.9296
94	60.3239	37.4659
95	60.4456	37.0903
104	60.5772	36.6830
105	60.7076	36.2791
114	60.8341	35.8883
115	60.9600	35.5000

TABLE XIII

SAMPLE OUTPUT FOR CASE 5

 OUTPUT BY CROSS SECTION

INCR 1

TIME 0.569E 00

DMAX 0.25E 00

CROSS SECTION NO. 1

NODE NO.	FRESH-WATER HEAD (CM.)	INTERFACE ELEVATION (CM.)
1	60.6830	35.7451
4	60.7081	35.7090
6	60.7211	35.6902
24	60.7623	35.6309
25	60.7958	35.5846
34	60.8266	35.5454
35	60.8549	35.5141
44	60.8800	35.4908
45	60.9016	35.4761
54	60.9191	35.4697
55	60.9329	35.4700
64	60.9431	35.4737
65	60.9501	35.4821
74	60.9549	35.4893
75	60.9577	35.4950
84	60.9594	35.4977
85	60.9602	35.4996
94	60.9603	35.5004
95	60.9603	35.5008
104	60.9601	35.5007
105	60.9602	35.4999
114	60.9601	35.5001
115	60.9600	35.5000

TABLE XIII (CONTD.)

OUTPUT BY CROSS SECTION

INCR 12

TIME 0.308E 02

DMAX 0.68E 00

CROSS SECTION NO. 1

NODE NO.	FRESH-WATER HEAD (CM.)	INTERFACE ELEVATION (CM.)
1	58.3595	42.7973
4	58.4924	42.3913
6	58.5603	42.1848
24	58.7678	41.5570
25	58.9447	41.0205
34	59.1111	40.5152
35	59.2756	40.0160
44	59.4310	39.5446
45	59.5846	39.0768
54	59.7299	38.6343
55	59.8732	38.1976
64	60.0090	37.7824
65	60.1411	37.3816
74	60.2651	37.0093
75	60.3837	36.6601
84	60.4933	36.3464
85	60.5953	36.0673
94	60.6943	35.8182
95	60.7655	35.6615
104	60.8327	35.5428
105	60.8864	35.4832
114	60.9274	35.4757
115	60.9600	35.5000

TABLE XIII (CONTD.)

OUTPUT BY CROSS SECTION

INCR 24

TIME 0.480E 03

DMAX 0.72E-02

CROSS SECTION NO. 1

NODE NO.	FRESH-WATER HEAD (CM.)	INTERFACE ELEVATION (CM.)
1	56.9028	48.3327
4	57.1490	47.5746
6	57.2722	47.1952
24	57.6066	46.1631
25	57.8870	45.2957
34	58.1279	44.5473
35	58.3635	43.8143
44	58.5752	43.1534
45	58.7835	42.5034
54	58.9749	41.9040
55	59.1637	41.3113
64	59.3394	40.7562
65	59.5132	40.2053
74	59.6769	39.6825
75	59.8392	39.1638
84	59.9927	38.6691
85	60.1451	38.1776
94	60.3039	37.6617
95	60.4321	37.2440
104	60.5690	36.7936
105	60.7036	36.3495
114	60.8325	35.9231
115	60.9600	35.5000

TABLE XIV
ANALYTICAL SOLUTION FOR CONFINED AQUIFER

NODE NO.	FRESH-WATER HEAD (CM.)	INTERFACE ELEVATION (CM.)
1	93.6458	45.3700
4	93.6850	38.8300
5	93.7147	33.8800
10	93.7396	29.7300
11	93.7615	26.0800
16	93.7813	22.7900
17	93.7994	19.7700
22	93.8163	16.9600
23	93.8321	14.3200
28	93.8471	11.8200
29	93.8613	9.4500
34	93.8749	7.1900
35	93.8879	5.0200
40	93.9004	2.9300
41	93.9125	0.9100
46	93.9242	0.0000
47	93.9355	0.0000
52	93.9465	0.0000
53	93.9572	0.0000
58	93.9677	0.0000
59	93.9778	0.0000

TABLE XV

SAMPLE OUTPUT FOR CONFINED AQUIFER EXAMPLE

NODE NO.	FRESH-WATER HEAD (CM.)	INTERFACE ELEVATION (CM.)
1	93.7523	37.5796
4	93.7644	35.5776
5	93.7787	33.1896
10	93.7902	31.2742
11	93.8043	28.9207
16	93.8157	27.0270
17	93.8297	24.6942
22	93.8409	22.8239
23	93.8547	20.5148
28	93.8658	18.6708
29	93.8795	16.3872
34	93.8904	14.5712
35	93.9039	12.3161
40	93.9146	10.5309
41	93.9280	8.3058
46	93.9385	6.5525
47	93.9517	4.3587
52	93.9620	2.6388
53	93.9749	0.4777
58	93.9825	0.0000
59	93.9778	0.0000

TABLE XVI

SAMPLE OUTPUT FOR RECHARGE MOUND
EXAMPLE WITH CAPILLARITY

OUTPUT BY CROSS SECTION

INCR 1

TIME 0.250E 00

DMAX 0.00E 00

CROSS SECTION NO. 1

NODE NO.	FRESH-WATER HEAD (CM.)	INTERFACE ELEVATION (CM.)
3	9.5228	0.0000
8	9.4782	0.0000
13	9.3253	0.0000
18	8.9591	0.0000
23	8.1827	0.0000
28	7.4011	0.0000
33	7.0293	0.0000
38	6.8564	0.0000
43	6.7749	0.0000
48	6.7365	0.0000
53	6.7192	0.0000
58	6.7108	0.0000
63	6.7074	0.0000
68	6.7050	0.0000
73	6.7043	0.0000
78	6.7032	0.0000
83	6.7031	0.0000
88	6.7024	0.0000
93	6.7026	0.0000
98	6.7020	0.0000
103	6.7023	0.0000
108	6.7015	0.0000
113	6.7014	0.0000
118	6.7003	0.0000
123	6.7000	0.0000

TABLE XVI (CONTD.)

 OUTPUT BY CROSS SECTION

INCR 5

TIME 0.125E 01

DMAX 0.00E 00

CROSS SECTION NO. 1

NODE NO.	FRESH-WATER HEAD (CM.)	INTERFACE ELEVATION (CM.)
3	20.2928	0.0000
8	20.0710	0.0000
13	19.4034	0.0000
18	18.2352	0.0000
23	16.5639	0.0000
28	14.6403	0.0000
33	12.9917	0.0000
38	11.4527	0.0000
43	10.2164	0.0000
48	9.1901	0.0000
53	8.4309	0.0000
58	7.8634	0.0000
63	7.4697	0.0000
68	7.1993	0.0000
73	7.0206	0.0000
78	6.9042	0.0000
83	6.8309	0.0000
88	6.7840	0.0000
93	6.7559	0.0000
98	6.7380	0.0000
103	6.7271	0.0000
108	6.7191	0.0000
113	6.7132	0.0000
118	6.7074	0.0000
123	6.7000	0.0000

TABLE XVI (CONTD.)

 OUTPUT BY CROSS SECTION

INCR 12

TIME 0.300E 01

DMAX 0.00E 00

CROSS SECTION NO. 1

NODE NO.	FRESH-WATER HEAD (CM.)	INTERFACE ELEVATION (CM.)
3	28.3553	0.0000
8	28.1529	0.0000
13	27.5389	0.0000
18	26.5366	0.0000
23	25.1803	0.0000
28	23.5683	0.0000
33	21.9767	0.0000
38	20.3503	0.0000
43	18.8127	0.0000
48	17.2789	0.0000
53	15.8774	0.0000
58	14.5186	0.0000
63	13.3105	0.0000
68	12.1764	0.0000
73	11.1986	0.0000
78	10.3170	0.0000
83	9.5806	0.0000
88	8.9451	0.0000
93	8.4296	0.0000
98	7.9999	0.0000
103	7.6563	0.0000
108	7.3744	0.0000
113	7.1439	0.0000
118	6.9454	0.0000
123	6.7000	0.0000

TABLE XVII

SAMPLE OUTPUT FOR RECHARGE MOUND
EXAMPLE WITHOUT CAPILLARITY

OUTPUT BY CROSS SECTION

INCR 1

TIME 0.250E 00

DMAX 0.00E 00

CROSS SECTION NO. 1

NODE NO.	FRESH-WATER HEAD (CM.)	INTERFACE ELEVATION (CM.)
3	9.6356	0.0000
8	9.6129	0.0000
13	9.5200	0.0000
18	9.1905	0.0000
23	8.1840	0.0000
28	7.1716	0.0000
33	6.8438	0.0000
38	6.7460	0.0000
43	6.7148	0.0000
48	6.7050	0.0000
53	6.7024	0.0000
58	6.7012	0.0000
63	6.7011	0.0000
68	6.7007	0.0000
73	6.7006	0.0000
78	6.7004	0.0000
83	6.7004	0.0000
88	6.7002	0.0000
93	6.7004	0.0000
98	6.7001	0.0000
103	6.7001	0.0000
108	6.7001	0.0000
113	6.7003	0.0000
118	6.7002	0.0000
123	6.7000	0.0000

TABLE XVII (CONTD.)

OUTPUT BY CROSS SECTION

INCR 5

TIME 0.125E 01

DMAX 0.00E 00

CROSS SECTION NO. 1

NODE NO.	FRESH-WATER HEAD (CM.)	INTERFACE ELEVATION (CM.)
3	18.0154	0.0000
8	17.8065	0.0000
13	17.1811	0.0000
18	16.0544	0.0000
23	14.3884	0.0000
28	12.3127	0.0000
33	10.6659	0.0000
38	9.1823	0.0000
43	88.1858	0.0000
48	7.4957	0.0000
53	7.1064	0.0000
58	6.8964	0.0000
63	6.7924	0.0000
68	6.7432	0.0000
73	6.7203	0.0000
78	6.7105	0.0000
83	6.7061	0.0000
88	6.7039	0.0000
93	6.7028	0.0000
98	6.7023	0.0000
103	6.7022	0.0000
108	6.7018	0.0000
113	6.7014	0.0000
118	6.7008	0.0000
123	6.7000	0.0000

TABLE XVII (CONTD.)

OUTPUT BY CROSS SECTION

INCR 12

TIME 0.300E 01

DMAX 0.00E 00

CROSS SECTION NO. 1

NODE NO.	FRESH-WATER HEAD (CM.)	INTERFACE ELEVATION (CM.)
3	25.3732	0.0000
8	25.1633	0.0000
13	24.5506	0.0000
18	23.4622	0.0000
23	21.9206	0.0000
28	20.0161	0.0000
33	18.2578	0.0000
38	16.4257	0.0000
43	14.7911	0.0000
48	13.1334	0.0000
53	11.7332	0.0000
58	10.3996	0.0000
63	9.3612	0.0000
68	8.4831	0.0000
73	7.8655	0.0000
78	7.4190	0.0000
83	7.1340	0.0000
88	6.9529	0.0000
93	6.8452	0.0000
98	6.7825	0.0000
103	6.7468	0.0000
108	6.7265	0.0000
113	6.7147	0.0000
118	6.7073	0.0000
123	6.7000	0.0000

APPENDIX F

FINITE-ELEMENT MESH LAYOUTS

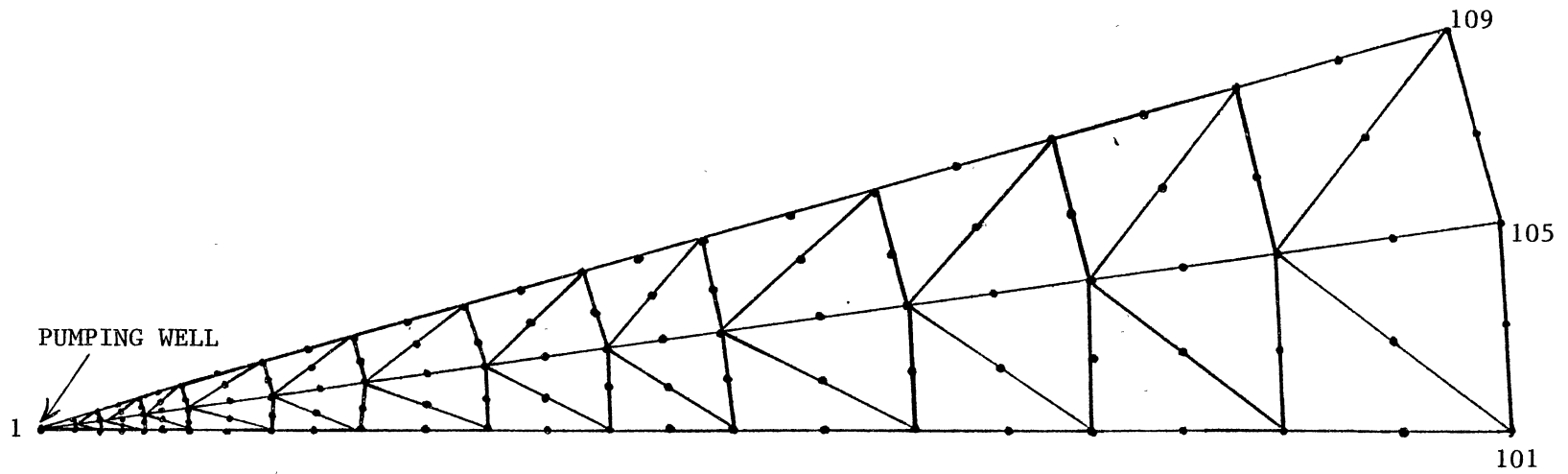


Figure 19. Detailed Finite Element Mesh Layout of Sahni's Model

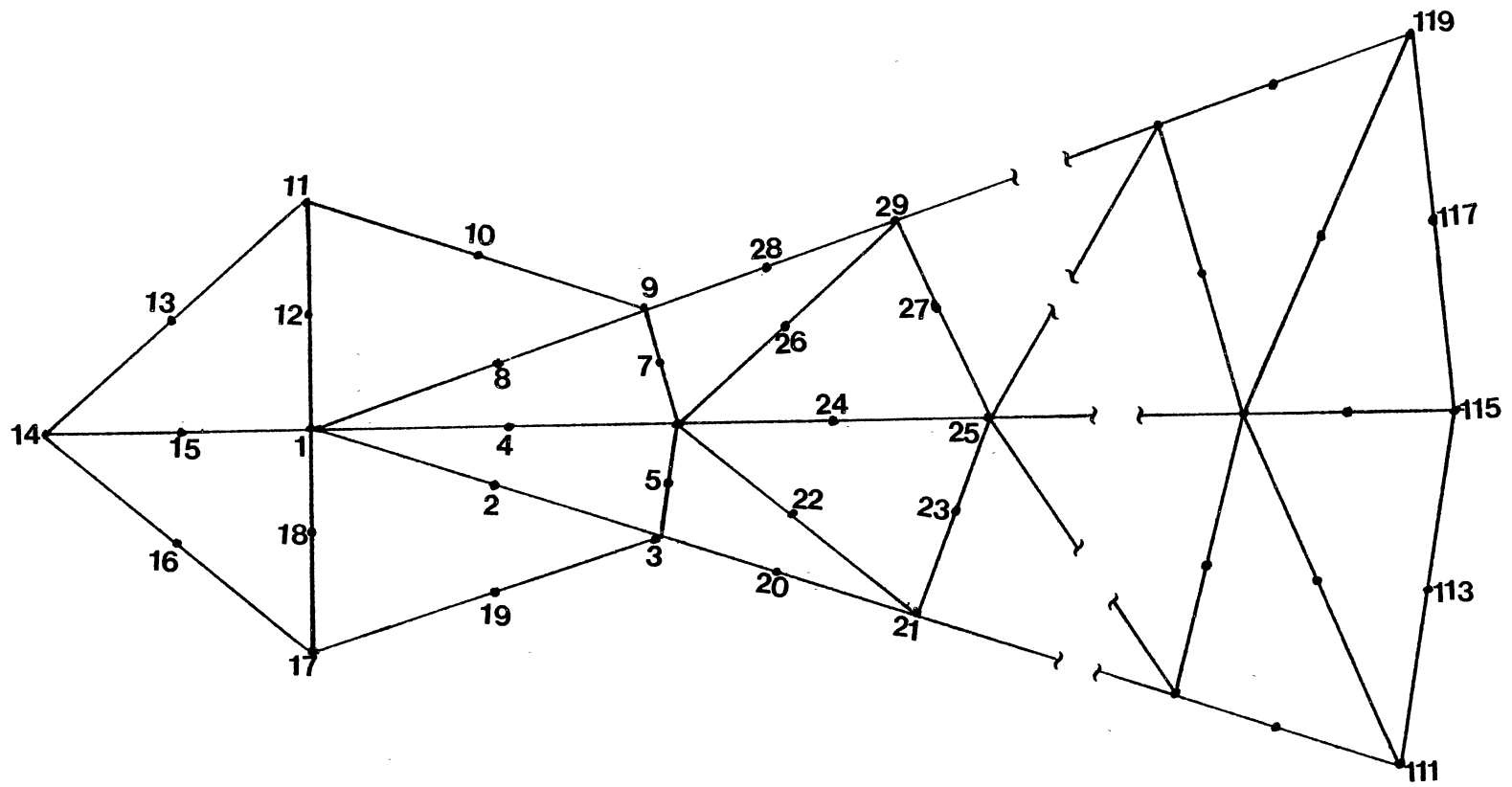


Figure 20. Expanded Finite Element Mesh Layout of Sahni's Model

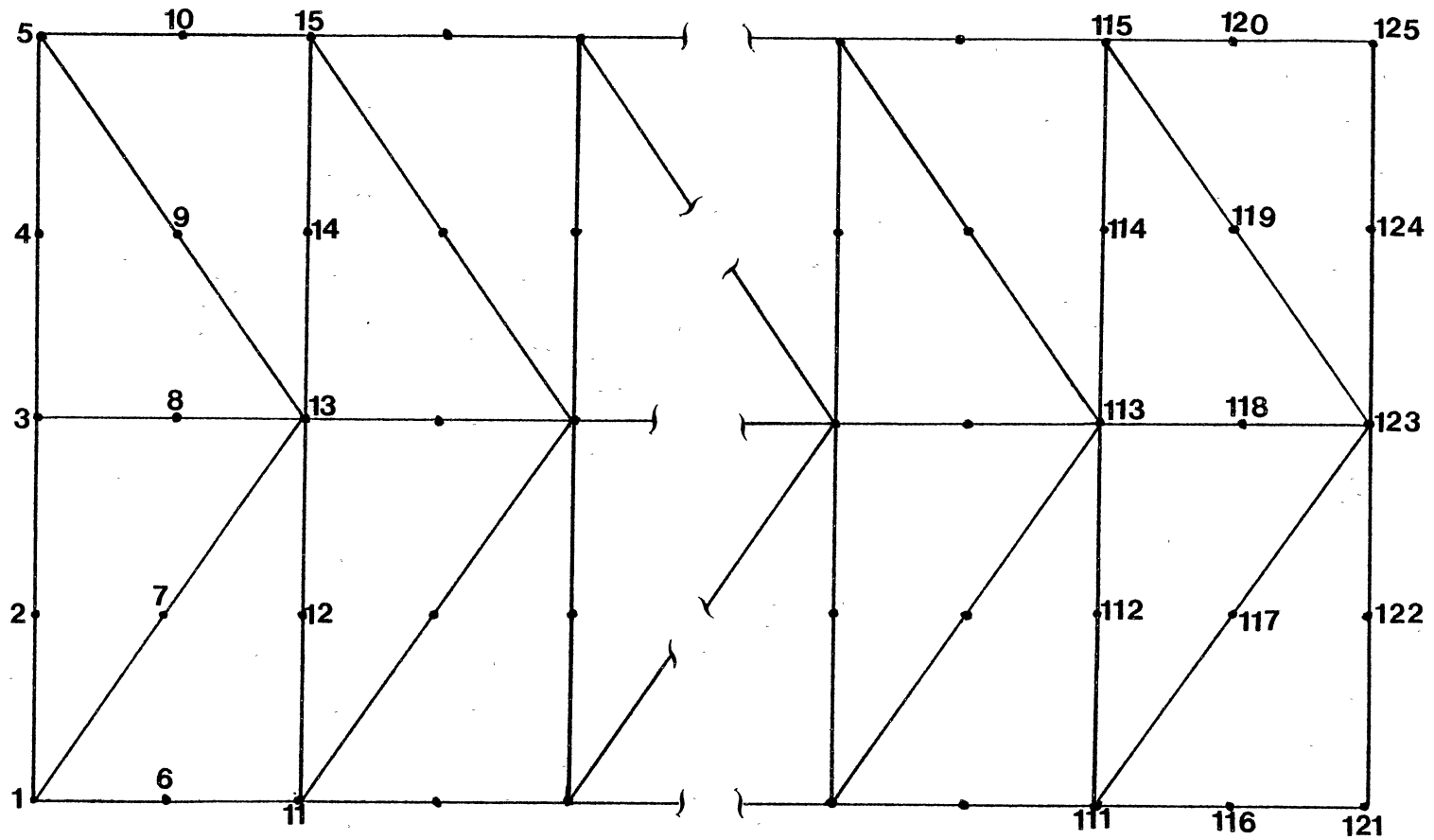


Figure 21. Finite Element Mesh Layout of the Experimental Model of Ortiz, et al.

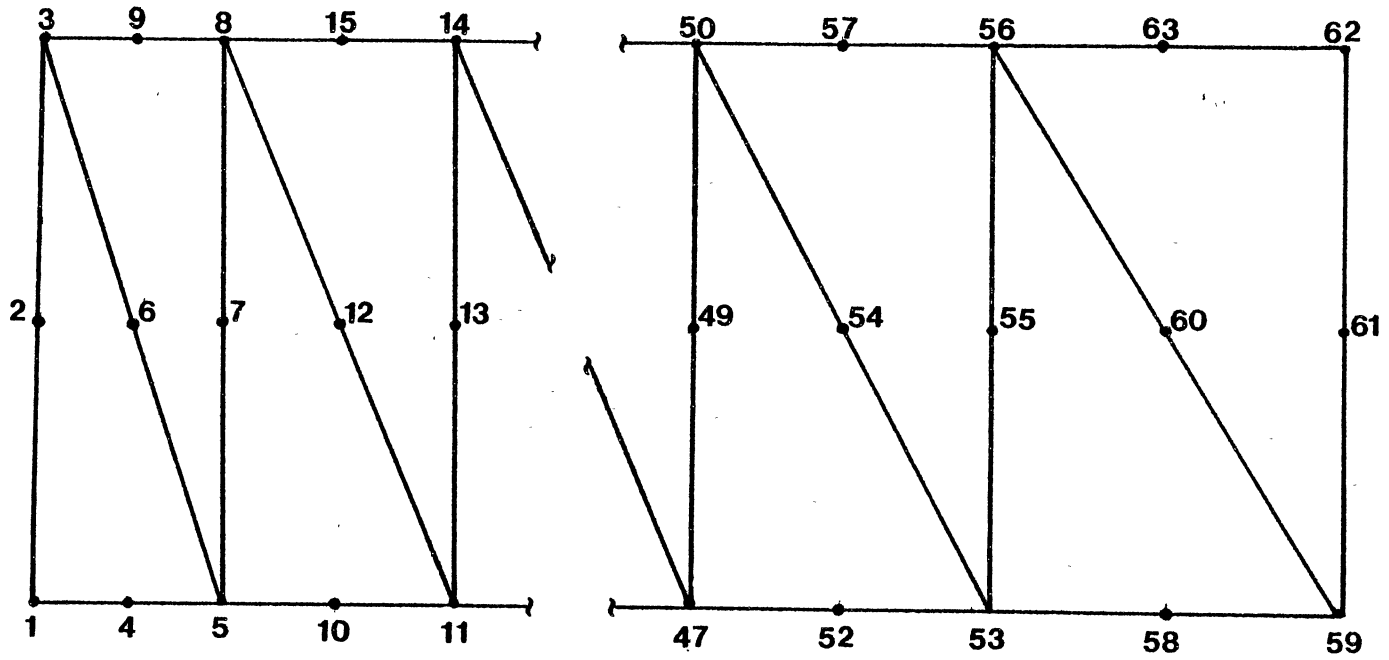


Figure 22. Finite Element Mesh Layout of Henry's Analytical Model

VITA 2

Roop Dasari Kumar

Candidate for the Degree of

Master of Science

Thesis: TRANSIENT SIMULATION OF THE IMMISCIBLE FRESH-WATER/SALT-WATER
INTERFACE IN AQUIFERS

Major Field: Chemical Engineering

Biographical:

Personal Data: Born in Hyderabad, India, August 10, 1958, the son
of Mr. and Mrs. D. V. Rao.

Education: Graduated from Hyderabad Public School, Hyderabad, India,
in March, 1975; received Bachelor of Technology degree in
Chemical Engineering from Osmania University in May, 1980;
completed requirements for the Master of Science degree at
Oklahoma State University in May, 1984.

Professional Experience: Research Assistant, School of Chemical
Engineering, Oklahoma State University, 1981-82; Teaching
Assistant, School of Chemical Engineering, Oklahoma State
University, 1981-82.